Imposing structure on odor representations during learning in the prefrontal cortex

Yiliu Wang

Submitted in partial fulfillment of the
requirements for the degree of
Doctor of Philosophy
in the Graduate School of Arts and Sciences

COLUMBIA UNIVERSITY

2019

ABSTRACT

Imposing structure on odor representations during learning in the prefrontal cortex

Yiliu Wang

Animals have evolved sensory systems that afford innate and adaptive responses to stimuli in the environment. Innate behaviors are likely to be mediated by hardwired circuits that respond to invariant predictive cues over long periods of evolutionary time. However, most stimuli do not have innate value. Over the lifetime of an animal, learning provides a mechanism for animals to update the predictive value of cues through experience. Sensory systems must therefore generate neuronal representations that are able to acquire value through learning. A fundamental challenge in neuroscience is to understand how and where value is imposed in brain during learning.

The olfactory system is an attractive sensory modality to study learning because the anatomical organization is concise in that there are relatively few synapses separating the sense organ from brain areas implicated in learning. Thus, the circuits for learned olfactory behaviors appear to be relatively shallow and therefore more experimentally accessible than other sensory systems. The goal of this thesis is to characterize the representation and function of neural circuits involved in olfactory associative learning. Odor perception is initiated by the binding of odors onto olfactory receptors expressed in the sensory epithelium. Each olfactory receptor neuron (ORN) expresses one of 1500 different receptor genes, the expression of which pushes the ORN to project with spatial specificity onto a defined loci within the olfactory bulb, the olfactory glomeruli. Therefore, each and every odor evokes a stereotyped map of glomerular activity in the bulb.

The projection neurons of the olfactory bulb, mitral and tufted (M/T) cells, send axons to higher brain areas, including a significant input to the primary olfactory cortex, the piriform cortex. Axons from M/T cells project diffusely to the piriform without apparent spatial preference; as a consequence, the spatial order of the bulb is discarded in the piriform. In agreement with anatomical data, electrophysiological and optical imaging studies also demonstrate that individual odorants activate sparse subsets of neurons across the piriform without any spatial order. Moreover, individual piriform neurons exhibit discontinuous receptive fields that defy chemical or perceptual categorization. These observations suggests that piriform neurons receive random subsets of glomerular input. Therefore, odor representations in piriform are unlikely to be hardwired to drive specific behaviors. Rather, this model suggests that value must be imposed upon the piriform through learning. Indeed, the piriform has been shown to be both sufficient and necessary for aversive olfactory learning without affecting innate odor responses. However, how value is imposed on odor representations in the piriform and downstream associational areas remain largely unknown.

We first developed a strategy to track neural activity in a population of neurons across multiple days in deep brain areas using 2-photon endoscopic imaging. This allowed us to assay changes in neural responses to odors during learning in piriform and in downstream associative areas. Using this technique, we first observe that piriform odor responses are unaffected by learning, so learning must therefore impose discernable changes in neural activity downstream of piriform. Piriform projects to multiple downstream areas that are implicated in appetitive associative learning, such as the orbitofrontal cortex (OFC). Imaging of neural activity in the OFC reveal that OFC neurons acquire strong responses to conditioned odors (CS+) during learning. Moreover, multiple and distinct CS+ odors activate

the same population of OFC neurons, and these responses are gated by context and internal state. Together, our imaging data shows that an external and sensory representation in the piriform is transformed into an internal and cognitive representation of value in the OFC. Moreover, we found that optogenetic silencing of the OFC impaired the ability of mice to acquire learned associations. Therefore, the robust representation of expected value of the odor cues is necessary for the formation of appetitive associations.

We made an important observation: once the task has been learned with a set of odors, the OFC representation decays after learning has plateaued and remains silent even when mice encounter novel odors they haven't previously experienced. Moreover, silencing the OFC when it was not actively engaged during the subsequent learning of new odors had no effect on learning. These sets of imaging and silencing experiments reveal that the OFC is only important during initial learning; once task structure has been acquired, it is no longer needed. Task performance after initial task acquisition must therefore be accommodated by other brain regions that can store the learned association for long durations.

We therefore searched for other brain regions that held learned associations long-term. In the medial prefrontal cortex (mPFC), we observe that the learned representation persists throughout the entire course of training. Unlike the OFC, not only does this representation encode the positive expected value of CS+ odors, it also encodes the negative expected value of CS- odors in a non-overlapping ensemble of neurons. We further show through optogenetic silencing that this representation is necessary for task performance after the task structure has already been acquired. Therefore, while the OFC representation is required for initial task acquisition, the mPFC representation is required for subsequent appetitive learning and performance. Why would a learned representation vanish in the OFC and be

transfered elsewhere? We hypothesize that the brain may allocate a portion of its real estate to be a cognitive playground where experimentation and hypothesis testing takes place. Once this area solves a task, it may unload what it has learned to storage units located elsewhere to free up space to learn new tasks.

We further imaged another associative area, the basolateral amygdala (BLA), and found a representation of positive value that appears to be generated from a Hebbian learning mechanism. However, the silencing of this representation during learning had no effect. This suggests that while multiple and distributed brain areas encode cues that predict the reward, not all may be necessary for the learning process or for task performance.

In summary, we have described a series of experiments that map the representation and function of different associational areas that underlie learning. The data and the techniques employed have the potential to significantly advance the understanding of learned behavior.

Contents

List of Figures

Acknowledgements

The work described in this thesis is the culmination of 6 years of work, none of which would have been possible without the contributions and support of those around me.

First and foremost I would like to thank my family. I would not have achieved all I have without your unconditional love and support.

Thank you to my undergraduate advisors, Joseph Fetcho and Carl Hopkins, who first introduced me to neuroscience. Thank you for giving me the chance to work with you and for believing that I had a future career as a neuroscientist.

I am also thankful to my collaborator, Cristian Boboila, for being an steadfast friend and colleague. I would also like to thank Ashok Litwin-Kumar as a long-term collaborator, and also to the technicians who have helped with this project: Kristen Lawlor, Matthew Chin, and Philip Shamash.

Thank you to Columbia's doctoral program in Neurobiology and Behavior for providing a great place to do good science. Thank you to Carol Mason, Darcy Kelley, Wes Grueber, and Ken Miller for your help in my early days at Columbia.

Thank you to all members in the Axel lab, as well as my friends in the Neurobiology program. Thank you to Phyllis Kisloff, Miriam Guiterrez, Adriana Nemes, Monica Mendelsohn, Nataliya Zabello, and Clayton Eccard for all your assistance over the years.

Thank you to Stefano Fusi, Rui Costa, and Bob Datta for serving on my committee. Your time and input are greatly appreciated.

Thank you to my friends outside of lab, Taiga Abe, Arnold Ha, Brien Lee, Max Liu, David Plotkin, Philip Shinn, Bert Vancura, Jeff Zhang, and Jay Zhang, and to my girlfriend, Connie Li, who have each made me so happy and have kept me mentally at peace towards the end of my PhD.

Finally, thank you to my thesis advisors, Richard Axel and Larry Abbott, who have both taught me invaluable lessons throughout my time at Columbia. You have shown me the importance of diligence, care, and creativity in experimentation, and have taught me how to think simply and critically. I would have achieved none of this without you and am forever indebted to you both, thank you.

To Richard, thank you for your patience, your understanding, and for your guidance over the years. I hope to make you proud in science in the years to come.

Dedication

To mom and dad

Chapter 1

Introduction

All organisms are alike: they must seek out food, shelter, and potential mates while avoiding danger in a constantly changing environment. Sensory stimuli such as mating calls or predator odors are highly predictive of future reward and risk, and organisms have evolved hardwired circuits that respond to these invariant predictive cues to drive appropriate behavioral repertoires. However, most stimuli do not have innate significance, and meaning must be imposed upon these stimuli through experience. The brain must therefore attach significance to specific sensory stimuli through learning. A fundamental challenge in neuroscience is to understand how and where meaning is imposed in the brain during learning.

Over the past 50 years, tremendous advances have been made in the understanding of neural circuits that underlie learned behaviors. More recently, the ease with which new genetic tools can be used to observe and perturb neural activity in defined neural populations in mice have made it a powerful model system to study neural circuits. We use the olfactory system to study learning in mice for two reasons. One, mice heavily rely on its sense of smell to interact with its surroundings. Many of its behavioral responses, such as predator avoidance or food scavenging, are mediated by its sense of smell. Two, the anatomical organization of the olfactory system is concise in that there are relatively few synapses separating the sense organ (nose) from brain areas implicated in learning. Thus, the circuits

for learned olfactory behaviors appear to be relatively shallow and more tractable that other sensory systems.

The mouse olfactory system

Odor perception is initiated by the binding of odors onto olfactory receptors expressed in the nasal epithelium. Olfactory receptors are a class of G protein-coupled seven-transmembrane proteins, and are encoded by the largest gene families known to exist in the animal genome (Mombaerts 1999). Each olfactory receptor neuron (ORN) expresses one of 1500 different receptor genes, and receptor neurons expressing the same olfactory receptor are dispersed randomly within the 4 zones of the nasal epithelium (Vassar et al. 1993; Ressler et al. 1993; Buck and Axel 1991; Godfrey et al. 2004; Zhang and Firestein 2002) (Figure 1.1). Each olfactory receptor binds to multiple structurally distinct odors; conversely, each odor binds to multiple olfactory receptors. As such, individual odors are detected by a unique subset of olfactory receptor neurons and therefore evoke activity in a spatially distributed pattern of neural activity within the nasal epithelium. This combinatorial coding underlies the mouse's ability to detect and discriminate between different odors (Malnic et al. 1999).

Neurons expressing a given receptor project with precision to two spatially invariant loci within the olfactory bulb, termed olfactory glomeruli (Ressler et al. 1994; Mombaerts et al. 1996; Vassar et al. 1994) (Figure 1.2). This convergence is genetically determined, as axons expressing the same receptor converge upon the same location across all mice. Therefore, any given odor induces the same pattern of glomerular activity across animals

(Soucy et al. 2009; Belluscio and Katz 2001; Bozza et al. 2004). Functional studies indicate that physiological concentrations of odor elicits activation in about 5% of all glomeruli (Lin et al. 2006). Therefore, odor activation in the sense organ is transformed into a discrete spatial map of glomerular activity in the olfactory bulb (Figure 1.3). Unlike other senses, no chemotopic order was apparent in responses elicited by odors in the olfactory bulb when glomeruli on the dorsal surface were imaged during odor presentation. Nearby glomeruli were as diverse in their odor sensitivity as distant glomeruli(Soucy et al. 2009). However, the bulb may be spatially organized to segregate innate odor responses from learned odor responses; genetic ablation of glomeruli on the dorsal olfactory bulb abolishes innate behavioral responses while leaving learned olfactory responses intact (Kobayakawa et al. 2007).

The axons of ORNs are received by mitral and tufted (M/T) cells, the main projection neurons of the olfactory bulb. M/T cells appear to be hardwired to receive input from a single glomerulus, and therefore faithfully preserve the segregation of ORN odor responses into distinct glomerular channels (Shepherd 1998). While M/T cells share similar tuning as their corresponding ORN inputs, local interneurons within the bulb appear to modulate and sharpen the selectivity of M/T odor responses compared to their ORN inputs, especially at high odor concentrations (Tan et al. 2010; Kikuta et al. 2013; Rinberg et al. 2006). M/T cells then send axons to 5 higher-order brain areas, including the cortical amygdala and the piriform cortex (Price and Powell 1970). The level of spatial stereotypy exhibited by M/T projections to downstream areas appears to reflect the function of the downstream areas. For instance, M/T projections to cortical amygdala appear to be spatially stereotyped across mice and appears to be necessary for behavioral responses to innately salient odors such as

predator scents (Sosulski et al. 2011; Root et al. 2014) (Figure 1.4). Indeed, optogenetic inhibition of the cortical amygdala abolishes hardwired responses to innate odors while sparing learned odor responses (Root et al. 2014).

In contrast, anatomic tracing reveals that axonal projections from M/T cells to the piriform cortex discard the spatial stereotypy of the olfactory bulb. These bulbar projections appear to be unstructured and distributed across the entirety of the piriform (Ghosh et al. 2011; Miyamichi et al. 2011; Sosulski et al. 2011) (Figure 1.4). In accord with this anatomy, electrophysiological and optical imaging studies demonstrate that individual odorants activate distributed ensembles of piriform neurons without apparent spatial preference (Stettler and Axel 2009; Poo and Isaacson 2009; Zhan and Luo 2010; Rennaker et al. 2007) (Figure 1.5). Therefore, the sensory representation in the primary olfactory cortex appears to be fundamentally different from cortices of other sensory modalities, where stimulus features are often topographically organized (HUBEL and WIESEL 1959; MOUNTCASTLE 1957).

These observations are consistent with a model where piriform neurons receive convergent input from random subsets of olfactory glomeruli (Stettler and Axel 2009; Apicella et al. 2010; Davison and Ehlers 2011). This model explains why individual piriform neurons have unique odor receptive fields and respond to structurally and perceptually distinct odors (Stettler and Axel 2009; Poo and Isaacson 2009; Zhan and Luo 2010; Rennaker et al. 2007; Davison and Ehlers 2011). Moreover, if piriform odor responses are different across different mice, it is unlikely that piriform neurons would be evolutionarily hardwired to drive specific behaviors. Rather, piriform neurons must acquire the ability to drive learned behaviors through experience. This suggests that the piriform cortex plays an important

role in olfactory learning. Indeed, the exogenous photo-activation of an arbitrarily chosen ensemble of piriform neurons can be entrained to elicit either appetitive or aversive behavioral responses through temporal pairing with rewards or punishments, respectively (Choi et al. 2011) (Figure 1.6). Moreover, silencing of posterior piriform using pharmacogenetics (DREADDs) blocks the retrieval of an olfactory fear memory while sparing innate odor responses (Sacco and Sacchetti 2010; Alexander et al. 2009). Therefore, the piriform is both necessary and causal for olfactory learning.

Sparse encoding of sensory stimuli in large neural populations has been proposed to facilitate learning in downstream associative circuits (Marr 1971). This framework has been applied not only to granule cells in the cerebellum, but also to piriform neurons and its invertebrate analogue, the Kenyon cells of the mushroom body. In this framework, inputs from M/T cells to piriform are random and fixed to generate a high dimensional odor representation that is stable during learning. A sparse and high dimensional representation allows for diverse and different odors to be encoded uniquely by non-overlapping neural ensembles. This enhances the discriminability of chemically similar odors and thus facilitates the accurate recall of trained odors after learning (Litwin-Kumar et al. 2017). Learning then modifies the connection strengths of piriform outputs to downstream associative areas. After learning, re-activation of the same ensemble would drive the conditioned response. Therefore, successful recall of a learned association depends upon the faithful re-activation of the same odor ensemble that is paired with a salient stimulus during learning. However, contrary to theory, past literature suggests that the response properties of piriform neurons are modulated by learning (Calu et al. 2007; Chen et al. 2011; Li et al. 2008; Roesch et al. 2007; Sevelinges et al. 2004).

Principal neurons of piriform cortex project to numerous areas that have been implicated in learned behaviors, including the orbitofrontal cortex, striatum, and amygdala (Miyamichi et al. 2011; Sosulski et al. 2011; Haberly and Price 1977). The potentiation of these projections may also drive learning-related changes in these downstream areas. Therefore, it is currently unclear whether value is imposed onto an odor representation within the piriform or in areas downstream. If value was imposed onto piriform neurons, then the representation of a trained odor would be different after learning as compared to before. Addressing this question directly would require a technique that tracks activity in a population of piriform neurons during learning.

Novel Approaches for Tracking The Representation of Odor During Learning in the Mouse Olfactory System and Beyond

Recording neural activity in deep brain structures has traditionally been done using extracellular multielectrode arrays (Buzsáki 2004). Currently, state of the art multielectrode arrays can record from as many as a thousand neurons simultaneously. Moreover, the precise spatial distribution of recording sites allows for the triangulation of the locations of recorded neurons (Csicsvari et al. 2003). Recent advances have also allowed for multi-electrode arrays to chronically record the activity of multiple neurons (Sato et al. 2007). However, this technique suffers from cell loss, glial scarring, and also drops in the number of functioning electrodes over time due to accumulated damage in both electrode and brain tissue (Biran et al. 2005).

Newly developed genetically encoded calcium indicators (GECIs) provides an alterna-

tive to large-scale recordings of neural activity (Broussard et al. 2014). These proteins are engineered to convert changes in calcium ion concentration into changes in fluorescence. Neural activity triggers large and rapid calcium influx through voltage-gated calcium channels. Therefore, the imaging of calcium activity through GECIs can be used as a reliable proxy to measure neural activity across populations of neurons. Moreover, genetic targeting through viral or transgenic approaches allow for the expression of GECIs to be restricted to defined cell populations (Chen et al. 2012). This gives unprecedented experimental control over the study of a particular neuron population, such as somatostatin neurons in the motor cortex or excitatory CA1 neurons in the hippocampus. In particular, the recently developed probe GCaMP6 allows for the detection of neural activity with extremely high signal-to-noise ratios in awake and behaving mice that are an order magnitude higher than previous GECIs (Chen et al. 2013).

However, imaging has traditionally been restricted to the brain surface (Chen et al. 2012). Recently, the application of optical microendoscopy has allowed for neural activity from deeper brain areas to be imaged. Miniature endoscopes called gradient index (GRIN) lenses can be inserted into deeper brain regions to transmit fluorescence emissions from deep brain tissue onto the surface of the lens to be collected. This can be combined with the imaging capabilities of a two-photon microscope to reduce bleaching and light scattering. A few groups have currently adapted 2-photon endoscopic imaging to image calcium dynamics in deep areas such as geniculate ganglion neurons (Barretto et al. 2015), the medial prefrontal cortex (mPFC) (Otis et al. 2017), and the basolateral amygdala (Grewe et al. 2017). Motion appears to be limited, especially in areas that lie closer to the dorsal surface of the brain and if mice are head-fixed. Moreover, this approach allows for the identi-

fication of neurons across multiple days of imaging. While neurons will certainly shift slightly across different days like in multielectrode array recordings, the high spatial resolution of 2-photon microscopy allows for neuronal shape to be visualized. Therefore, with current registration techniques, one can easily align and register the identities of neurons across multiple imaging days by aligning the spatial profiles of neurons across different days (Pnevmatikakis et al. 2016). Moreover, because the lens is firmly cemented against the cranium, there appears to be minimal amounts of tissue damage even after months of imaging following a brief post-surgery recovery period (Ziv et al. 2013).

We have adapted this microendoscopic imaging technique to track neural activities in the piriform cortex and its downstream regions, the orbitofrontal cortex, the basolateral amygdala, and the medial prefrontal cortex during learning. This method allows us to answer a fundamental question in all these brain areas: how do neural representations change as a function of experience? Specifically, in the piriform cortex, does the robust encoding of odor identity change dramatically as a function of learning, or is it preserved (Calu et al. 2007; Chen et al. 2011; Li et al. 2008; Roesch et al. 2007; Sevelinges et al. 2004)? Likewise, what specific changes occur in neural representations in downstream associative areas such as the OFC, bLA and mPFC during learning? The imaging of neural activity during learning in piriform and its downstream areas allows us to map how sensory information is transformed in cognitive areas.

The ability to track neural activity over time in genetically defined subpopulation of neurons allows us to study neural representations in unprecedented detail. First, we are able observe and quantify the consistency of neural responses across different days, which cannot be done using multi-electrode arrays. Second, we can answer fundamental questions

of neural coding by analyzing the properties of neurons that experience learning-related changes. For example, previous studies found that BLA neurons potentiate their responses to a CS after it is paired with an aversive US (Quirk et al. 1997). This has generated a Hebbian model in which CS inputs are potentiated specifically onto 'fear cells' that are also responsive to US. By imaging neural responses before and after learning, we can unequivocally answer this question by analyzing whether potentiated CS responses only occur in US-responsive neurons.

We have applied this imaging method in transgenic mice that express GCaMP6s in the majority of excitatory neurons to examine changes in odor representations during learning. The application of this new imaging technique has allowed us to gain insight into how odor information is represented in the piriform cortex, how odor information is transformed as it passes from the piriform to downstream associative areas, and finally, what roles these downstream areas may play in odor learning. The imaging method that we have developed is widely applicable and can be applied to image any deep brain area to understand how neural representations change through time. Informed by our imaging results, we can then directly test hypotheses on the roles of each downstream areas during learning, as revealed in chapters 2, 3, and 4. This approach can also be combined with newly developed optogenetic probes to conduct simultaneous optical perturbation and imaging experiments in awake, behaving mice (chapters 3 and 4).

Figure 1.1

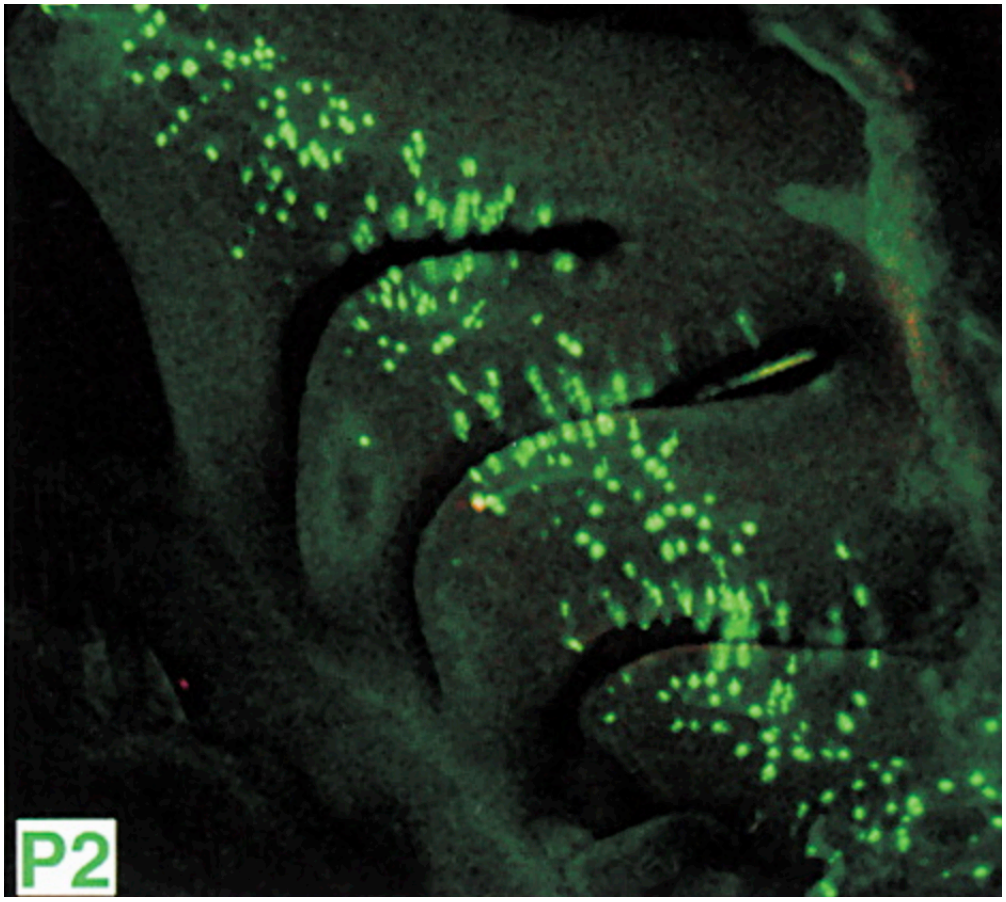

Figure 1.1. Sensory neurons expressing a single olfactory receptor are distributed in the nasal epithelium. Neuronal distribution of P2 OR expression in the olfactory epithelium was assayed in whole-mount specimens. P2-IRES-tauGFP Mice. GFP was imaged by its intrinsic green fluorescence. Adapted from Vassalli et al. 2002.

Figure 1.2

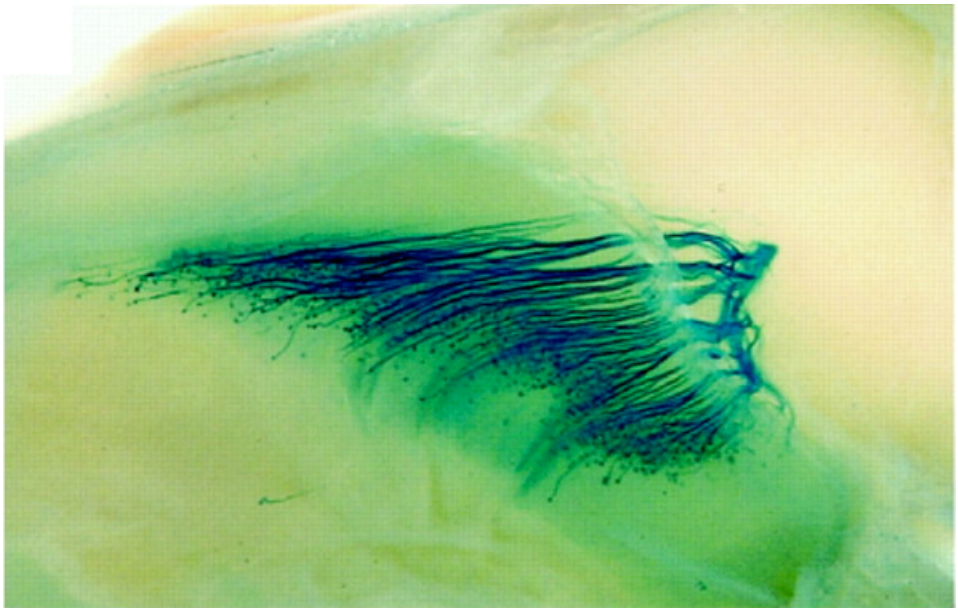

Figure 1.2. Axons of ORNs expressing a specific OR project with spatial precision to a defined loci within the bulb. View of the nasal septum and the medial aspect of the bulb. P2-IRES-tau-lacZ Mice, Stained with X-Gal. Adapted from Mombaerts et al. 1996.

Figure 1.3

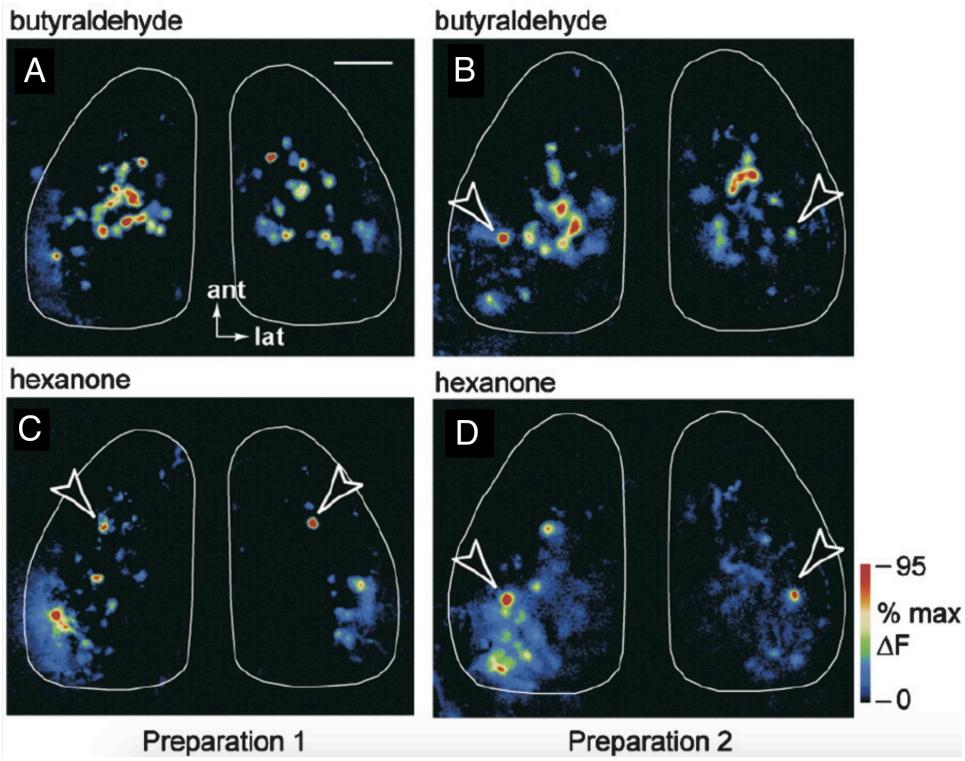
butyraldehyde
A
ant
lat
butyraldehyde
B
hexanone
C
hexanone
D
95
% max
ΔF
0
Preparation 1
Preparation 2

Figure 1.3. Odor-evoked responses in the olfactory bulb display spatial stereotypy. Odor response maps from two mice (butyraldehyde (A and B) and 2-hexanone (C and D)). Synapto-pHlouorin (sph), an indicator of synaptic release, was expressed in all ORNs (OMP-spH mice), and percentage change in fluorescence was quantified in pseudo-colored maps. Spatial patterns of odor-evoked activity are similar for the same odor in different mice, but were distinct for different odors in the same mouse. Scale bar, 500 μm. Adapted from Bozza et al. 2004.

Figure 1.4

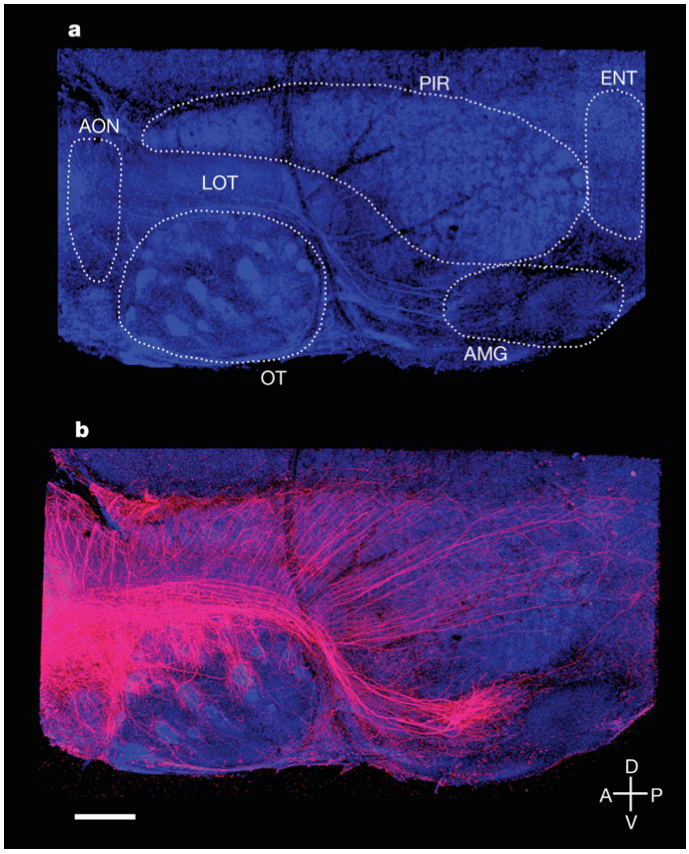

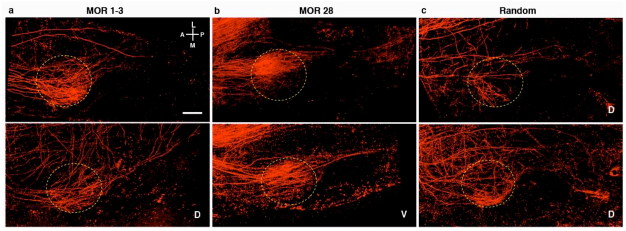

Figure 1.4. M/T cells projections to cortical and subortical structures. A. Flattened hemi-brain preparation with olfactory bulb targets outlined (AON, anterior olfactory nucleus; AMG, cortical amygdala; ENT, lateral entorhinal cortex; LOT, lateral olfactory tract; OT, olfactory tubercle). **B.** Flattened hemibrain preparation in which a single glomerulus was electroporated with TMR-dextran (shown in red) to label the axonal projections of M/T cells. Projection patterns to piriform are diffuse across different mice, whereas projection patterns to cortical amygdala display spatial stereotypy. **C.** Images of the cortical amygdala reveal similar projections from mitral and tufted cells that connect to the same glomeruli in two different brains (comparing top and bottom for glomeruli MOR1-3 and MOR28). However, these projection patterns are unique for different glomeruli, visualized when comparing the projection patterns from the MOR1-3, MOR28, or from a random glomerulus. Circle = approximate posterolateral cortical nucleus boundary; scale bar = 400 μM. Adapted from Sosulski et al. 2011.

Figure 1.5

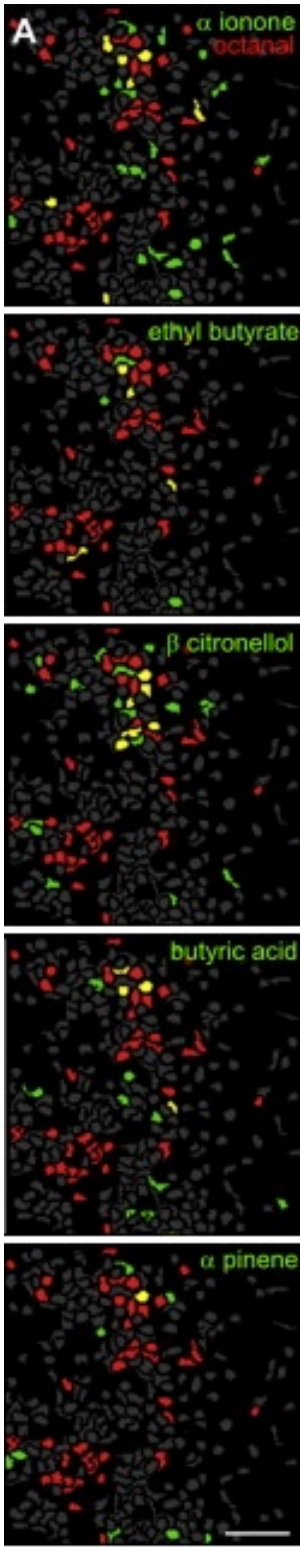
A
α ionone
octanal
ethyl butyrate
β citronellol
butyric acid
α pinene

Figure 1.5. Odor-evoked piriform ensembles are sparse and non-overlapping. Octanal-responsive cells (red) overlayed on the responses to five other odors (green) in the piriform cortex. Cells that respond to both odors are in yellow. Each odor evokes responses in largely non-overlapping ensembles of piriform neurons. Scale = 50 μm. Adapted from Stettler and Axel 2009.

Figure 1.6

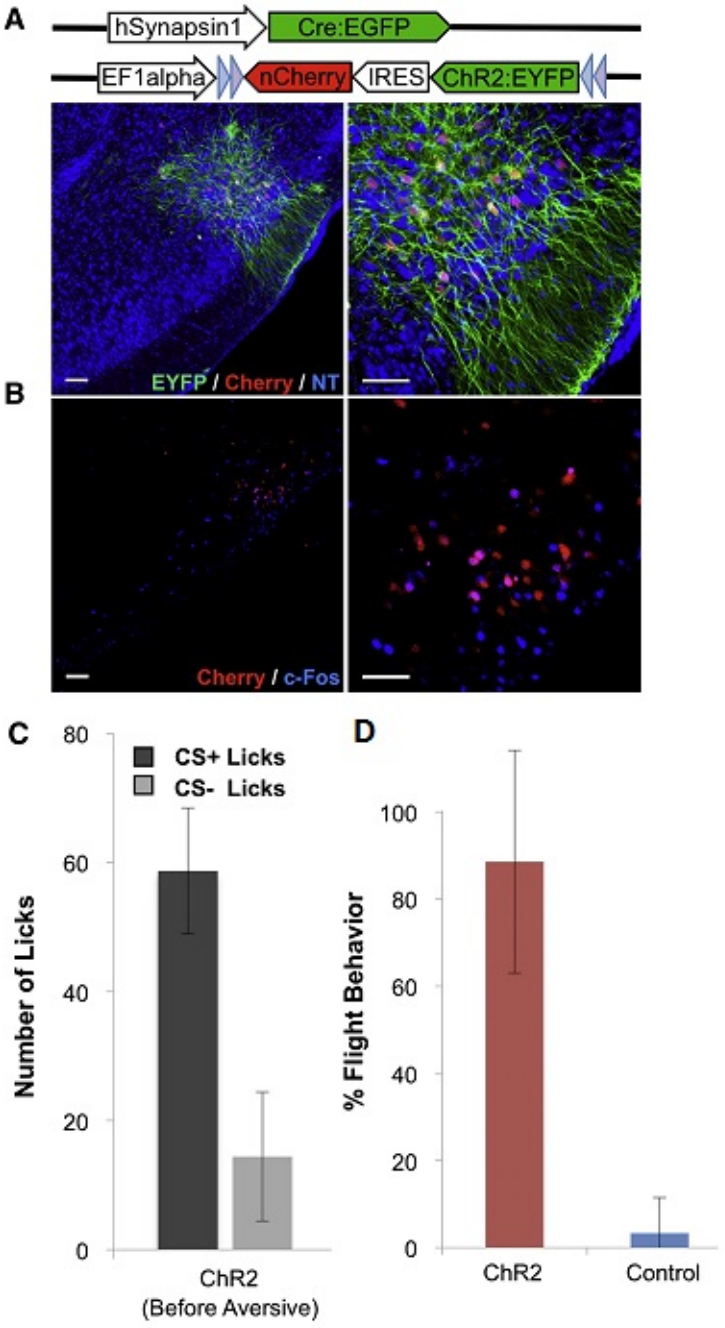
A
hSynapsin1
Cre:EGFP
EF1alpha
nCherry
IRES
ChR2:EYFP
B
EYFP / Cherry / NT
Cherry / c-Fos
C
CS+ Licks
CS- Licks
Number of Licks
80
60
40
20
0
ChR2
(Before Aversive)
D
% Flight Behavior
100
80
60
40
20
0
ChR2
Control

Figure 1.6. Activation of subsets of piriform neurons drives either appetitive or aversive behavior when paired with reward or shock, respectively. A. Lentivirus carrying ChR2:EYFP-IRES-nCherry (nuclear Cherry) flanked by loxP sites and under control of the EF1alpha promoter was coinjected into piriform with a second lentivirus carrying the hSynapsin1 promoter driving Cre:EGFP. This dual virus strategy was used to generate sparse labeling of piriform neurons expressing ChR2. nCherry (red) labels the cell bodies whereas EYFP (green) labels both cell bodies and processes. **B.** 40% of cells (right) expressing ChR2 also expressed c-Fos, a marker of neuronal activity, whereas 5% of cells were positive for c-Fos expression in uninjected controls (left). **C.** Average licks to rewarded odor when reward was paired with ChR2 activation (CS+) versus an unrewarded odor (CS-). **D.** Repeatedly pairing the activation of the same subset of piriform neurons with shock elicits a freezing response after training. Adapted from Choi et al. 2011.

Chapter 2

The Piriform Cortex

2.1 The Piriform Cortex

The piriform is the largest and most well-studied of all cortical areas that receive direct input from the olfactory bulb. Axons from M/T cells terminate in the superficial layer Ia of the piriform, whereas layer Ib contains fibers arising from the extensive recurrent connections that are made between the principal neurons of the piriform (Suzuki and Bekkers 2007). The cell bodies of principal neurons primarily reside in layers 2, and layer 3 is a combination of principal and GABAergic neurons (Protopapas and Bower 2000; Suzuki and Bekkers 2006). Principal neurons of the piriform cortex can be divided into two types, pyramidal and semilunar cells, each presumed to play different roles in the processing of olfactory information (Suzuki and Bekkers 2006). Further beneath layer 3 is the endopiriform cortex, which is populated with multipolar neurons (Bekkers and Suzuki 2013).

Imaging and electrophysiological studies have revealed that piriform odor responses can be either broadly or narrowly tuned to odor and often respond to odors that are molecularly diverse (Zhan and Luo 2010; Stettler and Axel 2009). Moreover, these studies demonstrate that odors evoke activity in sparse, spatially distributed neuron ensembles with no apparent spatial preference (Stettler and Axel 2009; Poo and Isaacson 2009). In addition, global in-

hibitory suppression is observed; neurons responsive to an odor presented by itself may not respond when the same odor is presented as a mixture (Stettler and Axel 2009). Moreover, supralinear enhancement of odor responses is also observed; neurons can respond more to a mixture of odors than would be predicted by the linear sum of the individual odor-evoked activities (Stettler and Axel 2009).

As mentioned in Chapter 1, the piriform mediates learned olfactory behaviors. However, it is open to debate whether changes in neural activity due to learning occur within the piriform, or if responses are preserved and then modified downstream. In support of the the former, olfactory learning appears to potentiate associational inputs from the orbitofrontal cortex onto the piriform, which is likely to alter piriform responses to odor (Cohen et al. 2008). Indeed, several studies have observed that learning drives changes in the odor responses of piriform neurons, particularly in the posterior piriform cortex (Calu et al. 2007; Chen et al. 2011; Roesch et al. 2007). Upon closer examination, however, most of these changes do not appear to be particularly striking. Even in the posterior piriform, changes in firing rates due to learning appears limited to a few spikes per second. Even when such changes were taken to be significant, most piriform neurons in reported studies appear to preserve their odor responses under task learning, especially compared to odor-evoked responses in associative areas such as the orbitofrontal cortex (Roesch et al. 2007).

Therefore, we sought to definitively answer the question of whether odor responses in the piriform are stable during learning. We first established a head-fixed associational learning assay that permitted simultaneous imaging of neural activity during behavior. Our requirements for the task were that it minimizes the number of variables that could potentially be encoded, that it could be learned within several imaging sessions, and that it is not

distressful to the mice as to permit stable imaging without appreciable head motion. For this purpose, we settled on a simple classical odor training paradigm where paired odors (CS+) predicted the onset of reward and other unpaired odors do not (CS-). Mice rapidly learn within 2 to 3 imaging sessions and display robust anticipatory licking to the CS+ odors. Moreover, mice are not distressed during this task and are almost never observed to struggle or head-jerk.

As introduced in Chapter 1, we employ 2-photon endoscopic imaging of calcium activity to track activity in piriform neurons during learning. We demonstrate the majority of piriform neurons do not alter their odor responses significantly during learning. Moreover, we imaged odor responses while passively exposing the same odors to mice over multiple days and found that piriform responses change to a similar degree as if the odors were associated with reward. Therefore, most piriform responses are preserved, and while changes in odor responses do exist, they appear to be unrelated to learning.

2.2 Results

We first asked whether odor representations in the piriform change during learning. Mice were trained in a classical odor discrimination task that permitted simultaneous imaging of neural activity. Mice were given trials of two odors (CS+) that predicted a water reward (US) after a short delay, two unrewarded odors (CS-), and the US by itself. Most mice displayed selective anticipatory licking to CS+ odors in three to four training sessions (10-15 trials of each odor per session) (Figure 2.1A). After learning, almost all mice display anticipatory licking in more than 95% of all CS+ odor trials. The anticipatory lick rate for

both CS+ and CS- odors is shown for all mice with GRIN lens placed in the piriform (n = 5) (Figure 2.1B). The intensity of anticipatory licking varies greatly across mice; while some mice will only lick 3 times before water delivery, others will lick on average 15 times in the 4.5 second period prior to water delivery for the CS+ odors. To monitor neural activity during training, we implanted a microendoscope above the piriform of transgenic GCaMP6S mice (VGLUT2-ires-Cre X rosa-FLEX-GCaMP6S) (Vong et al. 2011; Madisen et al. 2015). In future experiments, we assessed learning rate in the same task with lenses implanted in the OFC and BLA. Learning rate appears to be slightly affected by lens placement in the BLA relative to mice with lenses in piriform and OFC, but this change was not statistically significant ($p > 0.05$, Wilcoxon rank-sum test) (Figure 2.1C).

CS+, CS-, and US responses were imaged before, during, and after learning. Using this approach, we were able to track the neural activity of a population of neurons for over a week of training. A total of 350 neurons in 5 mice were tracked across an average of 4 training sessions. Odor-evoked responses typically are consistent, selective, and start immediate after odor delivery (Figure 2.2, Figure 2.3). On a population level we observe that odors activate sparse, distributed ensembles of piriform neurons characterized by low degrees of overlap with other odor ensembles (Stettler and Axel 2009; Poo and Isaacson 2009; Zhan and Luo 2010; Rennaker et al. 2007). We find that on average, 10% of neurons were active to a given odor prior to learning (Figure 2.6). Also consistent with previous work, we further observe global and non-selective suppression in response to odor delivery (Stettler and Axel 2009; Poo and Isaacson 2009) (Figure 2.4).

When we tracked the odor tuning of piriform neurons across learning, we observe that the majority of odor-evoked responses remained stable across learning. This is clear when

we sort responses by maximum odor-evoked activation before learning and align to responses after learning (Figure 2.5). To quantify this observation, we identified all significant responses to CS+ and CS- odors prior to learning (61 CS+ and 66 CS- responses after pooling both CS+ and CS- odors). We observed that 12/61 CS+ and 10/66 CS- responses decreased within 3-4 days of learning (Figure 2.7A). Conversely, 2/61 CS+ and 2/66 CS- responses that were significant prior to learning increased during learning.

We also assessed whether new odor responses were acquired during learning (Figure 2.7A). A neuron may be unresponsive to all four odors prior to learning and may acquire new responses to each odor during learning. Therefore, for each neuron, we counted each odor response as an independent data point, for a maximum of 2 silent CS+ responses and 2 silent CS- responses per neuron. We had a total of 657 silent CS+ responses and 652 silent CS- responses. We observed that 5% (32/657) of silent CS+ responses and 3.3% (23/652) of silent CS- responses converted to a significant response during learning. In other words, on average, 5% / 2 = 2.5% (1.6%) of neurons acquired a new CS+ (CS-) response.

While this appears to be a small fraction, we note that prior to learning, each odor only activates 10% of all piriform neurons, and therefore these new responses constitute a significant fraction of the odor-evoked ensemble. The net effect of all observed changes, while not being statistically significant ($p > 0.05$, Wilcoxon signed-rank test) increased the average odor ensemble size, from 10% before learning to 12% after learning (Figure 2.6A). This is also reflected by the observation that fewer neurons are unresponsive to odor post-learning (75% before learning to 61% after learning, $p > 0.05$, Wilcoxon signed-rank test) (Figure 2.6B-C). In conclusion, while significant changes in odor representation are observed, the majority of odor responses present prior to learning were retained during

learning.

We quantified the above changes in neural representation by setting a threshold over the level of fluorescence change that must be surpassed for a odor response to be considered as significantly altered during learning. Increasing this threshold decreases the frequency of observed changes, while lowering the threshold increases the rate of change. To show in an unbiased way that the threshold we picked reflects consistency of odor responses in the majority of piriform neurons, we asked whether we could decode odor identity from the population response on the last imaging day when it is trained on responses on the first imaging day, and vice versa. As a positive control, we trained the decoder on a subset of trials from two odors on the same day and confirmed that the decoder accurately classifies the identity of odors from held-out trials (3% error rate for all odor pairs). We then trained a binary linear decoder on a pair of odors on the first day and asked whether responses of the same odors on the last imaging day could be accurately classified. Indeed, the decoder was able to correctly classify odor identity with low error rates (8%, averaged across all odor pairs). We note that the error was higher when decoding the identities of two CS+ odors versus that of two CS- odors (10% versus 5%), which is likely due to more responses being lost and gained for CS+ odors than CS- odors during learning (Figure 2.7A). Therefore, while we have observed significant changes during learning, odor identity for both CS+ and CS- odors was largely preserved.

We next asked whether piriform responses observed before and after learning are predicted by a model where every piriform neuron has an equal probability of being activated by any odor. In this model, if odor A and B each activate a random 10% of piriform neurons, then 10% of the odor A ensemble will overlap with the odor B ensemble, and vice versa. For

the purpose of this analysis, we have excluded a subset of neurons that are non-selectively tuned to odors (3% vs .01%) because their existence is not predicted by a random model and may constitute a different population of neurons that receives input from large numbers of glomeruli (Stettler and Axel 2009). However, even after exclusion of non-selective responders, the level of overlap is still much greater than predicted by chance prior to learning, and also greater than previously reported studies (23% overlap vs 10% by chance, Figure 2.7B). This may be due to the use of odors that activate correlated sets of glomeruli, as such correlations in glomerular activation will also be passed onto the piriform as well (Schaffer et al. 2018).

Decoding analysis suggests that these odor ensembles are more separable post-learning compared to pre-learning (3% error rate pre-learning, 0% error rate post-learning). This decrease in overlap between different odor ensembles must reflect an increase in the degree of odor selectivity of individual neurons. Indeed, we find a larger percentage of neurons are selective to only 1 or 2 odors in the odor panel post-learning (18% before learning, 25% after learning). Therefore, while we observe more odor-responsive neurons post-learning (10% before learning, 12% after learning), we also observe that these ensembles share less overlap (23% to 19%, Figure 2.7B). These results are not what would be predicted from a random model, which predicts an increase in overlap if odor-evoked ensemble size increases. Therefore, while the effects are subtle, it is likely that there are active mechanisms either pre-synaptic to or within the piriform that decorrelate the piriform representations of odors that have been previously experienced. The combined effects of increased recruitment and increased selectivity of responsive neurons serve to enhance the discriminability of different odor ensembles.

Are these changes learning-dependent or simply a by-product of passive odor exposure across multiple days? Responses to both CS+ and CS- odors are altered during learning, and the level of overlap between CS+/CS+, CS-/CS+, and CS-/CS- ensembles appear to either stay the same or decrease slightly during learning 2.7A-B). Therefore, it appears that there is nothing special about the changes that occur in CS+ ensembles, and this lack of privilege suggests to us that the observed changes may largely be explained by repeated odor exposure.

We tested this hypothesis directly by imaging changes in neural representation during passive odor exposure. After mice were trained to perform the olfactory discrimination task, a new set of 4 odors were delivered for each experimental animal without training. Each odor was passively presented to mice for 12-15 trials per training session in a pseudo-random order. All experimental variables remained the same except that the water port was not present and odors were not paired with reward. We found that qualitatively similar changes occurred during passive odor exposure compared to during odor learning. While odor ensemble sizes did not increase (12% to 12%, Figure 2.9.A), piriform neurons became more selective to exposed odors after repeated exposure (Figure 2.9.B,C). More neurons were responsive to 1 or 2 odors out of the 4-odor panel, and fewer neurons were responsive to 3 or all odors out of the 4-odor panel after repeated exposure. This effect also manifested itself when we looked at the level of ensemble overlap between different odor ensembles. On average, odor ensembles shared less overlap after repeated odor exposure, with the percentage of overlapping neurons decreasing from an average of 20% of 10% ($p > 0.05$, Wilcoxon signed-rank test, Figure 2.7.B).

In summary, while we observe significant changes in odor representation within the

piriform during odor learning, we also observe qualitatively similar changes to occur during repeated odor exposure. The bulk of the changes that occur during odor learning are unlikely to be due to supervised or associational learning, but are likely reflective of an unsupervised mechanism that is sensitive to repeated odor exposure. These changes bias the piriform to respond to frequently experienced odors with greater selectivity, which may aid in the learning and discrimination of these odors in circuits downstream of the piriform.

2.3 Discussion

In accord with previous electrophysiological and imaging results, our results reveal that odor representations in the piriform are sparse, distributed, and unique. In agreement with previous reports, odors selectively activate 5-15% of piriform neurons and non-selectively inhibit another significant population (Stettler and Axel 2009; Poo and Isaacson 2009). Similar to previous experiments, we have also observed changes in odor representation during task learning. However, unlike other papers, we argue such changes are not due to learning. Rather, they appear to reflect an unsupervised mechanism that increases the discriminability in the piriform ensembles of experienced odors. Increasing the separability of different odor ensembles may aid in the future assignment of valence in the downstream projections of these ensembles during supervised learning.

We assume in a random model that 1) projections from the bulb to the piriform are random and 2) that odors activate independent and uncorrelated sets of glomeruli. The average overlap that we observe in our imaging studies between any pair of odor ensembles is significantly higher than predicted in this random model (24% compared to 12%), and

also higher than what has been previously described (Poo and Isaacson 2009; Stettler and Axel 2009). The calculation of overlap is highly susceptible to the arbitrary thresholds used to determine significant responses and significant overlap, so it is difficult to compare between studies. Moreover, odors that share high overlap in glomerular activation also shares high overlap in piriform responses (25% overlap). The odors that we selected may activate highly correlated sets of glomeruli and may in turn pass on these correlations upwards into the piriform (Stettler and Axel 2009).

In a random model, only 0.01% (0.1^{th}) of neurons will respond to all 4 odors if odors activate 10% of piriform neurons on average, as has been experimentally observed. However, in previous and current imaging experiments, we observe a small but significant subset of piriform neurons (3%) that respond robustly to all tested odors (Stettler and Axel 2009). Therefore, a model of random connectivity fails to account for the over-representation of non-selectively tuned odors, and we suggest that these neurons may constitute an unique subset of piriform neurons primed to receive inputs from a large collection of glomeruli.

While sparse and random connectivity will generate decorrelated odor ensembles, it does not constrain the sizes of odor-evoked piriform ensembles to be sparse. Without any normalization, the number of odor-evoked piriform neurons will be directly related to the number of active glomerular inputs, and large variances in ensemble size will result in poor classification performance. Indeed, we observe that odor-evoked inhibition is widespread and non-selective in the piriform. Prior work has shown that global inhibition is likely to reflect the fact that local interneurons receive ubiquitous odor-evoked excitation from a high convergence of M/T cells and output local inhibition to surrounding principal cells (Poo and Isaacson 2009). Within this scheme, inhibition will scale with total glomerular activity, and

only the cells that receive the strongest excitation will be driven to spike. Therefore, this inhibition is poised to normalize input activation such that odor-evoked piriform ensembles are constrained to be sparse regardless of the level of input activation.

Unsupervised Learning of Piriform Neurons

Previous work by our lab and others have suggested that the connections from the olfactory bulb to the piriform are sparse (Sosulski et al. 2011). Retrograde tracing studies have estimated that an average of 4 mitral outputs converge onto each piriform neuron, though this is likely to be a severe underestimate given the low efficiency of retrograde transport (Miyamichi et al. 2011).Indeed, a substantially higher estimate of 200 mitral outputs onto each piriform neuron was derived from functional studies that assesses connectivity by measuring piriform responses to glutamate uncaging of loci within the olfactory bulb (Davison and Ehlers 2011). Given that uncaging likely activates more than single glomeruli, and that the efficiency of trans-synaptic retrograde tracing was less than 100%, the true convergence number is likely between these two upper and lower bounds.

Previous work also suggests that the connectivity profile from the bulb to the piriform is random. Random synaptic wiring has been shown to maximize the dimensionality of odor representation in the piriform. This is because correlations between glomerular projections reduces the dimensionality of odor representations, and random wiring prevents such correlations from occurring (Babadi and Sompolinsky 2014; Litwin-Kumar et al. 2017). However, similar odors will activate similar sets of glomeruli, and existing input correlations will nevertheless persist downstream in piriform representations despite having random

connectivity (Schaffer et al. 2018). Therefore, it is difficult to accurately deduce projection patterns based upon the imaging of odor responses, especially without knowing what fraction of the bulb is activated by the odors.

Several previous results have suggested that piriform odor responses are modified as a result of associative learning (Calu et al. 2007; Chen et al. 2011; Roesch et al. 2007). While we observe that a significant fraction of odor-evoked responses were altered during learning, these changes are likely reflective of an unsupervised learning process that serves to decorrelate the odor ensembles of familiar odors. This is because we observe the same changes to occur in the piriform even when odors were passively presented without reward pairing over multiple days of imaging. What mechanism underlies unsupervised pattern separation within the piriform? Prior work has observed that mitral cells within the olfactory bulb also undergo pattern separation (Chu et al. 2016). Moreover, such enhancement of odor-evoked responses occur independent of any active learning process, as passive odor exposure over multiple days also leads to increased separability of distinct odor ensembles. Therefore, it is possible that the increase in discriminability that we have observed in the piriform is relayed by changes in glomerular activity upstream. Moreover, piriform neurons are also intricately connected through a network of recurrent excitatory and inhibitory synapses that may actively shape olfactory representations (Haberly and Price 1978; Johnson et al. 2000). Previous work have found that principal neurons project extensively across the entirety of the piriform to synapse onto other principal neurons and inhibitory cells, and these synapses serve to dynamically boost or inhibit the spiking of other principal neurons in response to glomerular activation (Franks et al. 2011). This study estimates that each piriform neuron may receive inputs from at least 2000 other piriform neurons. Such an

extensive recurrent network may shape the ensembles of odor-responsive neurons in an unsupervised manner during repeated odor exposure.

Multiple groups have shown that activity within the posterior piriform cortex may be critically required for olfactory associative learning, in particular learned olfactory fear (Sacco and Sacchetti 2010, Gore et al., unpublished data). Moreover, the exogenous photo-activation of an arbitrarily chosen ensemble of piriform neurons can be entrained to elicit either appetitive or aversive behavioral responses through temporal pairing with rewards or punishments, respectively (Choi et al. 2011). Therefore, the piriform is both necessary and sufficient for olfactory learning. We have currently shown that the majority of odor-evoked responses in the piriform were preserved during learning, and the changes that do occur are unsupervised in nature and therefore unrelated to associational learning. Therefore, learning must impose changes in neural activity in downstream associative regions. The piriform sends dense projections to multiple associational areas such as the basolateral amygdala, the orbitofrontal cortex (OFC), and the hippocampus. We first imaged learning-dependent changes in the OFC.

Figure 2.1

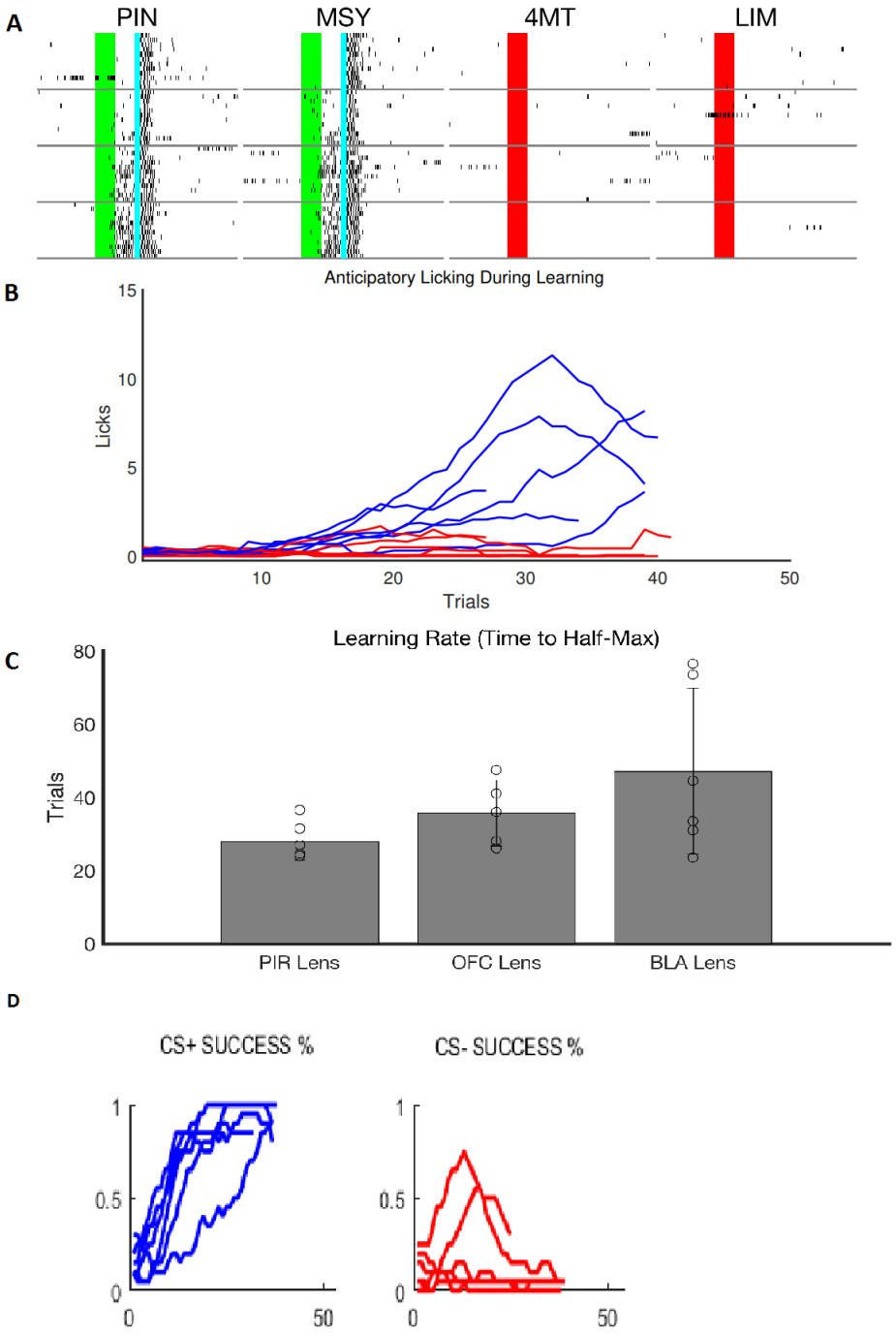
A
PIN
MSY
4MT
LIM
Anticipatory Licking During Learning
B
Licks
Trials
Learning Rate (Time to Half-Max)
C
Trials
PIR Lens
OFC Lens
BLA Lens
D
CS+ SUCCESS %
CS- SUCCESS %

Figure 2.1. Mice Display Robust and Selective Anticipatory Licking to CS+ odors. **A.** Licking responses to two CS+ and two CS- odors across 4 dseparate imaging sessions. Imaging was performed every other day. Days are separated by a gray line. Odor is presented for two seconds during the colored interval, and after a trace period of 2.5 seconds, water is given for CS+ odors while no reward is given for CS- odors. Licking is denoted by a black bar. 12 - 15 trials of each odor was given per day of imaging. This particular mouse learned within two days of training. **B.** Number of anticipatory licks for each mouse (n = 5). Each blue line denotes the number of anticipatory licks to CS+ odors for one mouse, and red denotes average number of licks to CS- odors. Traces were averaged by odors and also averaged across trials in a smoothing window of 5 trials. **C.** Learning rate was quantified using number of trials for anticipatory licking to reach half-maximum. The learning rate for mice with lenses implanted in the piriform, OFC, and BLA was compared. **D.** Percentage of trials with any anticipatory licking for CS+ and CS- odors. Each line the average percentage for two CS+ odors (left) and two CS- (right) odors for each mouse.

Figure 2.2

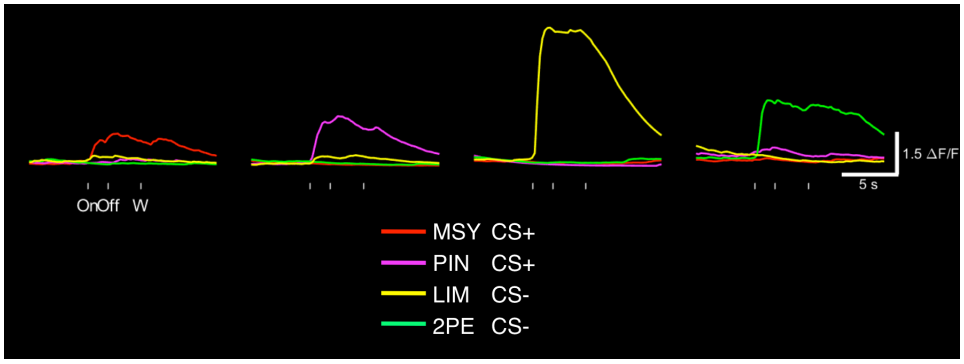

Figure 2.2. Piriform responses to odors are typically robust, selective, and have onsets at odor delivery. Responses of 4 example cells to odors. Each cell is selective to a different odor. MSY, methyl salicylate; PIN, pinene; LIM, limonene; 2PE, 2-phenylethanol.

Figure 2.3

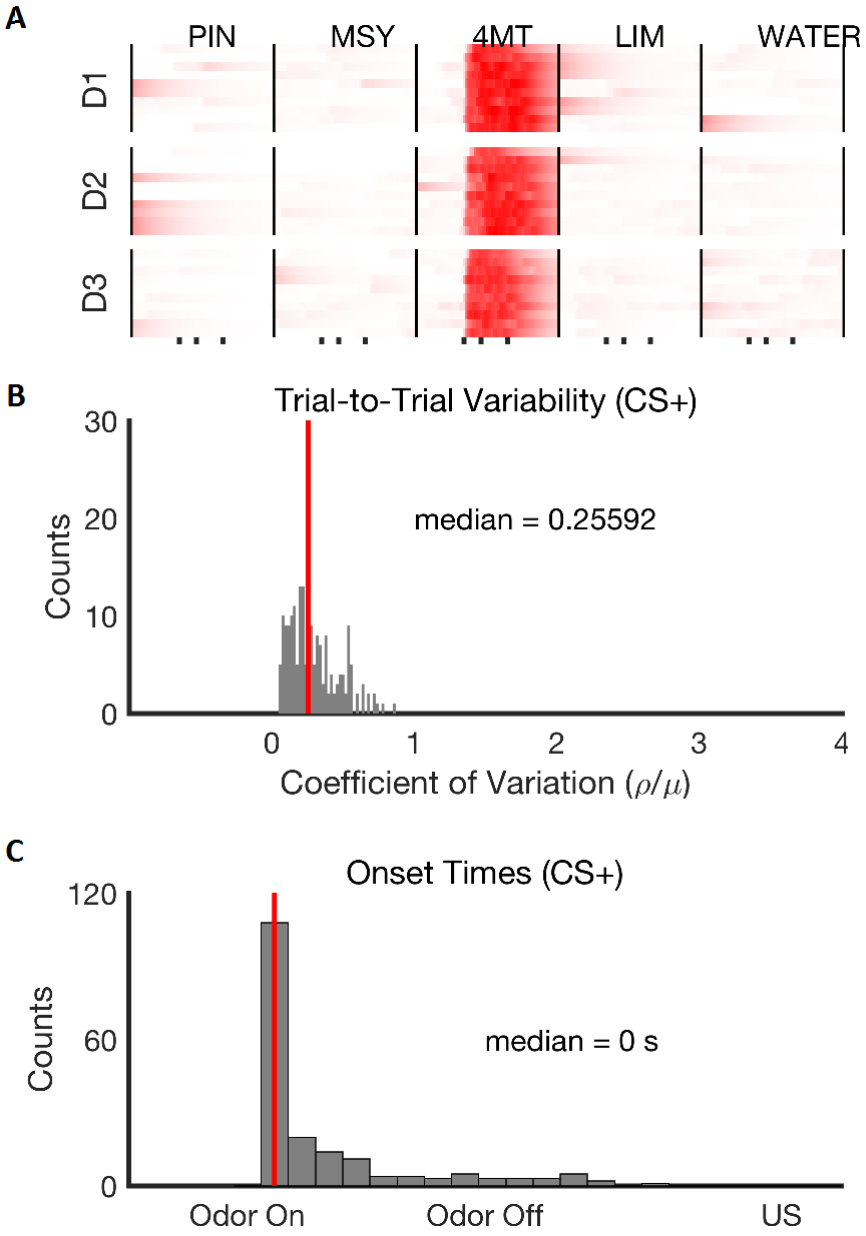
A
PIN
MSY
4MT
LIM
WATER
D1
D2
D3
B
Trial-to-Trial Variability (CS+)
median = 0.25592
Counts
30
20
10
0
0
1
2
3
4
Coefficient of Variation (ρ/μ)
C
Onset Times (CS+)
median = 0 s
Counts
120
60
0
Odor On
Odor Off
US

Figure 2.3. Piriform responses occur at odor onset and are consistent across trials. **A**. Responses to 4MT (4-methylthiazole) in an example piriform neuron for all trials across three days of training. The series of three tick marks on x axis denote odor onset, odor offset, and water onset. PIN and MSY are CS+ odors, 4MT and LIM are CS- odors. Y axis denote different days of imaging. Red denotes a positive DF/F, with saturation at 100% DF/F. **B**. Most odor responses display low trial-to-trial variability. The coefficient of variation (CV) was calculated for each time point between odor on and water on, and the maximum CV during this time was taken as an measurement of variability. CV values are shown for all significant odor responses. **C**. Most odor evoked responses onset immediately at odor-delivery. Only CS+ odors were counted to warrant a fair comparison with OFC and BLA behavior data later on.

Figure 2.4

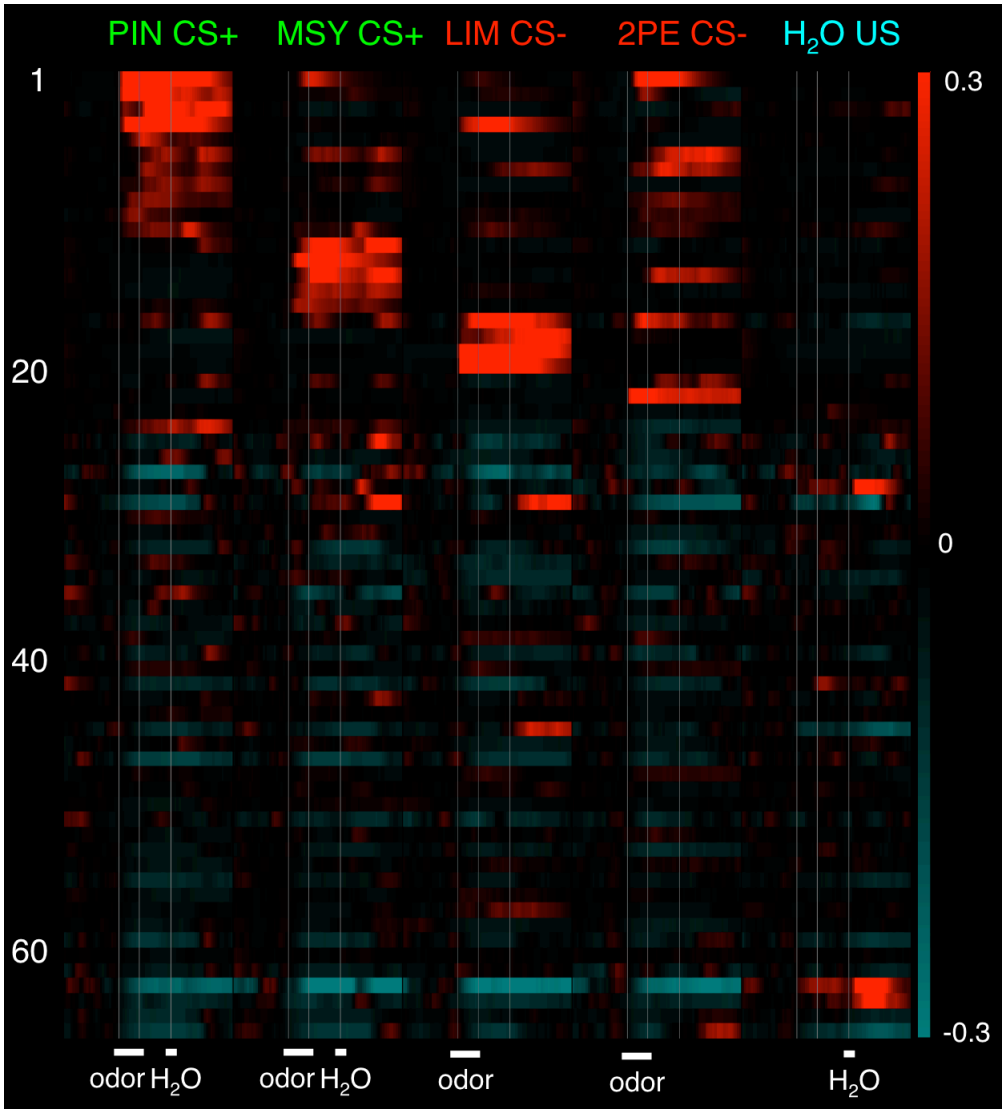
PIN CS+
MSY CS+
LIM CS-
2PE CS-
H2O US
1
20
40
60
0.3
0
-0.3
odor
H2O
odor
H2O
odor
odor
H2O

Figure 2.4. Population PSTH of Piriform Responses to Odors and US. Piriform responses in an example mouse. Each row denotes a single cell's trial-averaged responses to PIN, MSY, LIM, 2PE, and water. Scale bars indicate an increase in DF/F (red) or a decrease in DF/F (blue) relative to baseline. Odor-evoked ensembles of different odors share low overlap. Low activation to US was observed.

Figure 2.5

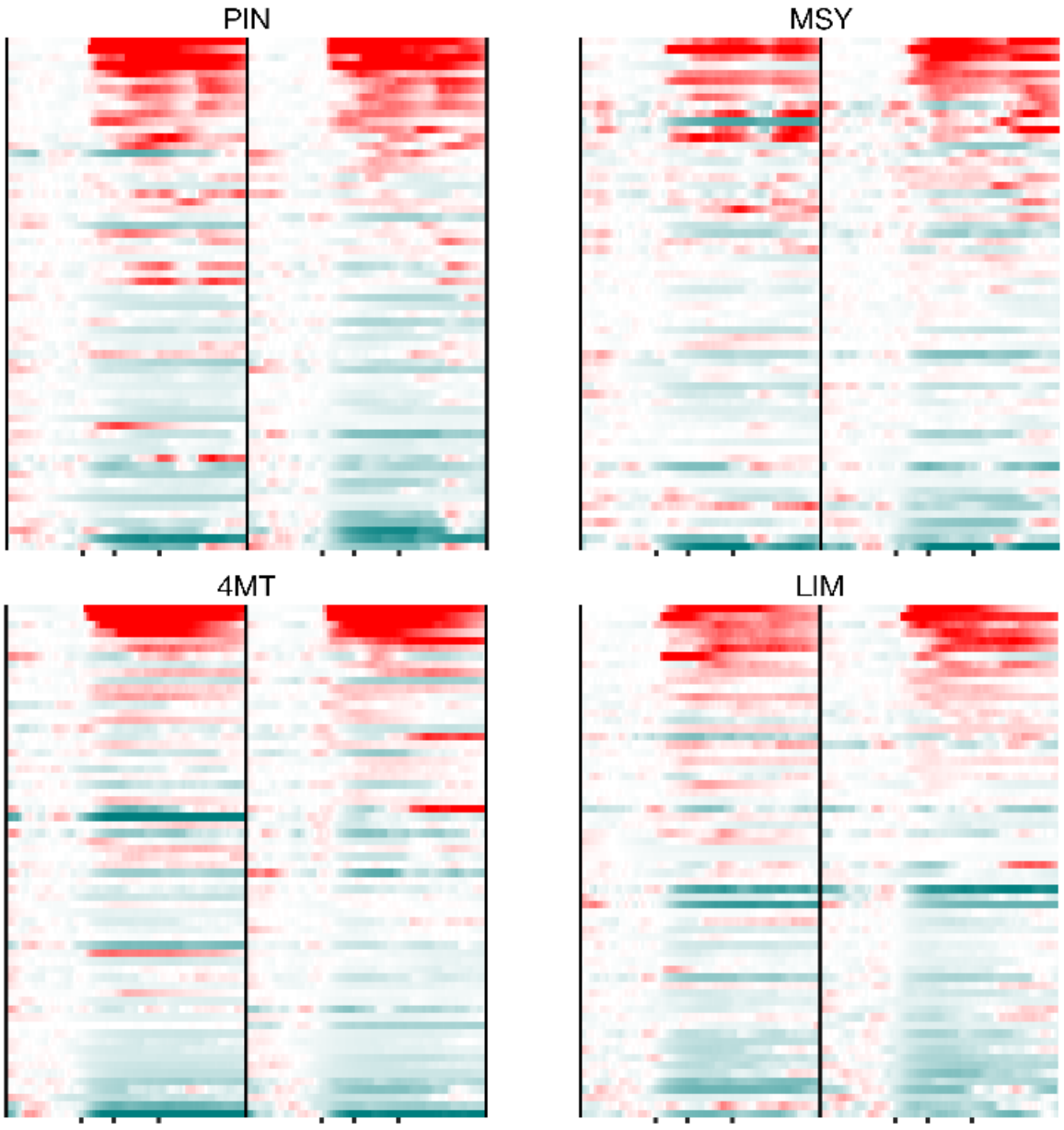

Figure 2.5. Piriform Responses Appear Largely Stable During Learning. A. Odor-evoked responses are shown for before learning (session 1, left side of each pane) and after learning (session 3, right side of each pane) for each odor. Responses are sorted based on maximal odor activation on last training day for each odor, and neurons are aligned across learning. While changes occur, most odor-evoked responses are stable across learning.

Figure 2.6

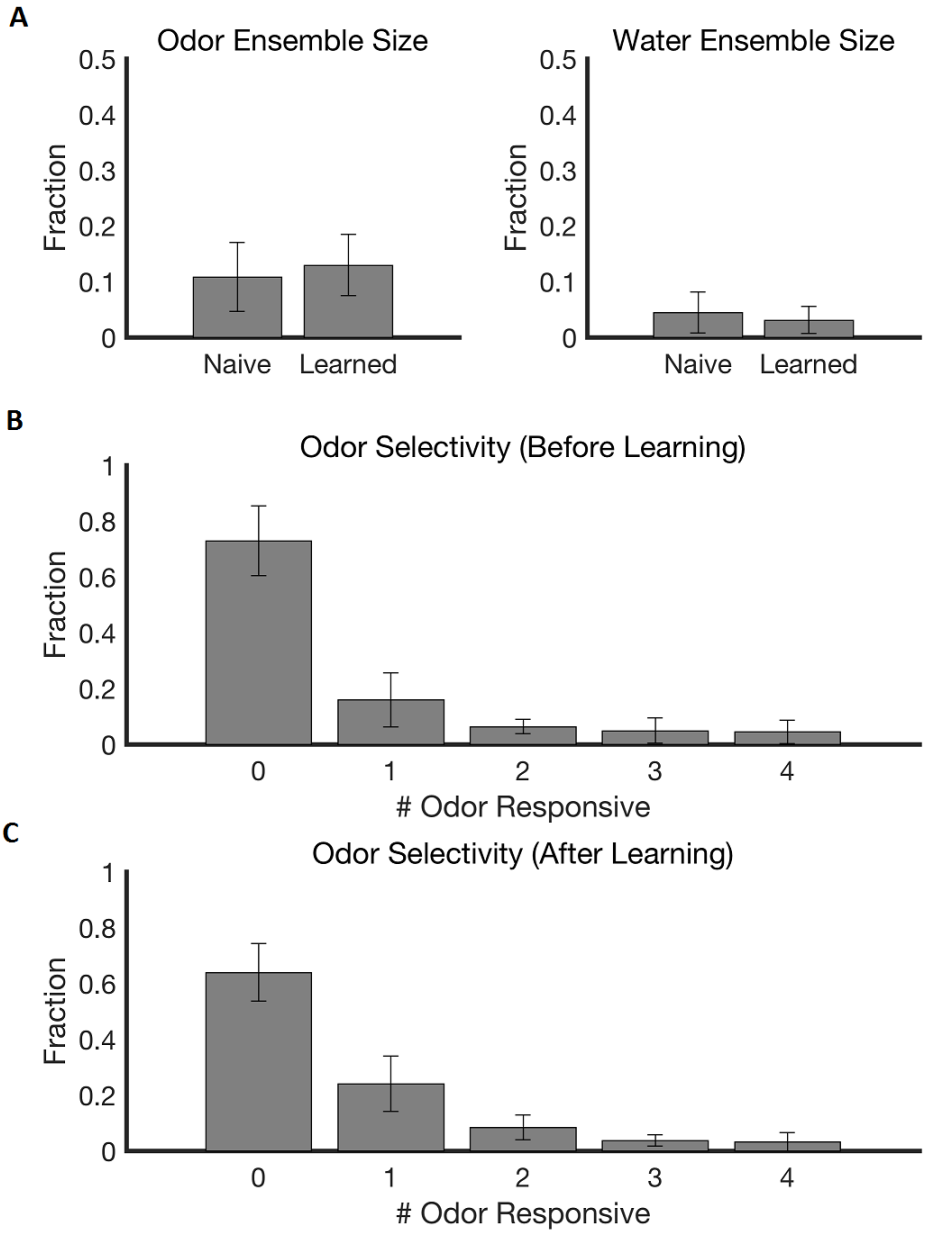
A
Odor Ensemble Size
Fraction
0.5
0.4
0.3
0.2
0.1
0
Naive
Learned
Water Ensemble Size
Fraction
0.5
0.4
0.3
0.2
0.1
0
Naive
Learned
B
Odor Selectivity (Before Learning)
Fraction
1
0.8
0.6
0.4
0.2
0
0
1
2
3
4
Odor Responsive
C
Odor Selectivity (After Learning)
Fraction
1
0.8
0.6
0.4
0.2
0
0
1
2
3
4
Odor Responsive

Figure 2.6. Odor-evoked Ensembles Experience Slight Increases in Size and Selectivity After Learning. **A**. On average, 13% of neurons are activated by a given odor after learning as compared to 11% before learning (left). Minimal response to US is observed either before or after learning (right). **B** and **C**. Fraction of neurons responsive to a given number of odors out of a total of 4 delivered odors. More neurons are response to odors after learning as compared to before learning.

Figure 2.7

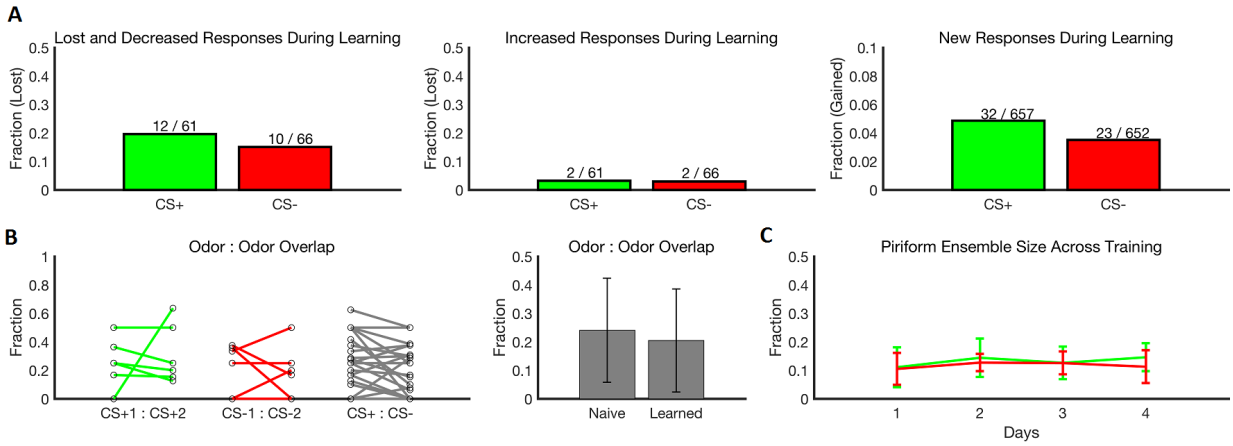
A
Lost and Decreased Responses During Learning
Fraction (Lost)
12 / 61
10 / 66
CS+
CS-
Increased Responses During Learning
Fraction (Lost)
2 / 61
2 / 66
CS+
CS-
New Responses During Learning
Fraction (Gained)
32 / 657
23 / 652
CS+
CS-
B
Odor : Odor Overlap
Fraction
CS+1 : CS+2
CS-1 : CS-2
CS+ : CS-
Odor : Odor Overlap
Fraction
Naive
Learned
C
Piriform Ensemble Size Across Training
Fraction
Days

Figure 2.7. Odor-evoked Ensembles Experience Slight Increases in Size and Selectivity After Learning. A. Left and Middle: fraction of CS+ and CS- responses that significantly decreased (left) or increased (middle) in amplitude during learning. Right: fraction of neurons that acquired new responses to a CS+ or CS- odor during learning **B**. Left: fraction of overlap between ensembles ofping neurons between CS+ odors, CS- odors, and between all CS+ and CS- odor pairs before and after learning. Right: pooled average ensembles of fraction overlaps between pairs of odor ensembles before and after learning **C**. Ensemble size as a function of learning across days. Ensemble size slightly increased duringincreases as a function of learning.

Figure 2.8

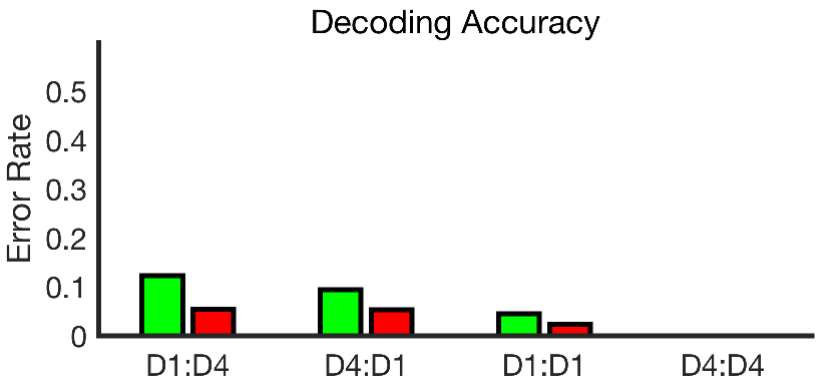
Decoding Accuracy
Error Rate
0.5
0.4
0.3
0.2
0.1
0
D1:D4
D4:D1
D1:D1
D4:D4

Figure 2.8. Odor Identities Can be Decoded from Piriform Neurons Across Many Days of Learning. Green: decoding performance between two CS+ odors (green) or two CS- odors (red). More errors were made in classifying the identities of CS+ odors when trained on pre-learning trials and tested post-learning (D1:D4) and vice versa (D4:D1). Performance became better for all conditions post-learning (D4:D4) compared to pre-learning (D1:D1), suggesting that representations are more separable post-learning.

Figure 2.9

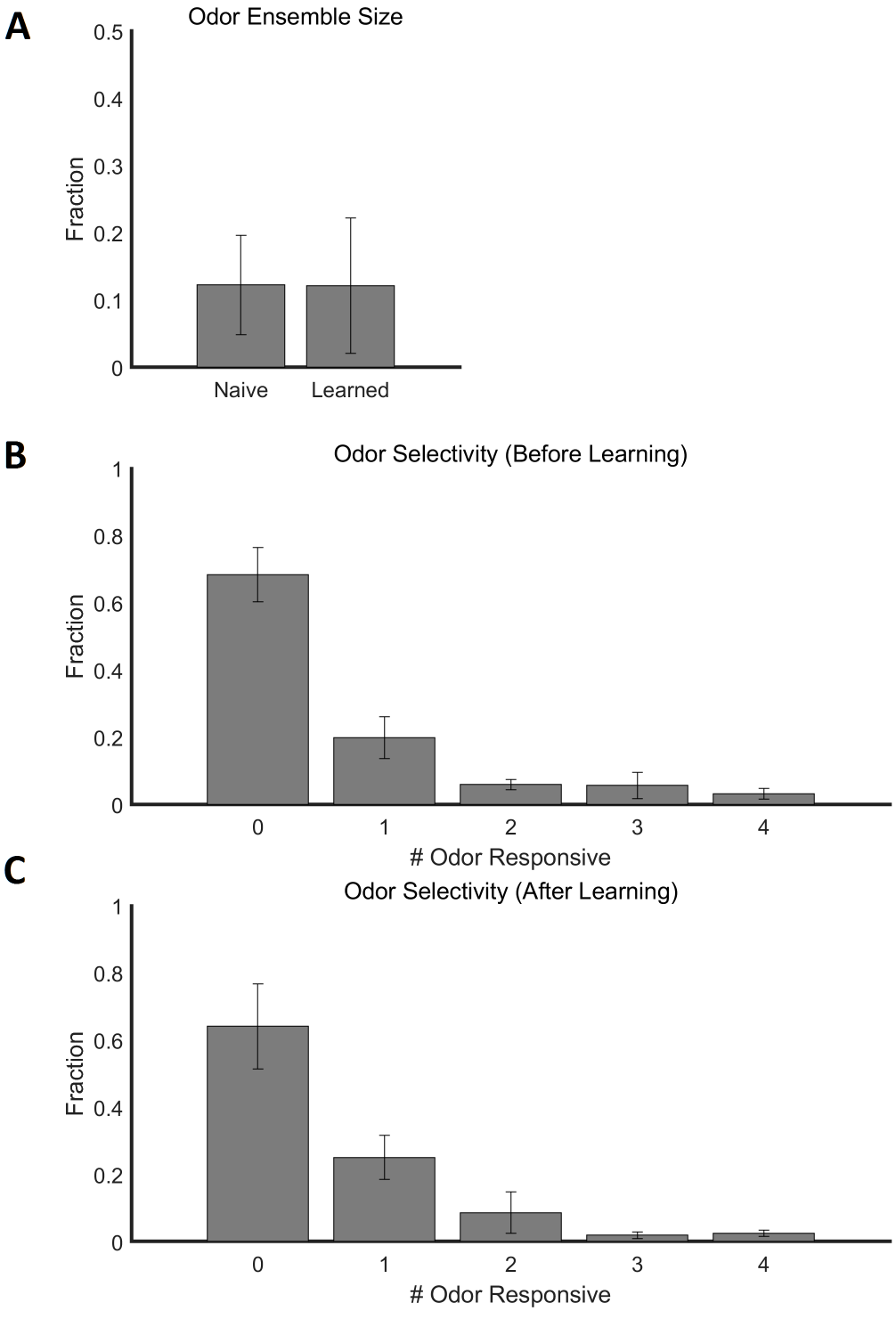
A
Odor Ensemble Size
Fraction
0.5
0.4
0.3
0.2
0.1
0
Naive
Learned
B
Odor Selectivity (Before Learning)
Fraction
1
0.8
0.6
0.4
0.2
0
0
1
2
3
4
Odor Responsive
C
Odor Selectivity (After Learning)
Fraction
1
0.8
0.6
0.4
0.2
0
0
1
2
3
4
Odor Responsive

Figure 2.9. Repeated odor exposure drives similar changes in piriform representations as during odor learning PT1 A. 12% of neurons are activated by a given odor before and after passive odor exposure. **B** and **C**. Fraction of neurons responsive to a given number of odors out of a total of 4 delivered odors. Neurons are slightly more odor selective after repeated odor exposure. More neurons are responsive to 1 or 2 of 4 presented odors as compared to 3 or all of the presented odors after repeated exposure.

Figure 2.10

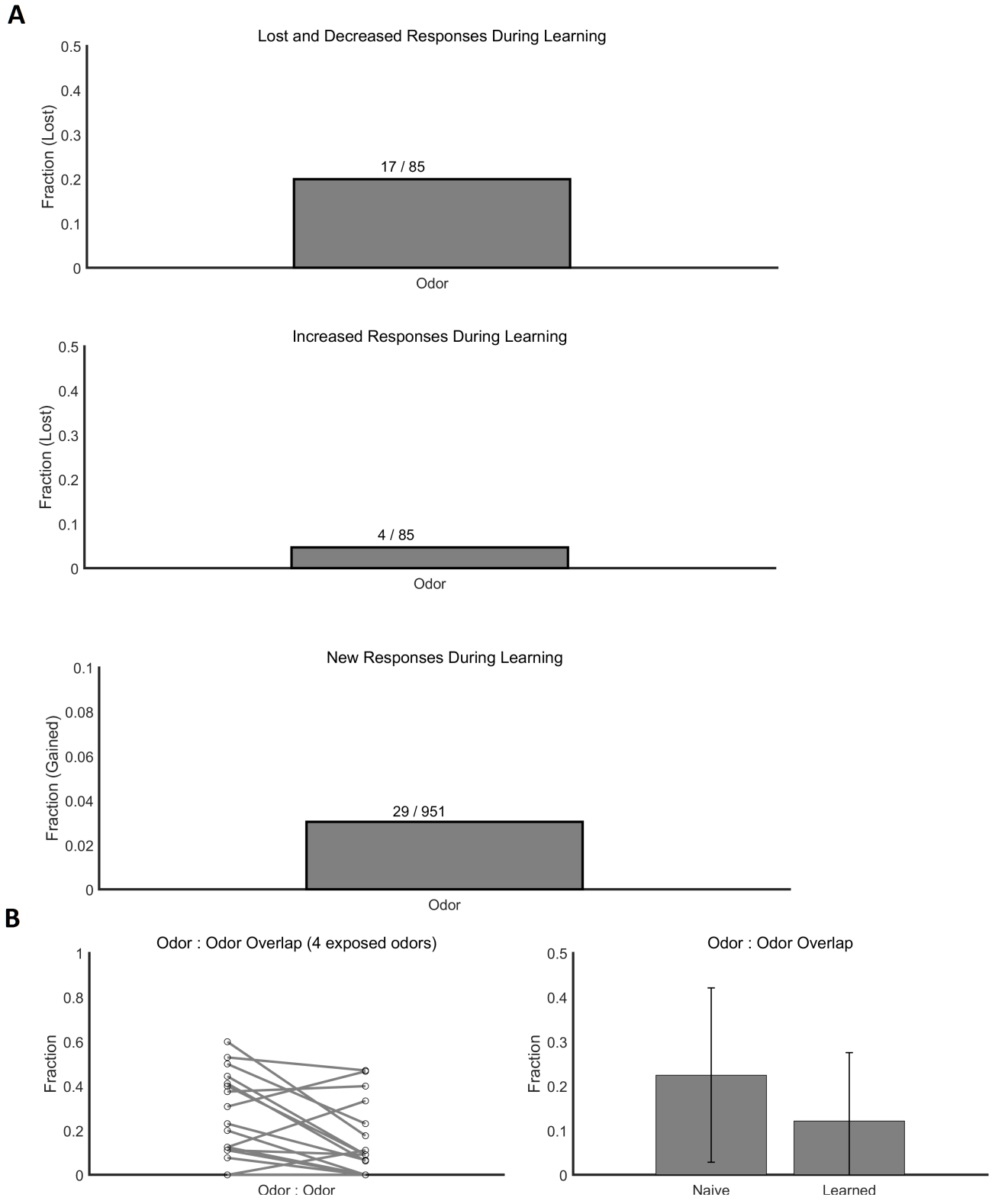
A
Lost and Decreased Responses During Learning
Fraction (Lost)
0.5
0.4
0.3
0.2
0.1
0
17 / 85
Odor
Increased Responses During Learning
Fraction (Lost)
0.5
0.4
0.3
0.2
0.1
0
4 / 85
Odor
New Responses During Learning
Fraction (Gained)
0.1
0.08
0.06
0.04
0.02
0
29 / 951
Odor
B
Odor : Odor Overlap (4 exposed odors)
Fraction
1
0.8
0.6
0.4
0.2
0
Odor : Odor
Odor : Odor Overlap
Fraction
0.5
0.4
0.3
0.2
0.1
0
Naive
Learned

Figure 2.10. Repeated odor exposure drives similar changes in piriform representations as during odor learning PT2 A. Similar fractions of neurons undergone changes during passive odor exposure as compared to odor learning. **B.** Overlap between any two odor ensembles also decreased after repeatedly odor exposure.

Chapter 3

The Orbitofrontal Cortex

3.1 The Orbitofrontal Cortex

The piriform sends both direct and indirect connections onto the OFC. The OFC has been intensely studied over the past 50 years, and many lesion studies have shown that it plays an important role for the learning of cognitively demanding tasks (Stalnaker et al. 2015). However, it has been difficult to distill a cognitive operation that is common to all of the observed behavioral deficits. Moreover, the myriad of neural recording studies in the OFC has shown that virtually any experimental variable can be represented by the firing of its neurons. The lack of consensus on its function has prompted reviews to be written on what it does not do rather than what it does do during learning (Stalnaker et al. 2015). I will start with a concise summary of OFC recording and lesion experiments and then describe a set of experiments that elucidates OFC function.

Anatomy

In rats and other rodents, the agranular parts of the prefrontal cortex is divided into medial orbital (MO), infralimbic (IL), prelimbic (PL), agranular insula (AI), ventrolateral orbital (VLO) and lateral orbital (LO) areas (Figure: 3.1). All orbitofrontal sections (MO, VLO,

LO) receives inputs from all sensory modalities and also from the striatum, amygdala, hippocampus, and other frontal and prefrontal areas amongst other areas. The LO and the VLO, in particular, appears to receive more connections from sensory areas compared to the more medial sections of the orbitofrontal network (Kahnt et al. 2012). The piriform cortex sends direct projections onto the VLO and the LO (Johnson et al. 2000), and indirect projections through the mediodorsal thalamus onto these areas (Groenewegen 1988). In primates, the piriform cortex also projects most densely to the VLO of all prefrontal structures (Morecraft et al. 1992). Given these projection patterns, I will refer to VLO and LO as the OFC for the remainder of this thesis.

OFC Computes Predicted Value

Humans with OFC damage have often led to changes in personality (Galleguillos et al. 2011; Cicerone and Tanenbaum 1997). These changes are also observed in studies of non-human primates, where OFC lesions often result in changes in aggressive behaviors (Butter et al. 1970; Raleigh et al. 1979; Beyer et al. 2014) and in emotional and social processes (Ishai 2007; Perry et al. 2016; Azzi et al. 2012; Izquierdo et al. 2005; Bechara et al. 2000). In addition, other studies have shown that OFC may also play roles both in working and in long-term memory (Frey and Petrides 2002; Meunier et al. 1997; Barbey et al. 2011).

One potential explanation of why the OFC underlies such a multitude of behavioral deficits is that the OFC computes predicted value. All of the tasks mentioned above require the subject to make informed decisions, and the value of each possible action must be computed for the subject to decide on an optimal action in a given state. Therefore,

impairing a system that computes value would cause widespread changes in the ability to make appropriate decisions in social, emotional, and cognitive tasks.

The theory that OFC encodes value is rooted in early primate OFC recordings (Padoa-Schioppa and Assad 2006; Tremblay and Schultz 1999). In these papers, the OFC was found to encode a general value representation that is independent of the sensory or motor features of the cue. This finding has been supported by a number of studies in rodents, monkeys, and humans (Thorpe et al. 1983; Gottfried et al. 2003; Schoenbaum et al. 1998). For example, in one study (Padoa-Schioppa and Assad 2006), OFC activity was recorded in monkeys while they chose between two different juice rewards. Visual cues conveyed the amount of juice that was offered to the monkey, and the monkey is able to choose which of the two options it preferred. The authors found that activity in a subset of OFC neurons encoded the value of the chosen juice regardless of the juice being chosen. In other studies, OFC activity was recorded when reward contingencies were switched such that a previously unrewarded cue (CS-) became rewarded, and a previously rewarded cue (CS+) became unrewarded (Thorpe et al. 1983; Roesch et al. 2007). During reversal learning, a significant percentage of OFC neurons was found to track reward outcome and not the sensory features of the cue itself. Moreover, internal state such as hunger and satiety modulates the responses of most OFC neurons to sensory cues predicting a food reward (Critchley and Rolls 1996). Based on these studies, the OFC indeed appears to create an abstraction of value that is appropriately sensitive to changes in outcome, context, and internal state.

The results of such electrophysiological studies suggest that OFC may play a crucial role during associative learning. Indeed, OFC lesions have generated behavioral deficits that are subtle and complex in a variety of cognitive learning tasks. Perhaps the most well-studied

has been reversal learning (Schoenbaum et al. 2002; Jones and Mishkin 1972; Meunier et al. 1997; Chudasama and Robbins 2003). If the computation of value is disrupted, subjects will be unable to update the value of new cue-outcome associations and therefore will be impaired in reversal learning. Indeed, OFC-lesioned animals take a significantly longer amount of time to outcome reversal (Schoenbaum et al. 2002; Chudasama and Robbins 2003; Izquierdo et al. 2004).

Moreover, OFC lesions also impair performance in delayed alternation tasks. In this task, subjects make a decision to choose between two cues. The cue that predicts reward alternates between different trials. Therefore, if subjects were unable to learn that alternation was the optimal strategy, they would not be able to receive reward in this task. Indeed, while control animals learn this task with ease, monkeys with OFC lesions fail to perform better than chance even after prolonged training (Mishkin and Manning 1978).

Lastly, OFC also affects performance in reinforcer devaluation tasks. In these tasks, animals first learn to associate a cue with a reward. The reward is then devalued outside the conditioning context by pairing the consumption of the outcome with a bitter substance for instance. After reward devaluation, cue presentation to a normal subject results in a decrease in relative preference to the devalued reward. However, OFC-lesioned subjects respond with equal vigor to cues both before and after reward devaluation, suggesting that was a failure to update the value of the cue during devaluation (Gallagher et al. 1999; Pickens et al. 2003; Izquierdo et al. 2004).

Caveats and Alternative Hypothesis

While the results of many electrophysiological and lesion studies support OFC's role in computing value, there are many important subtleties and caveats. For instance, while many studies have observed a reversal learning deficit from lesioning the OFC, the deficit only appears during the first reversal but not during subsequent reversals (Schoenbaum et al. 2002; Boulougouris et al. 2007). Moreover, in delayed alternation tasks, it appears that lesioning the OFC only influences task performance if a delay was introduced, suggesting that the OFC lesion does not impair value learning but rather the formation of working memory (Miller and Orbach 1972). Finally, probably the most glaring critique against OFC's role of computing value is that OFC-lesioned subjects are not impaired during initial value acquisition (Chudasama et al. 2007; Izquierdo et al. 2004; West et al. 2011). In these experiments, while the OFC was necessary for reversal learning, OFC lesions had no effect on initial discrimination learning; while the OFC was necessary for behavioral changes after devaluation, OFC lesions had no effect during simple associative conditioning. Therefore, in every classic paradigm, there are subtle but important caveats against the interpretation of OFC encoding general value.

The electrophysiological data is also nuanced. While there are certainly a significant subset of OFC neurons that track value, this subset of neurons appear to exist among a much more diverse population tuned for a variety of other variables. In rodent and primate studies, OFC neurons are found to be tuned to features such as stimulus identity, stimulus match-nonmatch comparisons, and stimulus location (Schoenbaum and Eichenbaum 1995; Ramus and Eichenbaum 2000; Lipton et al. 1999). OFC neurons also display a working

memory component and are influenced by prior contextual cues and whether rewards were given on preceding trials (Simmons and Richmond 2008; Saez et al. 2015). Moreover, while subsets of neurons appear to encode general value, many others are tuned to outcome identity and outcome location (Lipton et al. 1999; Padoa-Schioppa and Assad 2006; Feierstein et al. 2006). Some studies have also revealed that OFC even encodes motor responses in goal-directed learning tasks (Feierstein et al. 2006; Roesch et al. 2006) and confidence signals (Lak et al. 2014; Kepecs et al. 2008). Moreover, selectivity to one variable does not appear to predict responses to other variables, suggesting that OFC neurons exhibit mixed selectivity to any combination of task-relevant variables (Kennerley et al. 2011).

In summary, OFC neurons appears to be tuned not just to value but to a mixture of all relevant task variables. Moreover, the hypothesis that OFC computes value does not appear to account for all the subtleties apparent in many lesion studies. One alternative hypothesis of OFC function that attempts to take into account the complexity of recording and behavior data is that the OFC encodes task state. State, as defined in reinforcement learning, is a position in an abstract task map (Wilson et al. 2014). The complexity of the state representation depends upon the complexity of the task. In a classical conditioning task in which a single odor predicts reward, the states are as simple as ”odor present” or ”odor not present”. However, if a task is complex and requires working memory, such as the identity of cues presented on previous trials, then the state representation would encapsulate all such factors relevant towards the obtainment of reward, with the predicted value of a sensory stimulus being one of many contributing factors. Therefore, this theory offers an explanation of why the encoding of all relevant task variables appears within the OFC. However, the notion of state is abstract and difficult to define operationally, and it

offers little testable hypothesis or constraints on how task variables should be encoded to generate a representation of state.

Aim

Progress in elucidating OFC function has been limited by several factors. A potential source of confusion in almost all primate electrophysiology and lesion studies is that experimental subjects have already been well-trained on the current task prior to recording and lesion (for example, Thorpe et al. 1983; Mishkin and Manning 1978; Meunier et al. 1997). In particular, given the expensive nature of using monkeys as a model species, almost all experimental subjects have also been trained and tested on prior related tasks. Therefore, behavioral data extracted from lesion studies may be confounded by past learning in similar tasks, and recording data may also not only reflect current task variables, but also what the subject has previously learned. Similarly, in freely moving rodent studies, subjects are ”pre-trained” to be familiar with the task structure prior to recordings and prior to the assessment of deficits due to OFC lesion (for example, Schoenbaum and Eichenbaum 1995; Schoenbaum et al. 1998; Schoenbaum et al. 2002). The idea that different brain areas are responsible during different phases of learning has steadily gained experimental support (Jin et al. 2016; Roy et al. 2017; Kitamura et al. 2017). Therefore, if the OFC plays a crucial role during the acquisition phase of learning, this deficit would not be revealed by prior experiments that assess OFC function after animals have successfully acquired the task structure during pre-training. Therefore, OFC function should be assayed both during early and late phases of learning.

Understanding what OFC encodes is also severely limited by a lack of tools that allows for neural activity to be tracked in population of neurons during learning. In previous studies, it is unclear if responses to sensory cues, motor actions, working memory, and outcome were present prior to learning or if they were acquired during task learning. Therefore, tracking neural activity across time may distill the important variables that are potentiated during learning from background noise present throughout the entire task.

We sought out to understand what the OFC encodes by first tracking its neural activity during learning. We employed the same head-fixed, appetitive olfactory learning task as described in Chapter 2 and again used 2-photon endoscopic imaging to track activity in populations of OFC neurons. Imaging experiments reveal that odor representations in the OFC prior to learning are sparse and non-selective. However, after training over 30% of OFC neurons acquire robust responses to conditioned odors (CS+). Moreover, multiple and distinct CS+ odors activate the same population of OFC neurons. Furthermore, these responses are gated by context and internal state. We then explicitly asked whether piriform activity is sufficient to drive CS+ responses in the OFC by activating a random subset of piriform neurons that has been decorated with a red-shifted channelrhodopsin (ChrimsonR) while simultaneously imaging OFC activity (Klapoetke et al. 2014). We found that laser activation of this ensemble drove potentiated responses in the same set of OFC neurons as those activated by CS+ odors. Therefore, our data suggests that the representation of odor identity in the piriform is transformed by the convergence of sensory and cognitive information to create representations of predicted value in the OFC.

We then examined the functional role of the OFC in associative learning tasks. We divided our appetitive learning task into two epochs: pre-training, during which mice learn

that a single odor predicts water, and discrimination training, during which mice learn to distinguish between novel CS+ and CS- odors. Optogenetic silencing of OFC during pre-training results in a significant impairment in the learning of simple odor associations, whereas silencing of OFC during discrimination does not impair the learning of new associations. Imaging during these two epochs of the task reveals that the representation of the pre-training odor begins to decay when the animal has learned the appetitive task, and new CS+ odors are not represented as robustly during discrimination. Therefore, these results suggest that the OFC is necessary for task acquisition, but subsequent discrimination must be accommodated by other brain regions.

3.2 Results

OFC Discards Sensory Identity to Encode Predicted Value

As detailed in Chapter 1, we again implanted microendoscopes above the OFC of transgenic GCaMP6S mice (VGLUT2-ires-Cre X rosa-FLEX-GCaMP6S) and imaged population responses during the same head-fixed olfactory appetitive learning task (Vong et al. 2011; Madisen et al. 2015). We were able to track an average of 70 OFC neurons per animal across multiple training days, sometimes up to 15 days. CS+, CS-, and US responses were imaged before, during, and after learning.

Prior to learning, 15-20% of neurons were responsive to any given odor (Figure 3.2.A). However, these responses were unlike those observed in the piriform cortex. Whereas odors evoked piriform responses that were selective, consistent and high in amplitude, naive odor

responses in the OFC were inconsistent, low in amplitude, and non-selective to all odors. As a consequence, a binary linear decoder trained to decode odor identity in the OFC performed at near chance level for all pairs of odors, suggesting that odor identity is represented far weaker in the OFC than in the piriform (Figure 3.3.A). OFC neurons were responsive to the unconditioned stimulus, as water evoked significant excitation in 25% of imaged neurons (Figure 3.5.B).

Odor-evoked responses in the OFC dramatically changed as a result of learning. During the course of training, responses to CS+ odors gradually potentiated, and after mice have fully learned to lick in anticipation to CS+ odors in greater than 90% of trials, this potentiation matured into robust and consistent responses in 35% of OFC neurons (Figure 3.4, 3.2.B, 3.5.A). In contrast, there was little to no change in the activity to CS- odors during learning (Figure 3.5.A).

A defining feature of this representation is that most neurons exhibit identical or extremely similar responses to different CS+ odors in terms of onset, amplitude, and duration (Figure 3.4, 3.2.B). To quantify this observation, we first thresholded statistically significant responses and observed that the two CS+ odor ensembles shared high (70%, see Methods for overlap quantification) overlap after learning (Figure 3.6.A). However, the level of overlap is not near 100%, and this could suggest that either a low but significant proportion of CS+ responsive neurons encode the identities of distinct CS+ neurons, or that neurons classified as responsive to 1 CS+ odor are noisy and unreliable. If the former were true, then a linear decoder could use this population of identity-encoding neurons to decode the identities of the two CS+ odors. We trained a linear decoder on a subset of CS+1 and CS+2 odor trials, and found that odor identities of CS+ odors could not be reliably decoded when

tested on held-out trials (30% error rate) (Figure 3.3.B). Therefore, neurons that were classified as responsive to only one of two CS+ odors had weak and unreliable responses to that odor and thus did not aid in the decoding of odor identity. In addition, we also found that the identities of the CS- odors could not be decoded either before or after learning (Figure 3.3.B). Therefore, we conclude that the OFC does not encode sensory identity. The decoder could only accurate decode the identities between a CS+ odor and a CS- odor after learning, suggesting that the only quantity that is encoded within the OFC is predicted value (Figure 3.3.B).

Moreover, CS+ responses were temporally heterogeneous and had different waveforms, durations, and onset times (Figure 3.4, 3.2.B). In particular, we observe that less than half of all CS+ responses occur immediately at odor onset, and the rest tile the duration between odor onset and water onset (Figure 3.7.A). The diversity of temporal dynamics suggest that the OFC may be encoding time-sensitive events. However, if the underlying variability in the response dynamics to CS+ odors is very high, then downstream areas cannot decode it from OFC activity. Indeed, the OFC exhibits greater trial-to-trial variability than piriform responses (Figure 3.7.B). Preliminary analysis reveals that the OFC can indeed decode time better than other imaged brain regions that do not exhibit onset tiling, such as the BLA (analysis not shown).

Is having a US response predictive of the acquisition of a CS+ response during learning? In a simple model, the co-activation of sensory and US inputs will strengthen the connection weights of sensory inputs in a way that is suggestive of Hebbian learning(LeDoux 2000). Therefore, we would observe that US-responsive neurons would acquire CS+ responses, and neurons that are unresponsive to US will not acquire CS+ responses. We observe that

while it is more likely for a US-responsive neuron to acquire a CS+ response during learning as compared to chance, it does not occur with certainty (60% US responsive neurons acquire CS+ responses vs 35% from a random shuffling of CS+ and US responses) (Figure 3.6.B). Moreover, the number of US-responsive neurons is less than the number of CS+ responsive neurons (25% US-responsive vs 35% CS+ responsive), implying that many CS+ responsive responses were acquired by neurons that were unresponsive to the US (40% of CS+ neurons are US-responsive). Therefore the majority of CS+ responsive neurons were not US responsive (Figure 3.6.B). These results suggest that that CS+ responses in the OFC potentiate through mechanisms that cannot be explained by a simple Hebbian model.

We further assessed the consistency of odor-evoked responses across different days after mice have fully learned the task. We tracked neural activity across days and analyzed overlap in the CS+ responsive populations on consecutive imaging days. We found that 65% of OFC responses to CS+ were retained across consecutive imaging days, which is a lower fraction when compared to piriform responses across days (Figure 3.8). This lower consistency can be attributed to the observation that a significant proportion of CS+ responses decay after learning performance plateaus, a statistic that we will analyze in depth later on. Both CS- and US responses were less consistent compared to CS+ responses across days (40% for CS-, 40% for US). Therefore, responses to CS+ were the only responses that were consistently maintained across days.

Prior literature has also suggested that the OFC encodes motor action (Feierstein et al. 2006; Roesch et al. 2006). However, several lines of evidence suggest that there is minimal encoding of motor action within OFC activity in our appetitive conditioning task. First, if OFC neurons drive or encode motor action, neural activity should have a close

correlation with licking events. If strong responses are observed within CS+ trials, they should also be present during US-only trials since mice are licking for water in mice trial conditions. However, the majority of neurons (60%) that respond significantly to the CS+ do not respond to the US in US-only trials (Figure 3.2.B, 3.6.A). Second, if motor action was encoded in the OFC, population activity in trials where mice fail to display anticipatory licking to CS+ odors after learning should be similar to trials where mice withheld licking in CS- odor trials. However, non-lick CS+ odor trials were nearly always categorized as lick CS+ odor trials (26/30) rather than non-lick CS- odor trials, suggesting that the OFC encodes predicted value after learning irrespective of motor action (Figure 3.9). Finally, in a preliminary experiment, we entrained mice to lick left or to lick right in response to specific odors. We found that the representations of odors were similar between the odor signaling lick-left and the other signaling lick-right. All of these results suggest that motor action is unlikely to be encoded in the OFC.

OFC is Sensitive to Internal State, External Context, and Changes in Outcome

We have shown so far that the OFC responses discard sensory identity and appear to encode the value of the CS+ cues during task learning. If the OFC indeed encodes expected value of the odor stimuli, neural responses to odors should change when the value predicted by a learned odor also changes. We thus tested the hypothesis of value encoding by imaging OFC activity when the values of CS+ and CS- cues reverse during reversal learning. Mice were first trained on the same odor discrimination task, and once learned, cue reward con-

tingencies were reversed. During reversal learning, mice suppress anticipatory licking to the 'old' CS+ odors and learn to display anticipatory licking to the 'new' CS+ odors. Mice rapidly learn to reversal their behavioral responses, as both extinction and new licking take an average of 2 days or 30 trials of odor delivery per odor to for mice to complete.

Consistent with value encoding, the majority of neurons lost responses to the old CS+ and acquired responses to the new CS+ odors (Figure 3.10.A). We define odors A and B to be the old CS+ (or new CS-) odors, and odors C and D to be the old CS- (or new CS+) odors. We note that after reversal, responses to A and B did not fully subside but were significantly weaker in amplitude than responses to C and D. Therefore, counting responsive neurons by using only statistical significance without factoring in response amplitude would severely exaggerate the number of responses to AB after reversal. To use a metric that reflected the changes we observed, we counted neurons that not only had statistically significant responses, but also had a DF/F that was higher to AB than CD, and vice versa. Using this metric, we observe that most CS+ responsive neurons (55%) fully reversed their representation during reversal learning, or in other words, they have lost responses to AB and have gained responses to CD. The rest underwent partial reversal; 30% of neurons gained a response to CD during reversal when previously unresponsive to AB, and a final 15% lost responses to AB during reversal and did not gain responses to CD (Figure 3.10.C). On a population level, while 30% of neurons respond to AB more than CD after discrimination training, only 5% do so after reversal training. Conversely, while only 5% of neurons respond to CD after discrimination learning, 30% do so after reversal learning (Figure 3.10.B). Therefore, taken together, these results suggest that OFC responses adapt to changes in expected value.

We further manipulated the expected value of the CS odors by first satiating mice with water after they have learned discrimination training. Prior experiments have shown that significant subsets of OFC responses are modulated by state (Critchley and Rolls 1996). We first imaged OFC responses to odors when mice are well-trained and then sated them by delivering on average 2 mL of water in 10 minutes. After satiation, mice neither display anticipatory licking to odors nor do they collect the water once it is delivered, and we imaged OFC responses to odors during this period. We found that CS+ responses either completely vanish or were significantly attenuated after satiation (Figure 3.11.A). To quantify this change, we compared the evoked responses of all CS+ responsive neurons pre- and post-satiation, and observed a nearly complete suppression of CS+ responses (Figure 3.11.A). We also manipulated expected value by removing the water port after the mice have successfully completed discrimination learning. Upon removal of the water port, video recordings reveal that mice suppress anticipatory licking to the CS+ odors within 2-3 odor presentations (Figure 3.11.B). Similar to satiation, CS+ responses of nearly all OFC neurons either completely vanished or were significantly attenuated after water port removal (Figure 3.11.B).

In summary, during the manipulation of internal state, context, and changes in outcome, we did not observe subsets of OFC neurons encoding other factors such as sensory identity, motor actions or other task parameters. Instead, we found that nearly all OFC neurons updated their responses in a way that is consistent with a representation of expected value.

Entrainment of Piriform Neurons is Sufficient to Evoke CS+ Representation in OFC

We then asked whether the piriform alone is sufficient to drive value responses in the OFC by assessing whether entrainment of a random piriform ensemble drives potentiated CS+ responses in the same set of OFC neurons as odor entrainment. This was done in one mouse as a proof-of-concept experiment. We used an AAV virus to decorate a random piriform ensemble with a red-shifted rhodopsin (ReachR) whose activation wavelength is non-overlapping to the excitation and emission spectra of GCaMP6 (ChrimsonR-TdTomato) (Lin et al. 2013). We then paired the light activation of the ChrimsonR-expressing piriform ensemble with water reward while simultaneously imaging the evoked representation in the OFC during behavioral training. These laser-paired trials were alternated with CS+ odor and CS- odor trials. Mice, on average, took 2-3 times longer to learn to lick in response to light as compared to odor (80 trials for laser vs 25 trials for odor). However, once learned, the CS+ representation to laser was nearly identical to that evoked by CS+ odors (Figure 3.12). This experiment demonstrates that odor activation in the piriform is sufficient to drive the CS+ responses observed in the OFC, delineating a circuit whereby sensory identity in the piriform is transformed by the convergence of sensory and cognitive information to create a representation of expected value of the CS cues in the OFC.

OFC Is Necessary for Acquisition but not Expression of Learning

We have so far shown that the OFC encodes expected value and is sensitive to internal state, external context, and updates in outcome. However, does this representation of value

play a role during associative learning? To test this, we bilaterally silenced the OFC during discrimination learning using a red-shifted halorhodopsin, Jaws (Chuong et al. 2014). We chose Jaws because it provides an activation wavelength that is non-overlapping to the excitation and emission spectra of GCaMP6s, and therefore can allow simultaneous calcium imaging and optogenetic perturbation. Reliable inhibition was observed in >85% neurons using a 32-channel extracellular optrode array with an activation wavelength towards the tail end of Jaws' excitation spectrum (660 nm light, 10 mW output at fiber end) (Figure 3.13). A lens was also inserted on top of the BLA in these mice for simultaneous imaging, the results of which we will discuss in later chapters.

In this experiment, the induction of laser activation flanked odor delivery and water delivery, turning on 2 seconds prior to odor and turning off 2 seconds after water delivery. The same activation time was also used for CS- odors despite the lack of water delivery. The task structure of discrimination training remained the same as otherwise. We found that OFC silencing caused a profound learning deficit. While normal mice learn to lick in anticipation to CS+ odors within 2-3 days of training (12-15 presentations of each odor per day), inhibited mice failed to display robust anticipatory licking to CS+ odors even after 10 days of training (Figure 3.14). Collection licks after US delivery was unaffected in these mice, implying that inhibition did not impair the motivation to acquire water nor execution of motor actions in thirsty mice. OFC silencing also had no effect on suppression of licking to CS- odors. Therefore, the deficit observed during OFC silencing appears to only affect licking to CS+ odors but not in discriminating between CS+ and CS- odors. Our imaging results also support this interpretation, since the OFC does not significantly encode CS- odors either before or after learning.

We observed variability in our behavioral results. 3 of 5 mice did not learn the task after 10 days of training, and only initiated anticipatory licking in less than 30% of CS+ odor trials on day 10 of training (Figure 3.15). The rest learned within a normal number of trials relative to controls. We assessed fiber placement and virus infection post-fixation and found no observable defects in either parameter in these mice. Therefore, our inhibition results suggest that the OFC may be necessary for associative learning for some mice but not others.

These results runs counter to the corpus of literature claiming that the OFC does not impair either classical or operant associative conditioning. While in our task, discrimination training commenced without any form of prior odor training, others first "pre-train" animals to learn a simple association before discrimination training (Schoenbaum and Eichenbaum 1995; Schoenbaum et al. 1998; Schoenbaum et al. 2002). To the best of our knowledge, after the OFC is lesioned, deficits during pre-training were never assayed nor described, and only a lack of deficit during the ensuing discrimination training was reported. Therefore, we wondered whether the difference between our results and those that were previously published were due to the installment of a pre-training epoch prior to discrimination training.

We therefore implemented a head-fixed version of pre-training. Instead of presenting 4 different odors (2 CS+, 2 CS- odors), a single CS+ odor was paired with water delivery, and this was repeated for 30-50 trials in daily imaging sessions. As before, the red-shifted halorhodopsin Jaws was used to bilterally silence the OFC. We found that OFC inhibition impaired the acquisition of anticipatory licking by two-fold on average during pre-training (Figure 3.16). Control YFP mice learned this task in 50 CS+ trials over the span of two

days, with the slowest mouse learning in 70 trials. In contrast, 4 of 6 mice with bilaterally inhibited OFC learned this task in over 100 trials, whereas the other two mice learned as quickly as control mice (Figure 3.17). Therefore, just as before, the OFC is necessary for the acquisition of associative learning in a majority of mice. We also note silencing during pre-training resulted in a deficit that was less severe than silencing during discrimination training without any prior pre-training, as mentioned above (2-fold increase in learning time in pre-training vs. complete failure to learn during discrimination training).

Previous experiments only assayed discrimination learning after mice have undergone pre-training and have observed no deficit in discrimination learning. These results have been used to conclude that OFC does not play a role during associational learning. However, in our two sets of perturbation experiments, one inhibiting the OFC during pre-training and the other during discrimination learning without any prior pre-training, we observe that the OFC is necessary for the formation of learned associations. If our results and those of others both hold, then we suggest that the OFC is only important for learning task structure, and is dispensable for the learning of subsequent associations within the same task. We thus asked whether we can replicate the results of prior experiments by silencing the OFC during discrimination learning after mice have undergone pre-training.

In the first set of experiments, we pre-trained mice with an intact OFC and inhibited the OFC during discrimination training. We used the same pre-training and discrimination parameters as before, and silencing was again done using Jaws. Discrimination training proceeded only after mice have successfully learned pre-training (anticipatory licking in >90% of trials). The learning strategy was different for discrimination learning when preceded by pre-training. Instead of learning to lick to CS+ odors if there was no prior pre-training, con-

trol mice generalize what they have learned during pre-training by licking in anticipation to all odors at the start of discrimination training (Figure 3.18.A). They then rapidly adapt their behavioral strategy to suppress licking to CS- odors, with full suppression occurring in an average of 10 trials. Therefore, selective anticipatory licking to CS+ odors during discrimination training was rapid and often occured within a day of training (Figure 3.18.B). We observed no deficit in OFC inhibition during discrimination training after pre-training (Figure 3.18.A). Inhibited mice also learn to generalize licking to all odors at the start of discrimination and no deficit was observed for suppression to CS- odors. This result implies that once a simple association has been learned with an intact OFC, the OFC is not required for the learning of subsequent associations.

In the second set of experiments, we matched the experimental protocol of prior experiments by inhibiting the OFC during both pre-training and discrimination epochs. In agreement with previously published results, we again observed no deficit in OFC inhibition. Mice again generalized anticipatory licking for all odors and quickly learned to suppress to CS- odors (Figure 3.18). Together, these sets of results suggest that no matter if a simple association is learned with or without an intact OFC, the OFC is not required past the point of initial task acquisition.

We further replicated these sets of findings with a freely moving behavioral paradigm. In this task, mice were free to move within a behavioral apparatus. Trials were initiated with a nose poke into a nose port located at one end of the box, and odor was then delivered inside the nose poke port after a successful nose poke. Water was then given for CS+ odors through a lick port situated directly underneath the odor port. Each mouse was left within the behavioral apparatus for an hour and were able to initiate trials freely during

this period. Motivated mice initiated an average of 100-200 trials in this 1 hour period. We found that OFC inhibition during pre-training significantly impaired the ability to learn this task (Figure 3.19). Most experimental mice were unable to initiate trials even after 5 days of training whereas control mice learned the task structure within three days, and initiated an average of 200 trials on the 5th day with robust anticipatory licking. When OFC inhibition was released in mice that failed to learn pre-training, these mice were able to learn to initiate trials and displayed normal anticipatory licking to the pre-training CS+ odor. Therefore, similar to head-fixed inhibition results, OFC inhibition during the freely moving task also prevented mice from acquiring task structure.

Once mice learned pre-training, they then underwent discrimination training, which consisted of discriminating between one CS+ odor and one CS- odor. The majority of mice again generalized anticipatory licking to both odors and rapidly suppressed licking to CS- odors (Figure 3.19). Again, we silenced the OFC during discrimination training either after mice learn pre-training with an intact OFC or with an inhibited OFC. We observed no behavioral deficit in discrimination learning in either experiments. Therefore, results from freely moving experiments were similar to head-fixed experiments. OFC appears to be strictly necessary for task acquisition.

OFC Activity Peaks During Initial Learning and Decays After Learning Plateaus

Our silencing experiments reveal that the OFC appears to be important during the early stages of associative learning. This is presumably reflected by the robust CS+ representa-

tion that is observed by imaging the OFC during learning. By that logic, the lack of deficit observed when silencing during the learning of subsequent associations implies that the OFC may be inactive and unresponsive to CS+ odors after initial learning. Therefore, we would predict that the OFC should not be engaged during discrimination learning after pre-training. Initial imaging results suggested that OFC responses may decay after learning has plateaued, but neural responses were not tracked for long periods of time so no definitive conclusions could be reached. We therefore conducted a series of long-term imaging experiments in a new cohort of mice where OFC activity was tracked long after initial learning. Like before, we observe that a robust CS+ representation emerges during initial learning, when mice display anticipatory licking in >85% of trials for the first time (Figure 3.20). Imaging was conducted for an average of 5 sessions past complete learning. We observe that robust responses to CS+ odors decay when learning performance plateaus. The decline appears to be gradual, progressively decaying from a peak response where 35% of OFC neurons respond to CS+ odors during initial task acquisition to 15% on the 4th training session after having completely learned the task (Figure 3.21).

We now ask whether OFC will respond as robustly to the learning of new associations during discrimination training once mice have already learned an example association during pre-training. The structure of this task was identical to that used in prior optogenetic experiments, consisting of a pre-training epoch (1 CS+ odor) and a subsequent discrimination epoch (2 CS+, 2 CS- odors). As expected, a significant fraction of OFC neurons (35%) acquired robust and consistent responses to the CS+ odor during pre-training (Figure 3.22). This fraction is similar to the fraction of neurons that were responsive to CS+ odors when mice underwent discrimination training without prior pre-training (40% in discrimination

training vs 38% in pre-training, Figure 3.23). While we did not over-train animals past the point of initial acquisition, we observed (but did not quantify) that the representation to the CS+ odor decays after initial task acquisition. Once pre-training is complete, we then switch to discrimination learning. When mice have successfully learned discrimination training, we observe that fewer neurons were responsive to the new CS+ odors as compared to the pre-trained CS+ odor (38% after pre-training vs 28% after discrimination training, Figure 3.22). Moreover, on average, there was no increase in the size of the CS+ odor ensemble or of the CS- odor ensemble after discrimination learning. Therefore, the OFC does not appear to be actively encoding learned associations past the acquisition of the first association. We thus conclude that the OFC is not needed for either behavioral generalization to novel CS+ odors nor for learning lick suppression once mice have already learned the task structure.

In summary, these series of imaging results reflect the behavioral deficits that we observe from OFC inhibition. Responses to CS+ odors in the OFC is only robust during initial task acquisition, whether it is pre-training or discrimination without prior pre-training. Likewise, silencing the OFC during this period causes dramatic impairments in associational learning. However, silencing the OFC during the learning of subsequent associations produces no behavioral deficits, and imaging results also reveal that the OFC does not appear to be engaged during this time period. Both imaging and inhibition results suggest that the OFC is important for initial task acquisition.

3.3 Discussion

Previous recording studies have isolated neurons that were sensitive not only to the expected value of CS cues but also to sensory identity and a myriad of other factors such as nose-poking, past odor identity, and reward history (Schoenbaum and Eichenbaum 1995). Responsivity to a diverse array of task-relevant variables in prefrontal regions has led to the hypothesis that such a representation increases the information content, or "dimensionality", of the encoding (Rigotti et al. 2013; Schoenbaum and Eichenbaum 1995). While we have not yet quantified the dimensionality of the temporal dynamics of OFC responses, most OFC neurons do not appear to discriminate between CS+ odors and do not encode CS- odors. Therefore, the dimensionality of OFC's odor representation appears to be low and is reflected by the higher percentage of variance explained by the first principle component in a PCA of OFC population activity (50 % variance explained). Moreover, CS+ neurons also respond homogeneously to perturbations in state, context, and changes in reward contingencies during reversal learning. Therefore, the only quantity that we observe the OFC to encode is expected value. With this said, we acknowledge that we have intentionally defined a minimal set of task parameters, and we have not assessed, for example, whether the OFC is encoding motor actions in tasks where motor planning is integral to the retrieval of reward (Roesch et al. 2006; Feierstein et al. 2006). Moreover, we have also not explored whether responses in the OFC generalize across sensory modalities.

Many previous behavioral experiments have assayed OFC function only after first performing the lesion and then shaping animals on a pre-training task. In agreement with our results, these experimenters have observed that OFC does not impair subsequent learning

(Chudasama et al. 2007; Izquierdo et al. 2004; West et al. 2011). In light of our results, the prior conclusion that OFC is dispensable for forming simple associations may be based on experiments that did not assay OFC function when the OFC was engaged during task acquisition. Indeed, when OFC function is assessed during the first learning bout, it appears to be essential for the learning of a simple association. Moreover, nearly all electrophysiological studies in the OFC, particularly in primates, have also been performed on experimental subjects that are already well-trained (Saez et al. 2015; West et al. 2011). Given that we observe that the OFC is dispensable after initial task acquisition, and that there is a strong decay in the CS+ representation after task acquisition, recording OFC activity in animals that are well-trained may not reflect what the OFC is encoding during initial task acquisition, when it is necessary for learning. With that said, many previous tasks in primates and rodents are more cognitively complex and have a larger number of task-relevant variables compared to the simple classical conditioning task that we have employed, and it is currently unclear whether the increase in cognitive demand may require the OFC to be active not only during the learning period but throughout the entire task.

Several future experiments can further define what the OFC is encoding. First, is the encoding of expected value modality-specific? To resolve this question, both odor and tone could be paired with reward, and the overlap in their representations after learning could be examined. Second, is the encoding valence-specific? To resolve this question, different odors could be paired to both appetitive and aversive USs, and the overlap in their representations could be examined. Third, is the encoding motor-specific? To resolve this question, mice could be trained to perform two different actions that both result in water delivery, and the overlap in the representations of these two motor actions could be

examined. We reason that the OFC cannot dedicate unique neural ensembles to encode sensory modality, or valence, or motor action. Given that 35% of OFC neurons encode a learned appetitive association, I expect that any other associative learning will also take up an equally dense representation. Thus, representations of opposing valences, of distinct modalities, and of distinct motor actions must share significant overlap. Indeed, when mice were trained to perform different motor actions upon the delivery of odors to retrieve the same reward, the representations of the two odors cuing different motor actions are highly overlapping in the OFC (unpublished).

Figure 3.1

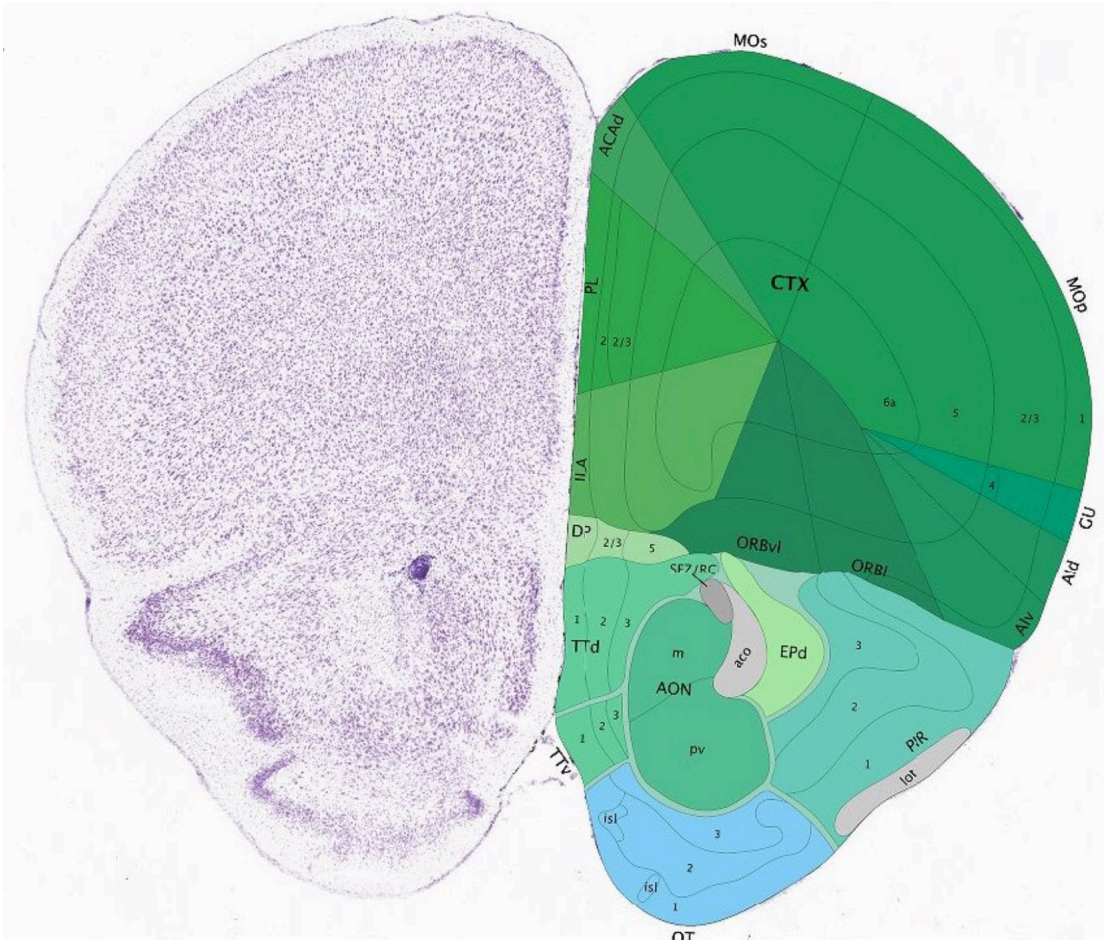
MOs
ACAd
CTX
PL
2
2/3
MOp
6a
5
2/3
1
4
ILA
GU
DP
2/3
5
ORBvl
ORBl
SF7/RC
Ald
Alv
1
2
3
TTd
m
aco
EPd
3
AON
2
3
2
1
pv
PIR
1
lot
TTv
isl
3
2
isl
1

Figure 3.1. Antero-posterior view of the orbitofrontal cortex. the OFC comprises of the lateral orbitofrontal (ORBl) and the ventrolateral orbitofrontal cortex (ORBvl). Adapted from the Allen Brain Atlas.

Figure 3.2

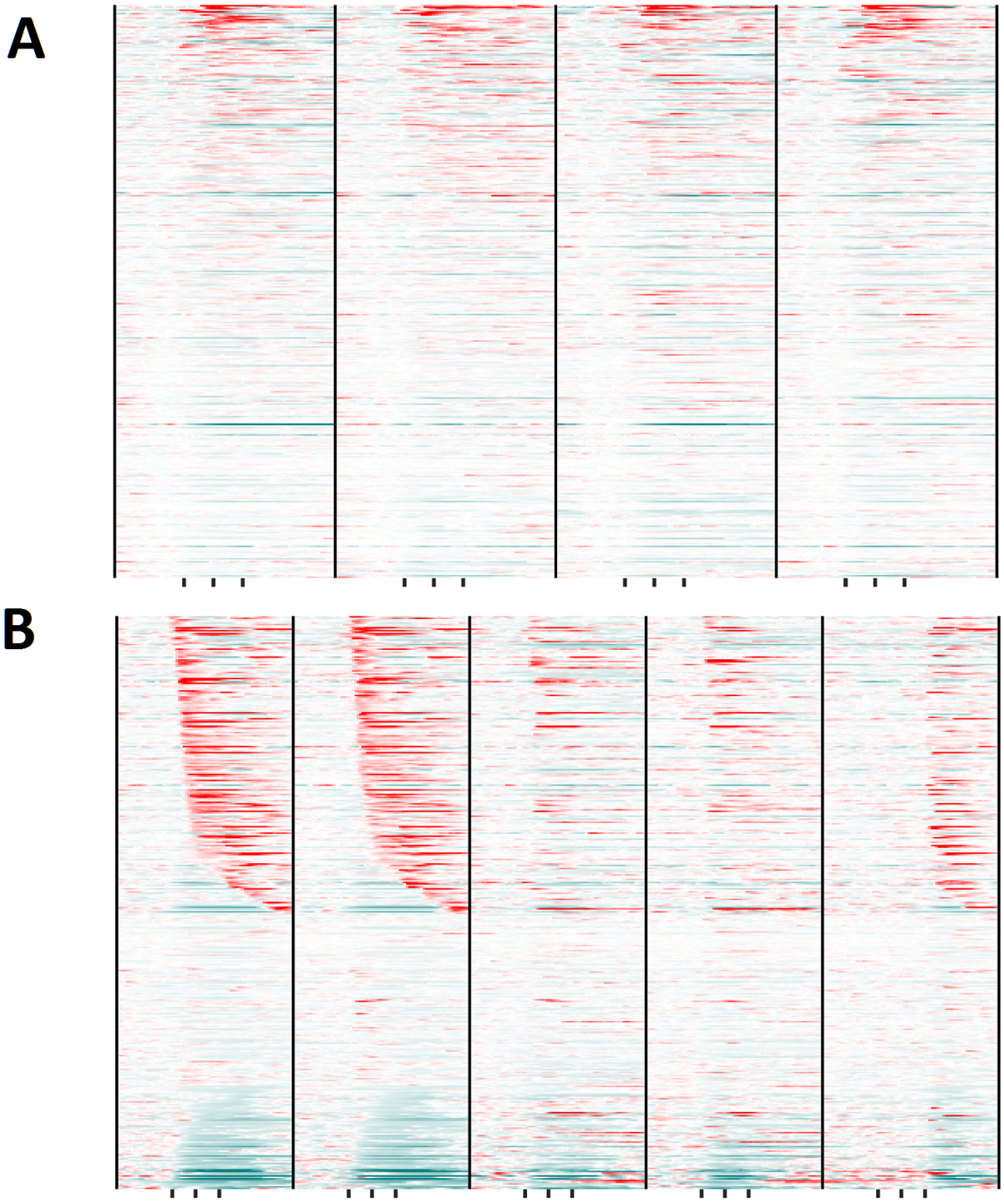

Figure 3.2. OFC Population Activity Before and After Learning. OFC responses in all neurons recorded from 5 mice. Each row denotes a single cell's trial-averaged DF/F responses to CS+1 (PIN), CS+2 (MSY), CS-1 (EUY), CS-2 (LIM). Response to water is the 5th column in the part B. Scale bars indicate an increase in DF/F (red) or a decrease in DF/F (blue) relative to baseline. **A**. Responses prior to learning are non-selective. **B.** 35% of neurons respond to CS+ odors after learning. These responses tile the entire task period are almost identical for two distinct CS+ odors paired with the same reward.

Figure 3.3

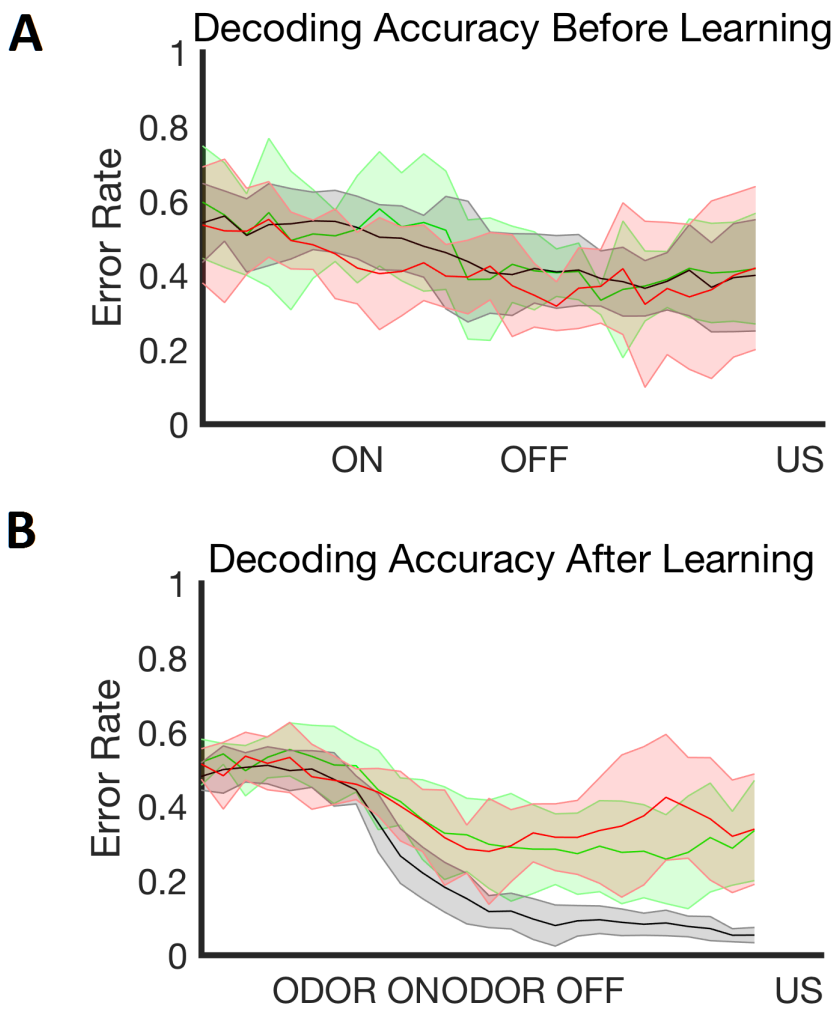
A
Decoding Accuracy Before Learning
Error Rate
1
0.8
0.6
0.4
0.2
0
ON
OFF
US
B
Decoding Accuracy After Learning
Error Rate
1
0.8
0.6
0.4
0.2
0
ODOR ON
ODOR OFF
US

Figure 3.3. Pairwise Decoding of Odors Using OFC Population Activity. For each mouse, a binary linear decoder was trained on population OFC activity from a subset of odor trials and was then asked to decode the identity of the odor using held-out trials. Green curve indicates decoding between CS+1/CS+2 odors, red curve indicates decoding between CS-1/CS-2 odors, and gray indicates all 4 pairwise combinations of CS+/CS- odors. Error bars indicate standard deviations of decoding performance across different mice. The decoder was trained and tested at each time-point (see Methods). **A**. Prior to learning, decoding accuracy was poor for all odor pairs. **B**. After learning, decoding performance only improved for pairs of CS+/CS- odors, suggesting that OFC acquired a representation of expected value.

Figure 3.4

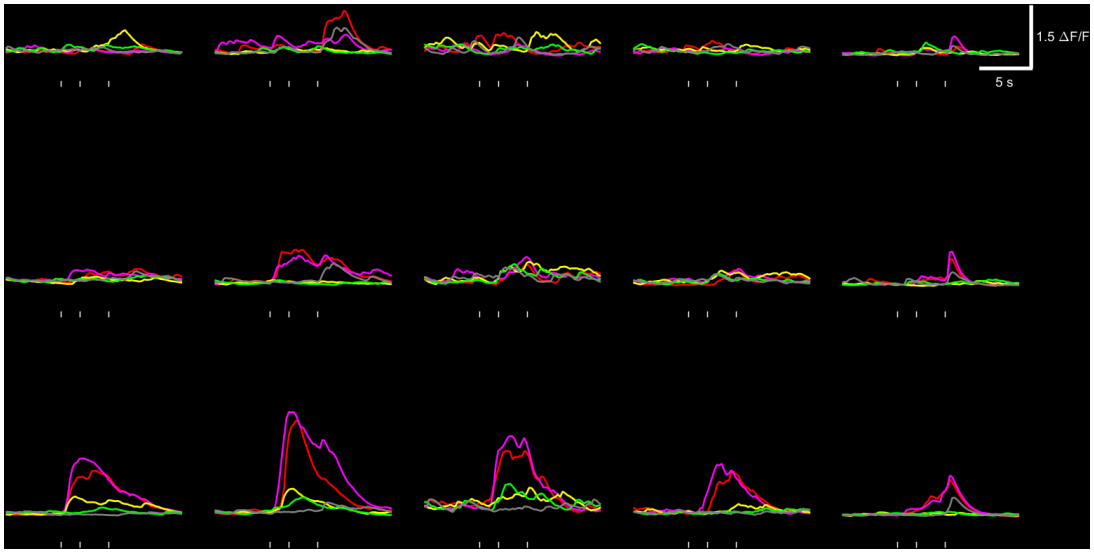

Figure 3.4. OFC neurons acquire responses to CS+ odors during learning. Tracking responses of 5 example cells to odors before learning (naive odor presentation), during learning (anticipatory licking in 50%), and fully learned (anticipatory licking in >90% of CS+ trials) in the three rows from top to bottom, respectively. All 5 cells acquired responses to CS+ odors, with some cells acquiring it earlier in training and others later. These responses have varied response dynamics and onset times, but were identical for multiple and distinct CS+ odors in the same neuron. Each point is a single mouse, and connected lines relate fractions responsive before and after learning in each mouse.

Figure 3.5

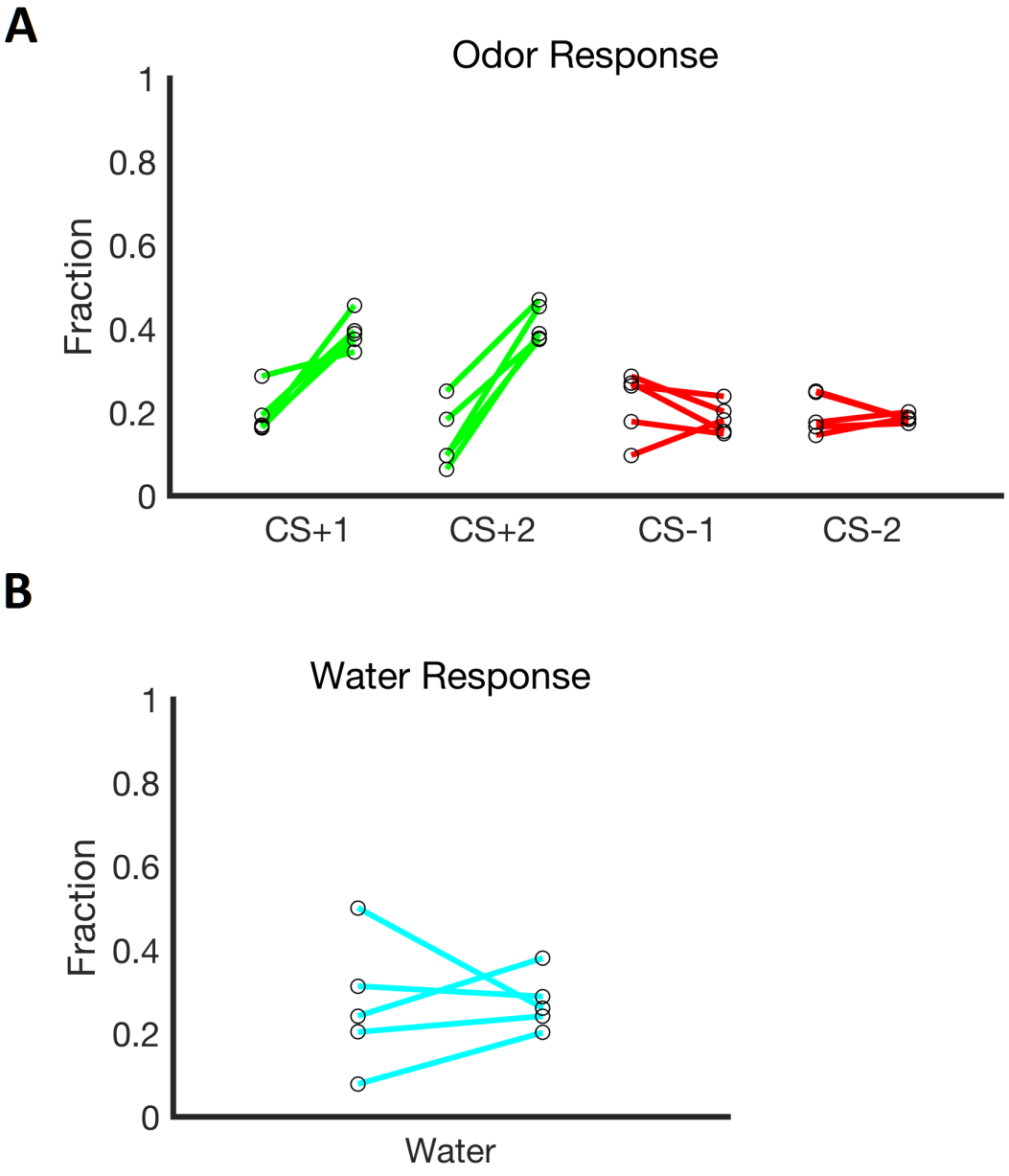
A
Odor Response
Fraction
1
0.8
0.6
0.4
0.2
0
CS+1
CS+2
CS-1
CS-2
B
Water Response
Fraction
1
0.8
0.6
0.4
0.2
0
Water

Figure 3.5. Quantification of Odor-Evoked Responses Before and AFter Learning. A., B. Fraction of neurons responsive to CS+ odors increased, while responses to CS- odors and to the US remained constant after learning.

Figure 3.6

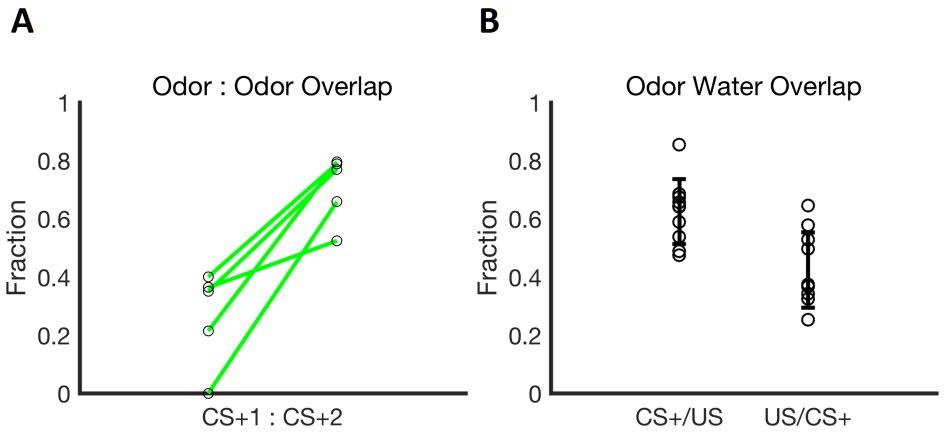
A
Odor : Odor Overlap
Fraction
1
0.8
0.6
0.4
0.2
0
CS+1 : CS+2
B
Odor Water Overlap
Fraction
1
0.8
0.6
0.4
0.2
0
CS+/US
US/CS+

Figure 3.6. Quantification of Overlap Before and After Learning. A. Fraction of cells responsive to both CS+ odors increased as a function of learning. **B.** CS+/US: 60% of neurons responsive to US have a significant CS+ response. US/CS+: 40% of CS+ responsive neurons are US responsive after learning.

Figure 3.7

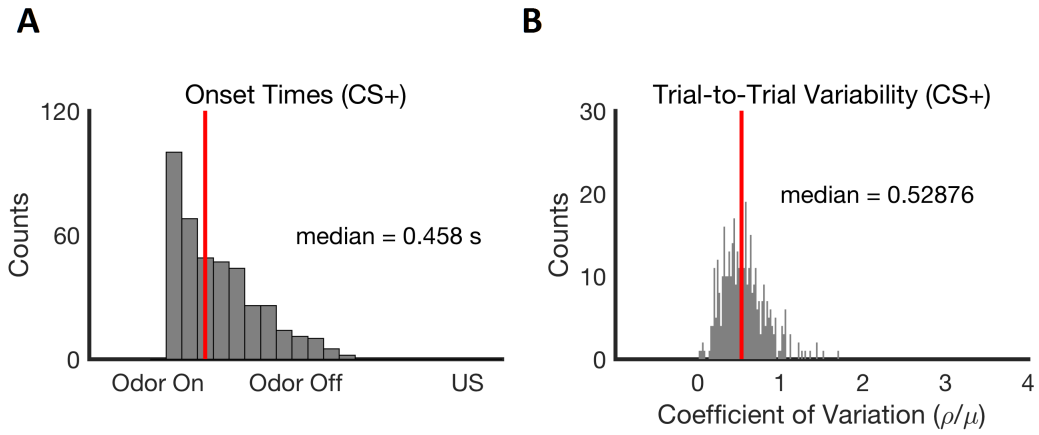
A
Onset Times (CS+)
120
60
0
Counts
median = 0.458 s
Odor On
Odor Off
US
B
Trial-to-Trial Variability (CS+)
30
20
10
0
Counts
median = 0.52876
0
1
2
3
4
Coefficient of Variation (ρ/μ)

Figure 3.7. OFC responses are variable and temporally heterogeneous. A. The onsets of CS+ responses in the OFC tile the duration between odor onset and water onset. **B.** OFC responses exhibit almost double the trial-by-trial variability as compared to piriform responses.

Figure 3.8

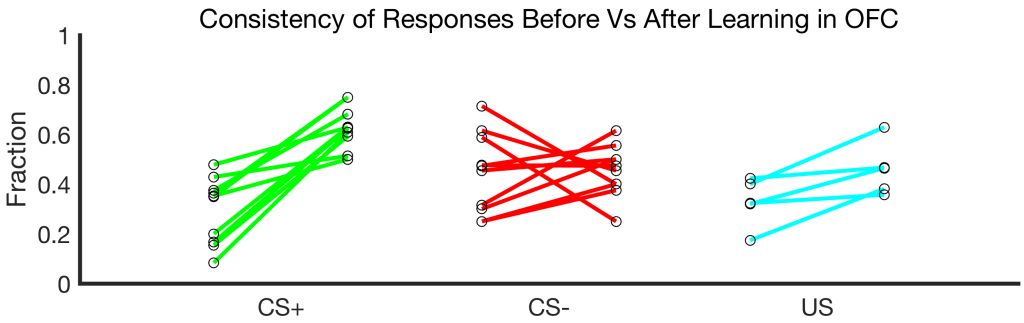
Consistency of Responses Before Vs After Learning in OFC
Fraction
1
0.8
0.6
0.4
0.2
0
CS+
CS-
US

Figure 3.8. Consistency of OFC Responses to Odors Before and After Learning. Consistency of response was measured by assessing the fraction of neurons that are responsive to CS+ odors on consecutive imaging days. This was done for each mouse before and after learning (each line). Responses to CS+ odors become more consistent after learning, but CS- responses did not grow more consistent after learning. US responses appear to increase slightly in consistency as a result of learning.

Figure 3.9

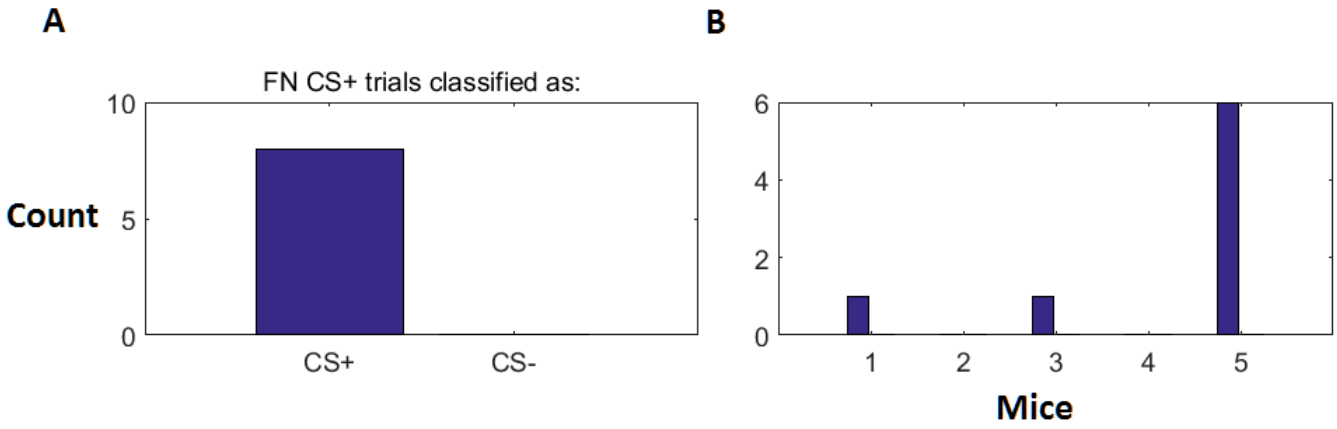
A
FN CS+ trials classified as:
Count
10
5
0
CS+
CS-
B
6
4
2
0
1
2
3
4
5
Mice

Figure 3.9. False negative CS+ trials are similar to true positive CS+ trials. A binary decoder was trained on CS+ lick trials and CS- non-lick trials, and then asked to decode the identity of false positive (no lick) CS+ trials. **A.** Decoder categorized false positive trials as CS+ lick trials, suggesting that motor action is not significantly encoded in the OFc. Cumulative data from 5 mice. **B.** Trials as grouped by different mice.

Figure 3.10

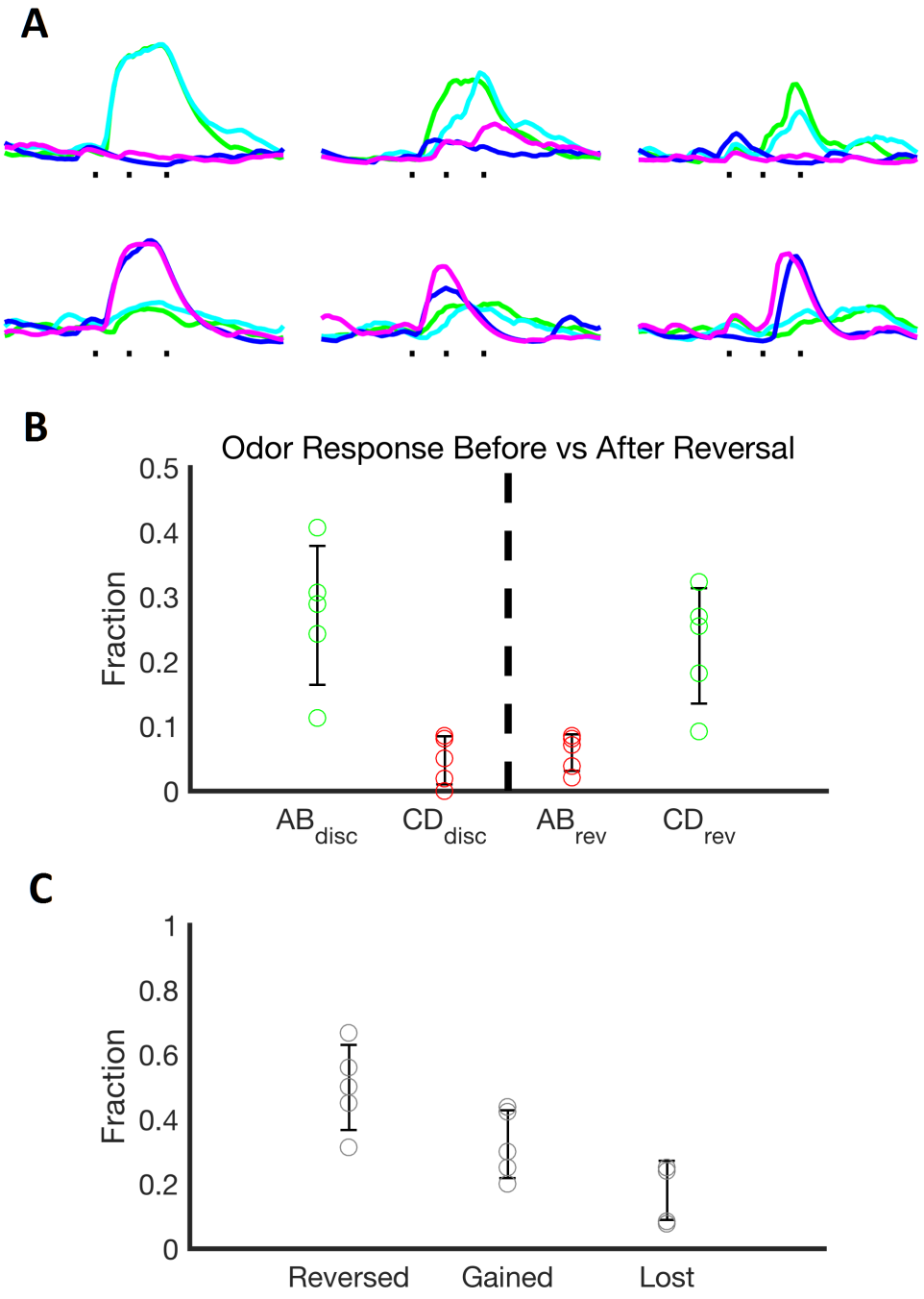
A
B
Odor Response Before vs After Reversal
Fraction
0.5
0.4
0.3
0.2
0.1
0
AB disc
CD disc
AB rev
CD rev
C
Fraction
1
0.8
0.6
0.4
0.2
0
Reversed
Gained
Lost

Figure 3.10. Responses to CS+ and CS- Odors Reverse After Reversal Learning. A. Tracking the odor responses of 3 example cells before and after reversal learning. Prior to reversal learning, robust responses are observed to CS+ odors. After reversal, these responses diminish and are replaced by responses to new CS+ odors. Note that responses to old CS+ odors never fully diminish despite complete behavioral suppression of anticipatory licking to these odors. **B.** Quantification of fraction of cells responsive to CS+ and CS- odors before and after learning. Green color denotes CS+, red color denotes CS-. **C.** For all cells that display significant responses to CS+ odors either before or after reversal, we found that 55% of cells fully reversed their responses during reversal. 30% of neurons were not responsive to CS+ odors pre-reversal but gained a response post-reversal, whereas 15% of neurons were responsive to CS+ odors pre-reversal but were not responsive to the new CS+ odors post-reversal.

Figure 3.11

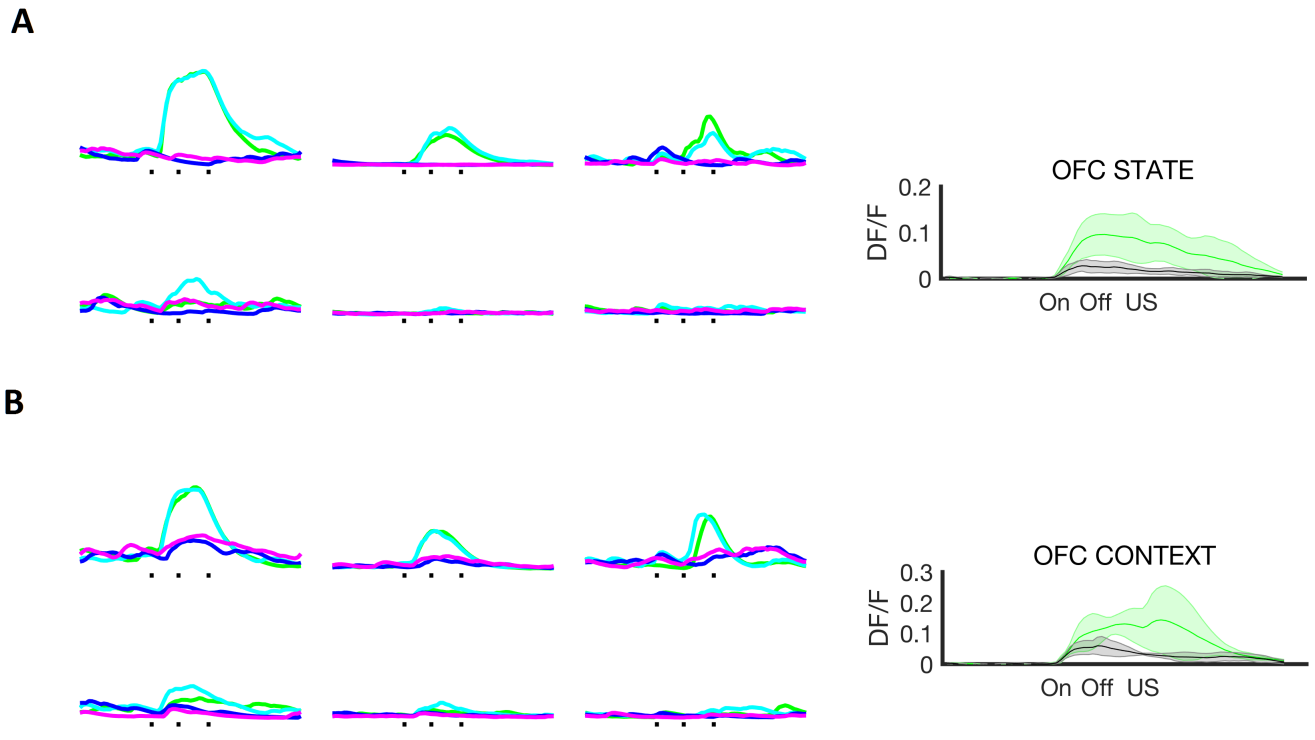
A
OFC STATE
DF/F
0.2
0.1
0
On Off US
B
OFC CONTEXT
DF/F
0.3
0.2
0.1
0
On Off US

Figure 3.11. OFC Responses are Gated by State and Context. A. Left: tracking responses of 3 example cells before and after quenching thirst. When mice are sated, responses to CS+ responses vanish. Right: average DF/F of all CS+ responsive neurons before and after satiation. **B.** Same as A, except for water port removal.

Figure 3.12

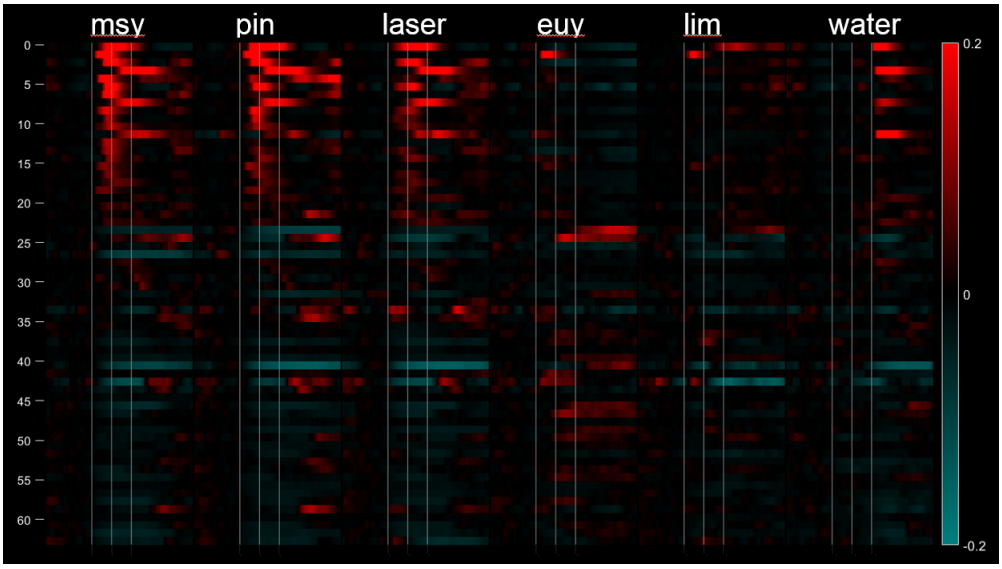
msv
pin
laser
euv
lim
water
0
5
10
15
20
25
30
35
40
45
50
55
60
0.2
0
-0.2

Figure 3.12. Pairing Laser Activation with Reward Evokes Similar CS+ Responses in OFC as Odor-Pairing. Population OFC responses to CS+ odors (MSY, PIN), CS- odors (EUY, LIM), Laser trials (Laser), and US only trials (Water). Responses to laser after learning evoked activity in similar sets of neurons as evoked by CS+ odor delivery.

Figure 3.13

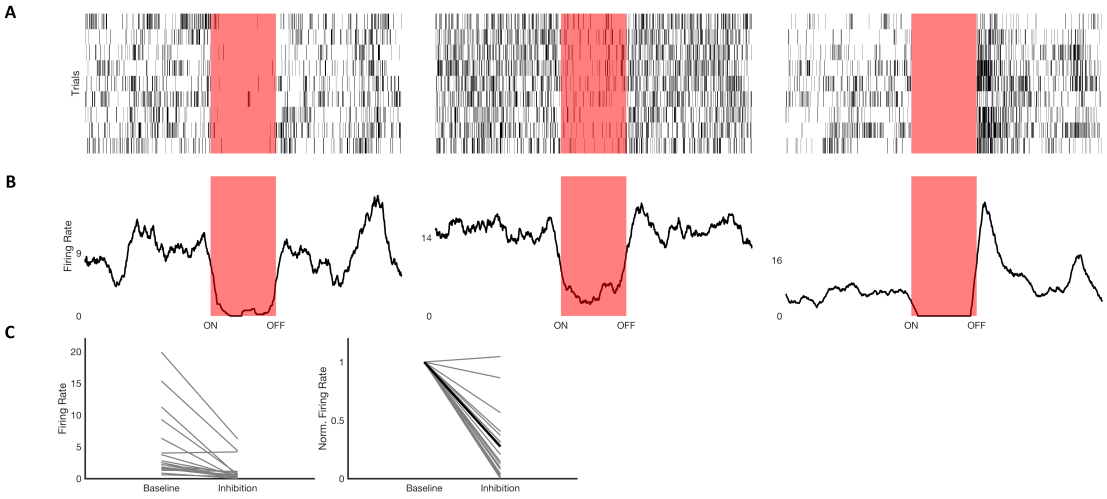
A
Trials
B
Firing Rate
0
14
16
ON
OFF
C
Firing Rate
20
15
10
5
0
Baseline
Inhibition
Norm. Firing Rate
1
0.5
0
Baseline
Inhibition

Figure 3.13. Activation of Jaws reliably inhibits neural activity in OFC. A. Spike rasters of 3 example neurons with Jaws activation denoted by the pink bar. Neural activity was reliably inhibited. **B.** Spike rate summary of the correspond cells in part A. **C.** Quantification of spike rates before and during inhibition for all recorded neurons. Inhibition was apparent in over 80% of all recorded neurons.

Figure 3.14

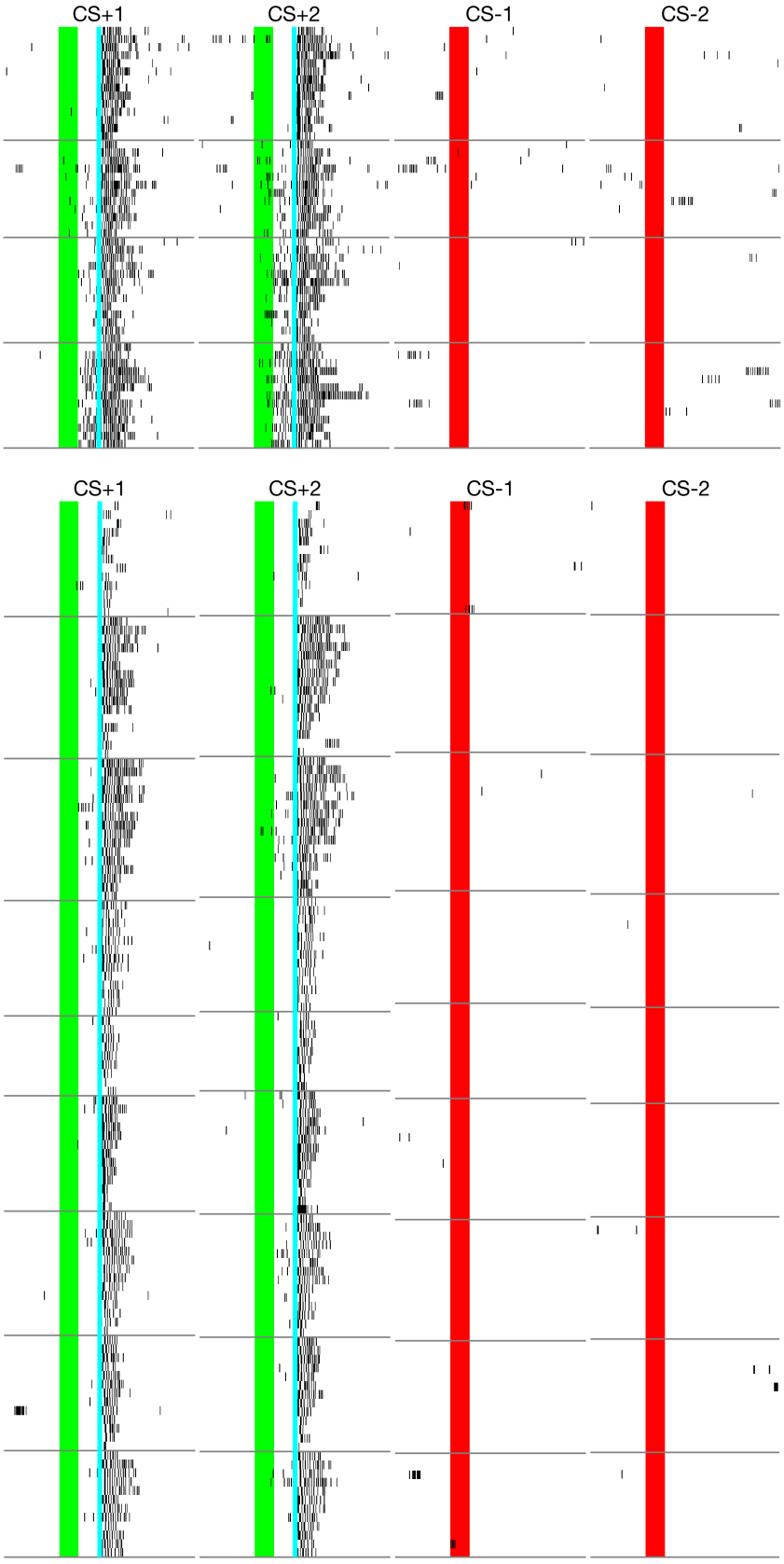

Figure 3.14. OFC Inhibition Impairs Associational Learning During Discrimination. Behavioral data for an example control mouse (top) and an OFC-inhibited mouse (bottom). The control mouse learn to lick to CS+ odors within 30 trials, whereas the OFC-inhibited mouse never learns.

Figure 3.15

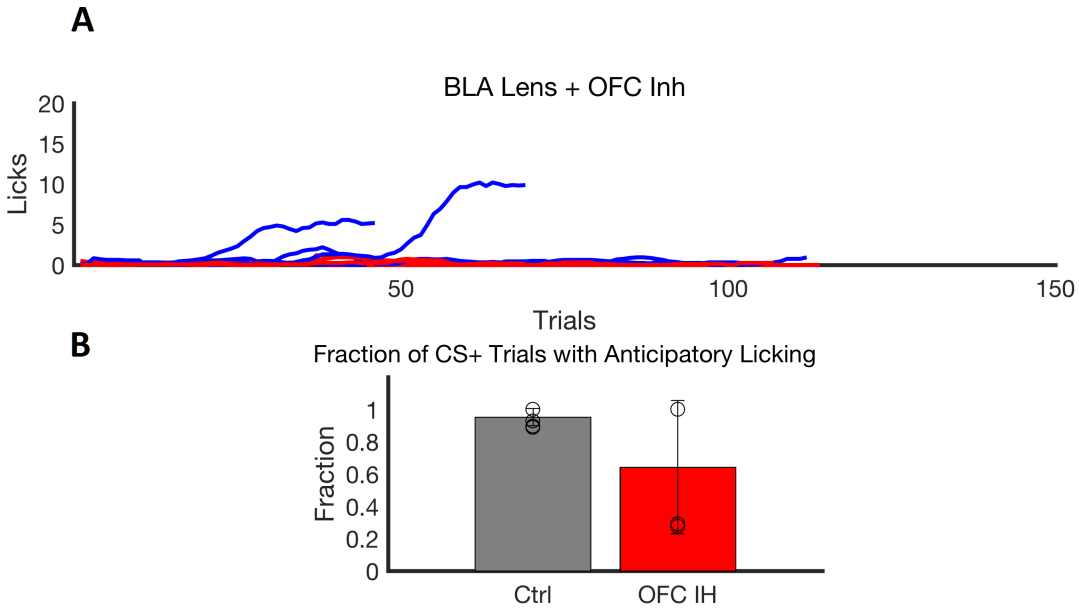
A
BLA Lens + OFC Inh
Licks
20
15
10
5
0
50
100
150
Trials
B
Fraction of CS+ Trials with Anticipatory Licking
Fraction
1
0.8
0.6
0.4
0.2
0
Ctrl
OFC IH

Figure 3.15. Quantification of Behavioral Effects with OFC inhibition. A. Anticipatory licking as a function of trials for all 4 mice. Blue denotes the average anticipatory lick rate to the two CS+ odors for one mice, whereas red is the same for CS- odors. Control mice take 30-50 trials to learn to display robust anticipatory licking to CS+ odors. 2 mice never learned the task, whereas the other 2 learned it within a normal range of trials. **B.** Quantification of false positive rate on last day of training.

Figure 3.16

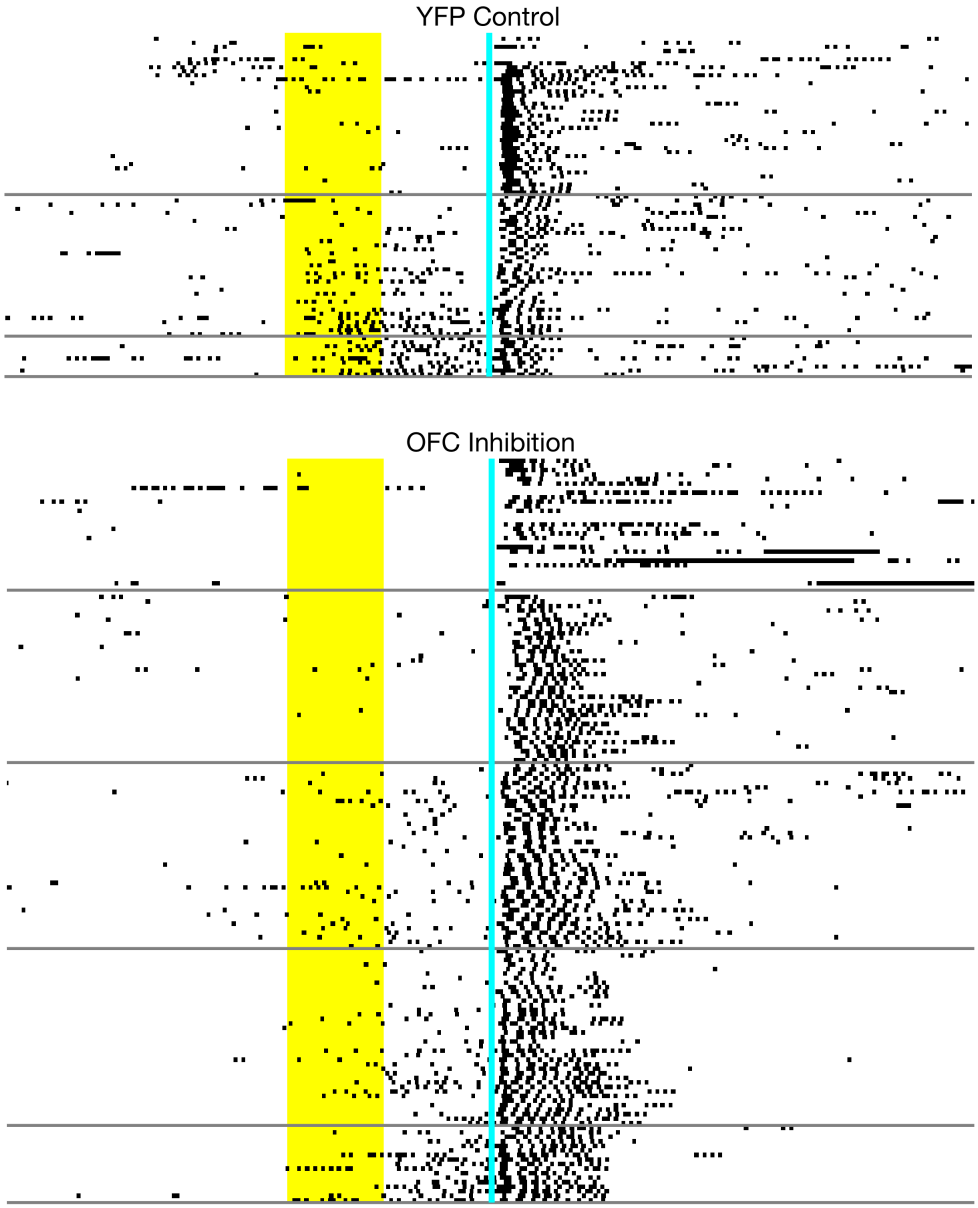

Figure 3.16. OFC Inhibition Impairs Associational Learning During Pre-Training. Behavioral data for an example control mouse (top) and an OFC-inhibited mouse(bottom) during pre-training. The control mouse learn with 50 trials (2 days of training) whereas the OFC-inhibited mouse learn in 150 trials (4 days of training).

Figure 3.17

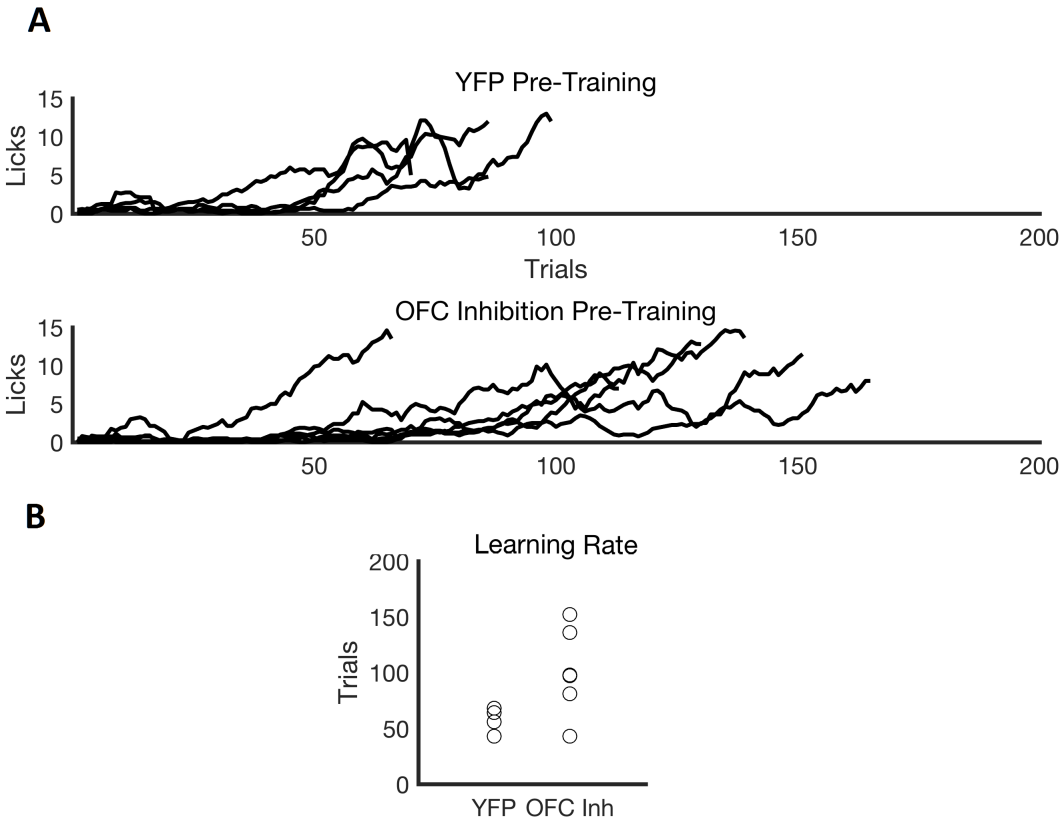
A
YFP Pre-Training
Licks
15
10
5
0
50
100
150
200
Trials
OFC Inhibition Pre-Training
Licks
15
10
5
0
50
100
150
200
B
Learning Rate
Trials
200
150
100
50
0
YFP
OFC Inh

Figure 3.17. Quantification of Behavioral Effects During Pre-training with OFC inhibition. A. Anticipatory licking as a function of trials for 4 YFP mice (top) and 5 OFC-inhibited mice (bottom). **B.** Control mice take 55 trials to learn to display robust anticipatory licking to CS+ odors, whereas OFC-inhibited mice take 100 trials.

Figure 3.18

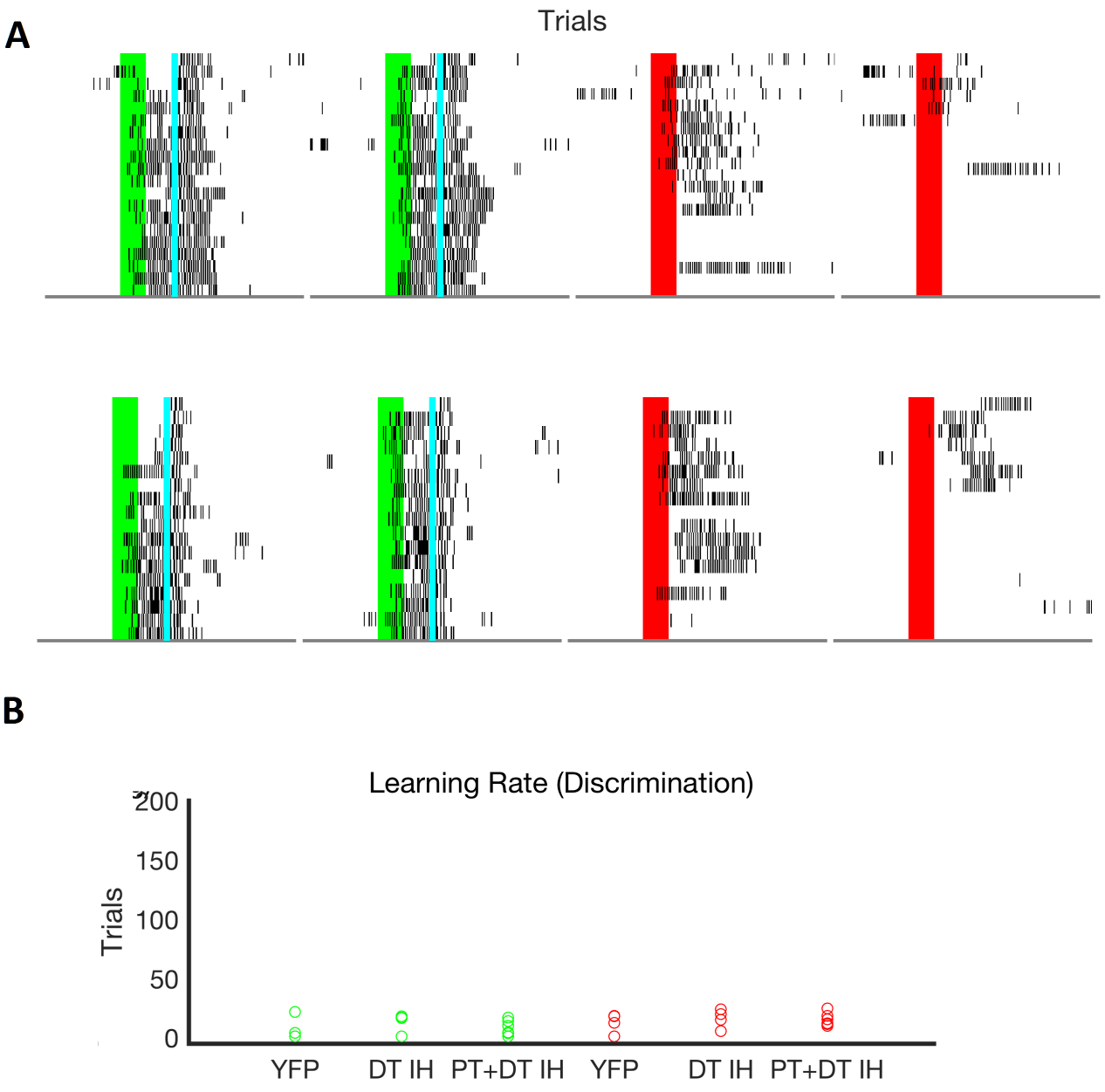
A
Trials
B
Learning Rate (Discrimination)
Trials
200
150
100
50
0
YFP
DT IH
PT+DT IH
YFP
DT IH
PT+DT IH

Figure 3.18. OFC Inhibition Does not Impair Discrimination Learning After Pre-Training. A. Behavioral performance during discrimination learning immediately after pre-training for an example YFP control mouse (top) and an mouse with OFC silencing during discrimination but not pre-training (bottom). In both conditions, mice generalize licking and rapidly suppress to CS- odors. **B.** Summary of learning rate for control mice (YFP), inhibition only during discrimination (DT IH), or inhibition during both pre-training and discrimination (PT+DT IH). Green denotes number of trials to lick to CS+ odors, and red denotes time to suppress to CS- odors. Inhibition in all conditions had no effect on learning.

Figure 3.19

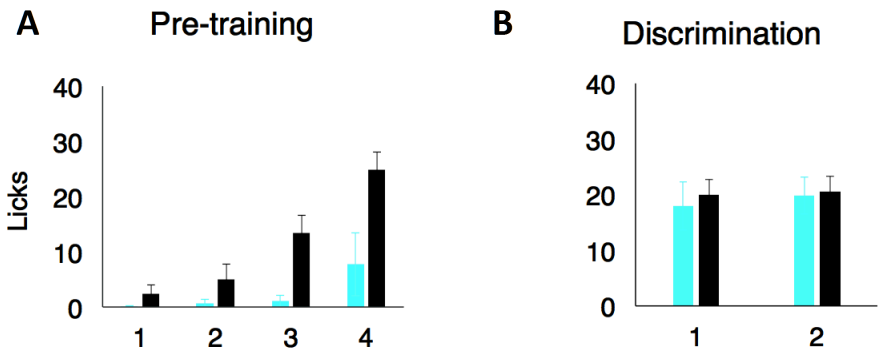
A
Pre-training
B
Discrimination
Licks
40
30
20
10
0
1
2
3
4
40
30
20
10
0
1
2

Figure 3.19. OFC Inhibition Causes Same Behavioral Deficits in a Freely Moving Behavioral Paradigm. A. Quantification of learning rate during pre-training with and without OFC inhibition. Red: OFC inhibition with halorhodopsin. White: YFP controls. Learning performance was quantified as average anticipatory lick rate for each day of training. Silencing the OFC impairs licking to CS+ odors **B.** Silencing the OFC during discrimination training after pre-training with an intact OFC does not impair learning.

Figure 3.20

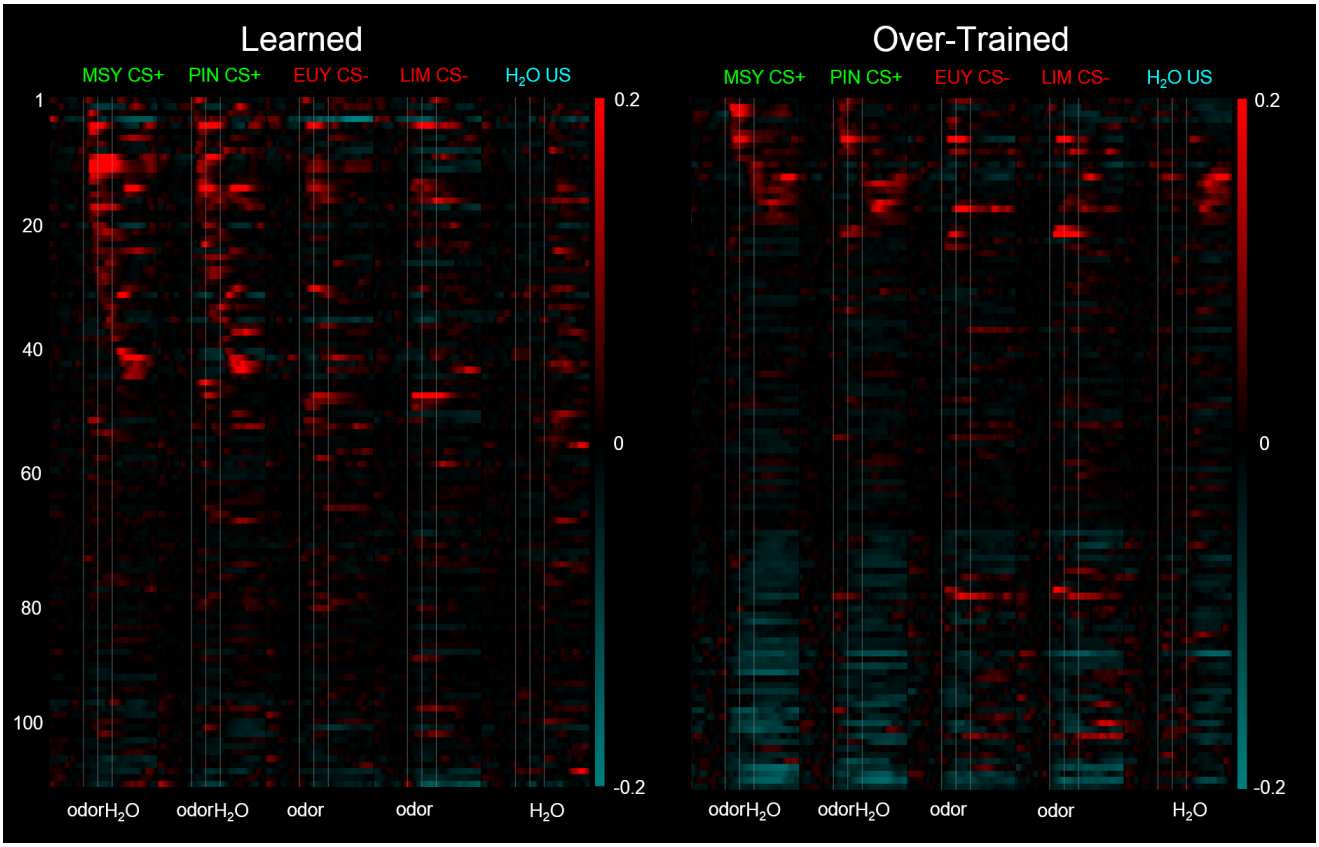
Learned
MSY CS+
PIN CS+
EUY CS-
LIM CS-
H2O US
1
20
40
60
80
100
0.2
0
-0.2
odorH2O
odorH2O
odor
odor
H2O
Over-Trained
MSY CS+
PIN CS+
EUY CS-
LIM CS-
H2O US
0.2
0
-0.2
odorH2O
odorH2O
odor
odor
H2O

Figure 3.20. OFC Responses Decay After Learning has Plateaued. Population response of OFC neurons to CS+ and CS- odors during initial learning and 5 days of training past initial learning. Significantly less neurons respond to CS+ odors after over-training.

Figure 3.21

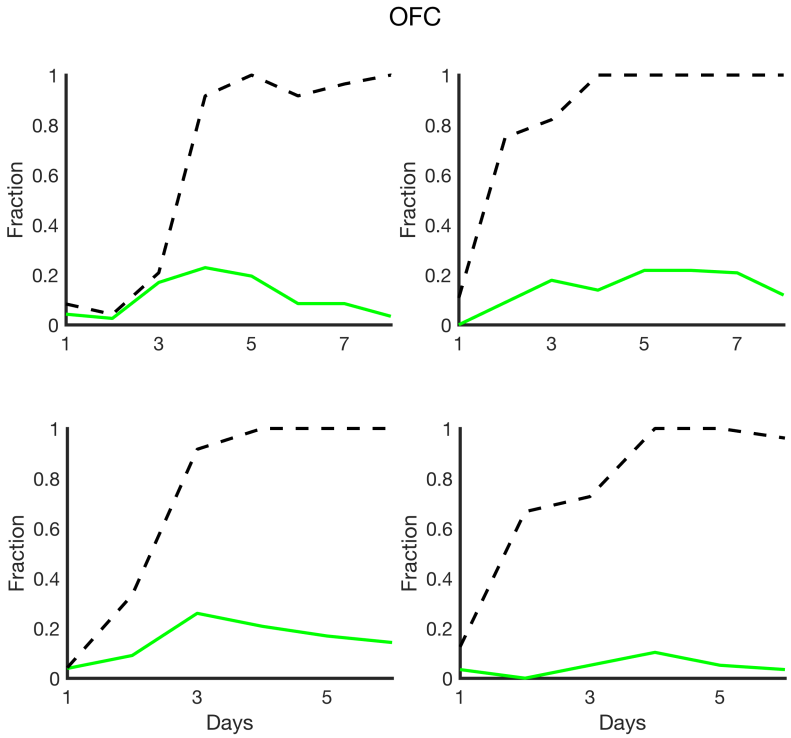

Figure 3.21. Quantification of Response Decay After Initial Learning. Number of neurons that are more responsive to CS+ odors than CS- odors, quantified on each day of imaging for 4 mice. Dotted line denotes fraction of trials that mice displayed anticipatory licking to CS+ odors. Responses in 3/4 mice peak during initial learning and progressively declines after learning perfroamcne plateaus.

Figure 3.22

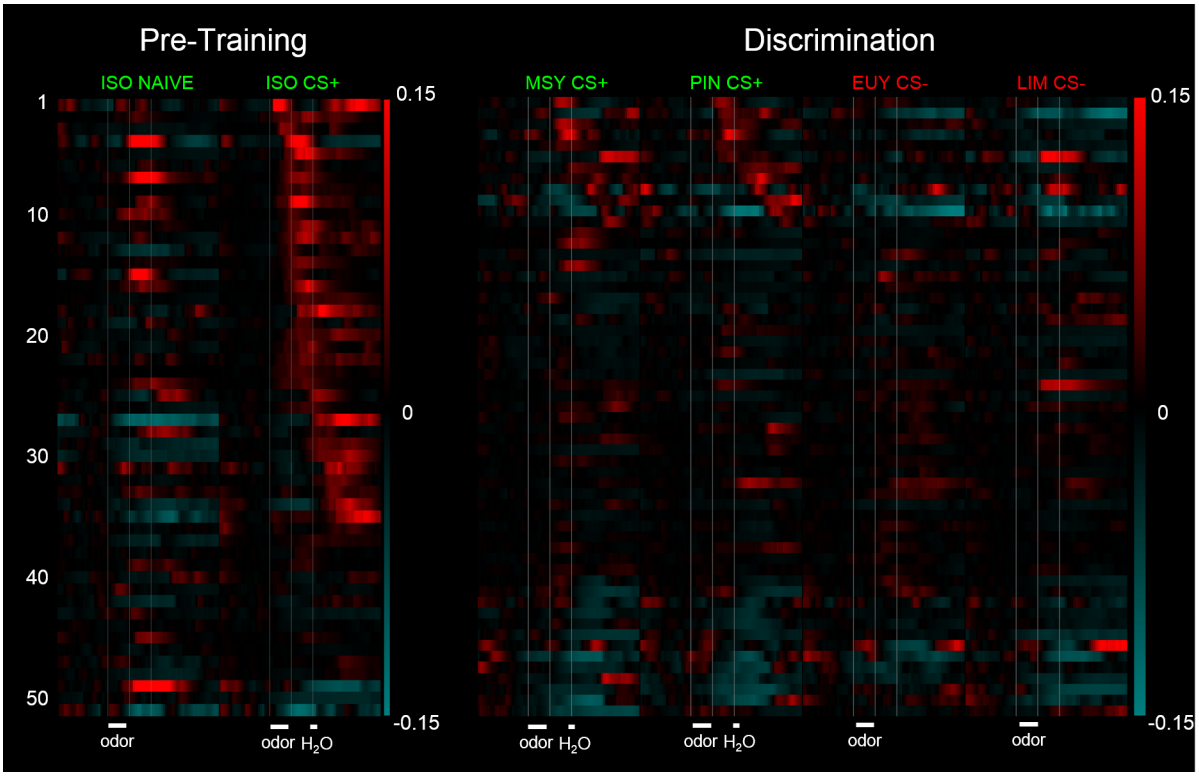
Pre-Training
ISO NAIVE
ISO CS+
Discrimination
MSY CS+
PIN CS+
EUY CS-
LIM CS-
1
10
20
30
40
50
0.15
0
-0.15
odor
odor H2O
odor H2O
odor H2O
odor
odor

Figure 3.22. OFC is not Engaged During Learning of Subsequent Associations. Population response of OFC neurons to CS+ and CS- odors during pre-training and discrimination. Left: the CS+ odor used was ISO, or isoamyl acetate. Potentiated responses were observed after learning the pre-training task compared to prior to pre-training. Right: responses to CS+ and CS- odors when mice have learned to lick to CS+ odors and suppress to CS- odors. Minimal activation was observed to CS+ odors during subsequent discrimination learning.

Figure 3.23

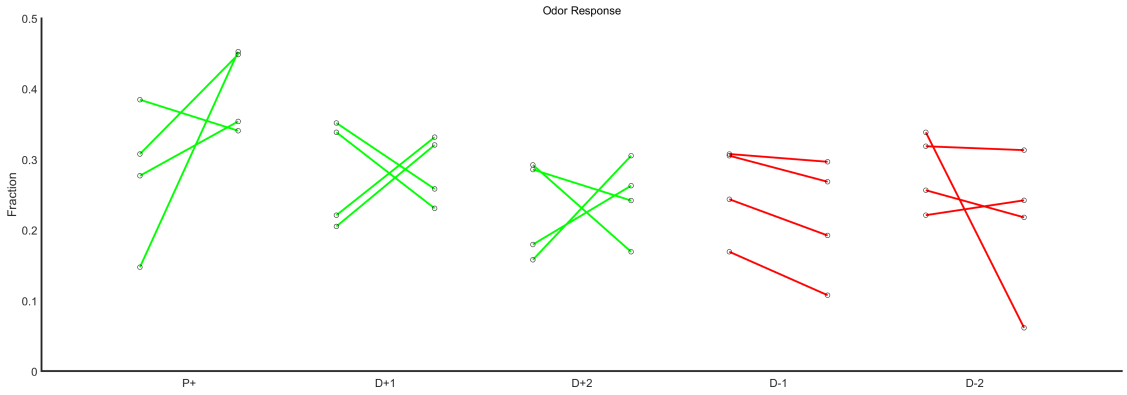

Figure 3.23. OFC is not Engaged During Learning of Subsequent Associations. Responses to odors during pre-training and during discrimination. Responses to the pre-trained CS+ odor is potentiated during pre-training, rising from 25% before pre-training to 40% after pre-training. However, responses to new CS+ odors during discrimination learning is not potentiated after pre-training, staying constant at 26% on average. Representation to CS- odors also do not change significantly during discrimination learning.

Chapter 4

The Medial Prefrontal Cortex

4.1 Introduction

We have delineated a circuit where sensory identity from the piriform is transformed into a representation of predicted value downstream in the OFC. This representation is necessary for the acquisition of task structure but not for subsequent learning once task structure has been learned. Therefore, learning must be transfered into a brain area for long-term storage. Potential candidate brain regions must satisfy two criterion: it must maintain a stable representation of the learned cues after initial learning, and the inhibition of these areas must necessarily impair task performance. We describe a set of inhibition experiments carried out in brain regions that have previously been implicated in task performance and associational learning, the basolateral amygdala and the medial prefrontal cortex.

The Medial Prefrontal Cortex

In rodents, the mPFC is identified as the agranular frontal lobe and is partitioned into the anterior cingulate (ACC), the prelimbic (PL), and the infralimbic (IL) cortices. Here we will focus on the PL and IL. PL and IL are defined by different cytoarchitectonic features, laminar organization, and projection patterns, with the PL dorsal to the IL (Giustino and

Maren 2015). The IL receives and projects to autonomic areas such as the parabrachial nucleus, the lateral preoptic areas, central amygdala, nucleus accumbens, and posterior hypothalamus (Vertes 2004). Thus, IL is thought to be critical for modulation of autonomic or affective functions. In contrast, the PL mainly receives and targets cognitive and limbic structures such as the striatum, the basolateral amygdala, the orbitofrontal cortex, and the raphe nuclei.

Several previous studies have demonstrated that the PL and IL may have opposing roles in fear learning (Vidal-Gonzalez et al. 2006; Sierra-Mercado et al. 2011). While inactivation of IL appears to impair the acquisition and expression of extinction learning, it had no effect on fear learning. In contrast, while inactivation of PL impaired learned fear expression, it had no effect on extinction learning. Therefore, whereas PL promotes fear learning, IL promotes fear extinction. However, a recent study has shown that pyramidal neurons in PL project to pyramidal neurons in IL, and that the activation of this connection enhances fear extinction, thus redefining the role of the PL in extinction learning (Marek et al. 2018).

The role of the IL and PL in appetitive learning is less well-understood. Previous recording studies in the mPFC have revealed correlates that are thought to be related to the anticipation of reward (Pratt and Mizumori 2001; Miyazaki et al. 2004; Mulder et al. 2003). Recent imaging experiments have revealed that the PL acquires responses to rewarded but not unrewarded auditory cues in a classical conditioning task (Otis et al. 2017). Segregated populations of pyramidal neurons project to the striatum and thalamus; while striatal projectors acquire excitatory responses to rewarded cues, thalamic projectors develop inhibitory responses. Bidirectional manipulation of these neurons reflect their tuning; exogenous activation of corticostrial neurons promotes reward-seeking behavior, while corticothalamic

neurons suppresses reward-seeking. Moreover, it does not appear that PL and IL responses differ significantly; both the PL and IL exhibits prominent excitatory responses during rewarded but not unrewarded lever presses in an operant learning task (Burgos-Robles et al. 2013). We therefore asked whether the mPFC (PL and IL) encodes learned sensory cues and whether it is necessary during appetitive learning.

4.2 Results

mPFC Encodes Positive and Negative Value and Is Necessary for Continued Task Performance

Using same methods as described in Chapter 2, we imaged mPFC population responses. We were able to track an average of 60 mPFC neurons per animal across multiple training days. Prior to learning, few mPFC neurons were responsive to naive odors (15% to a given odor, Figure 4.1.A). Moreover, neural responses in mPFC were also largely unresponsive to water (>10% to water, Figure 4.1.B).

We then trained a single mouse in the head-fixed discrimination assay as described in earlier chapters. Unlike what we have previously observed in the OFC, mPFC neurons acquired potentiated responses to both CS+ and CS- odors. These responses also appear to be independent of US responses, and most responses appear to start immediately or close to odor onset. One subpopulation of cells (30%) acquired strong responses to CS+ odors, and another subpopulation (30%) acquired strong responses to CS- odors (Figure 4.1). Moreover, the ensembles of distinct CS+ odors shared high overlap after learning,

and this was similarly the case for CS- odors. Overlap increased from an average of 30% before training to 70% after training when comparing the two CS+ ensembles, and from 30% to 60% for CS- ensembles. However, the ensembles of any CS+ and CS- odor were largely non-overlapping, decreasing from 50% to 20% after training. Therefore, unlike the OFC, not only do CS- odors activate the mPFC, the representation of CS- odors are also non-overlapping with CS+ odors after learning (Figure 4.8). Therefore, the mPFC appears to encode both positive and negative value while discarding odor identity. The encoding of signed value suggest to us that the mPFC may be driving both the licking to CS+ odors and also the suppression of licking to CS- odors.

We then asked whether this representation is maintained after initial task acquisition, unlike what we have observed in the OFC. To test this, we imaged the mPFC using the same composite pre-training and discrimination task that we have used in OFC learning tasks, as described in Chapter 3. Like before, mice underwent pre-training to a single CS+ odor and once they have learned the task, they were then switched onto a discrimination assay where two new CS+ and CS- odors were presented. When we imaged the mPFC within this composite task, we observed responses that had time courses that were the opposite of what we had previously seen in the OFC.

mPFC neurons did not acquire significant numbers of CS+ neurons during pre-training (25% before learning to 28% after learning). However, during discrimination training, mPFC neurons acquired robust and numerous responses to both CS+ and CS- odors, similar to what we have previously observed during discrimination training without pre-training (Figure 4.2). After learning discrimination training, the number of neurons responsive to CS+ odors increased from an average of 18% before learning to 30% after learning, and

this was also the case for neurons responsive to CS- odors, increasing from 20% before learning to 30% after learning (Figure 4.3.A).

In contrast, we observe the exact opposite in the OFC. Within the OFC, the biggest change in representation occurred during pre-training, where the CS+ representation increased from 28% to 40%. However, during subsequent discrimination training, the size of the CS+ ensemble did not significantly change when learning the value of new CS+ odors (26% to 28%) (Figure 4.3.B). These sets of results suggest that the mPFC is more engaged during discrimination learning compared to during pre-training, whereas the exact opposite is true in the OFC.

Moreover, not only are mPFC odor responses more consistent after discrimination learning compared to after pre-training, they are also stronger. When we pooled the set of neurons responsive to CS+ odors and computed the average odor-evoked DF/F of this population, the response was greater after discrimination learning as compared to after pre-training (Figure 4.4.A-C). This was also the case if we compared either CS- or CS+ responses after discrimination training to responses evoked by the same respective odors before training started. However, this was not the case for responses in the OFC (Figure 4.4.A-C).

Our past OFC imaging results reveals that the OFC is active early during task acquisition but not late during the learning of subsequent associations. These imaging results generated the hypotheses that silencing the OFC early may produce learning deficits, whereas silencing it late may have no effect, and both were confirmed using optogenetic perturbation experiments. Our current mPFC imaging results now reveals that the mPFC is silent early during task acquisition but is recruited during the learning of subsequent associations. In the same way, we hypothesize that the mPFC be necessary for generalizing what mice

have previously learned for the learning of new associations. We therefore silenced the mPFC during pre-training and separately during discrimination training to assess mPFC's contribution to both task acquisition and task generalization.

For this purpose, we used the same freely moving paradigm described before in Chapter 3, and optogenetically inhibited the mPFC bilaterally either during the pre-training epoch or during the subsequent discrimination epoch. Silencing the mPFC during the pre-training phase did not appear to inhibit task performance, as mice took an average of 500 trials to learn in either the control or experimental condition (Figure 4.6). As described earlier, control mice in this task generalize their learned behavior in pre-training by licking in anticipation to all new CS+ odors at the start of discrimination. However, silencing the mPFC during discrimination training impairs the mouse's ability to generalize. Licking at the onset to CS+ odors is drastically reduced from an average of 30% time spent licking to 8%, suggesting that mice have forgotten what it has previously learned during pre-training (Figure 4.7). Mice then appear to re-learn licking to CS+ odors by initially licking to all odors (CS+ and CS- odors, during trials 0-100) and then refining anticipatory licking to only CS+ odors. In addition to impairing initial generalization, mPFC silencing also appears to impair licking to CS+ odors in a subset of mice for a prolonged duration. The rate of false negatives to CS+ odors (failure to display anticipatory licking to CS+ odors) remained high throughout the entire training period for 2/5 mice during mPFC inhibition, whereas other mice were similar to controls (Figure 4.7). Suppression of licking to CS- odors was unaffected in all mice; the rate of false positive licking to CS+ odors were similar to controls (Figure 4.7).

In summary, whereas OFC silencing drastically impairs task acquisition during pre-

training, mPFC silencing impairs the learning of new associations after initial acquisition (Figure 4.5). This suggests to us that the brain learns to form associations through a set of parallel but interconnected series of brain regions that are specialized during different phases of learning.

4.3 Discussion

We observe multiple deficits in learning the discrimination task when silencing the mPFC using halrhodopsin. First, mice fail to generalize what they have learned during pre-training and appear to re-learn the task anew. This result implies that at the very start of discrimination, the mPFC is required for generalizing what it has previously learned to new odor stimuli. Early in discrimination learning, most odor-evoked responses are non-specific, suggesting that the mPFC is treating CS+ and CS- odors similarly. Therefore, it is possible this population of non-selective odor-responsive neurons in the mPFC is responsible for driving odor generalization during the initial phase of discrimination learning after pre-training. Some mice (2/5 mice) fail to learn even after pro-longed training when the mPFC is silenced. These results agree with our observation that mPFC activity tracks the value of both CS+ and CS- odors during discrimination learning. We give reasons for why different prefrontal areas may be engaged in during different phases of learning in chapter 5.

A recent imaging paper also imaged CS+ and CS- odors during an auditory classical conditioning task (Otis et al. 2017). The task variables that Stuber and colleagues have employed were virtually identical to ours except that they also used a viral approach to transfect neurons with GCaMP6s. They observed that 35% of mPFC neurons acquired

responses to CS+ odors, and no neurons acquired responses to CS- odors as a consequence of learning. In contrast, we observe slightly fewer neurons that acquire responses to CS+ odors (30%), but we also observe a significant fraction of neurons that acquire responses to CS- odors (30%). Injection coordinates used were also similar in both studies, focusing on the PL cortex (Stuber: +1.85 mm AP, +- 0.50 mm ML, -2.20 mm DV; us: +1.65 mm AP, +- 0.40 mm ML, -2.00 DV). One possible explanation for this difference is that auditory cues may elicit a different learned representation than olfactory cues. Another possible is that these differences may be due to a viral transfection issue as described in the subsequent chapter.

Figure 4.1

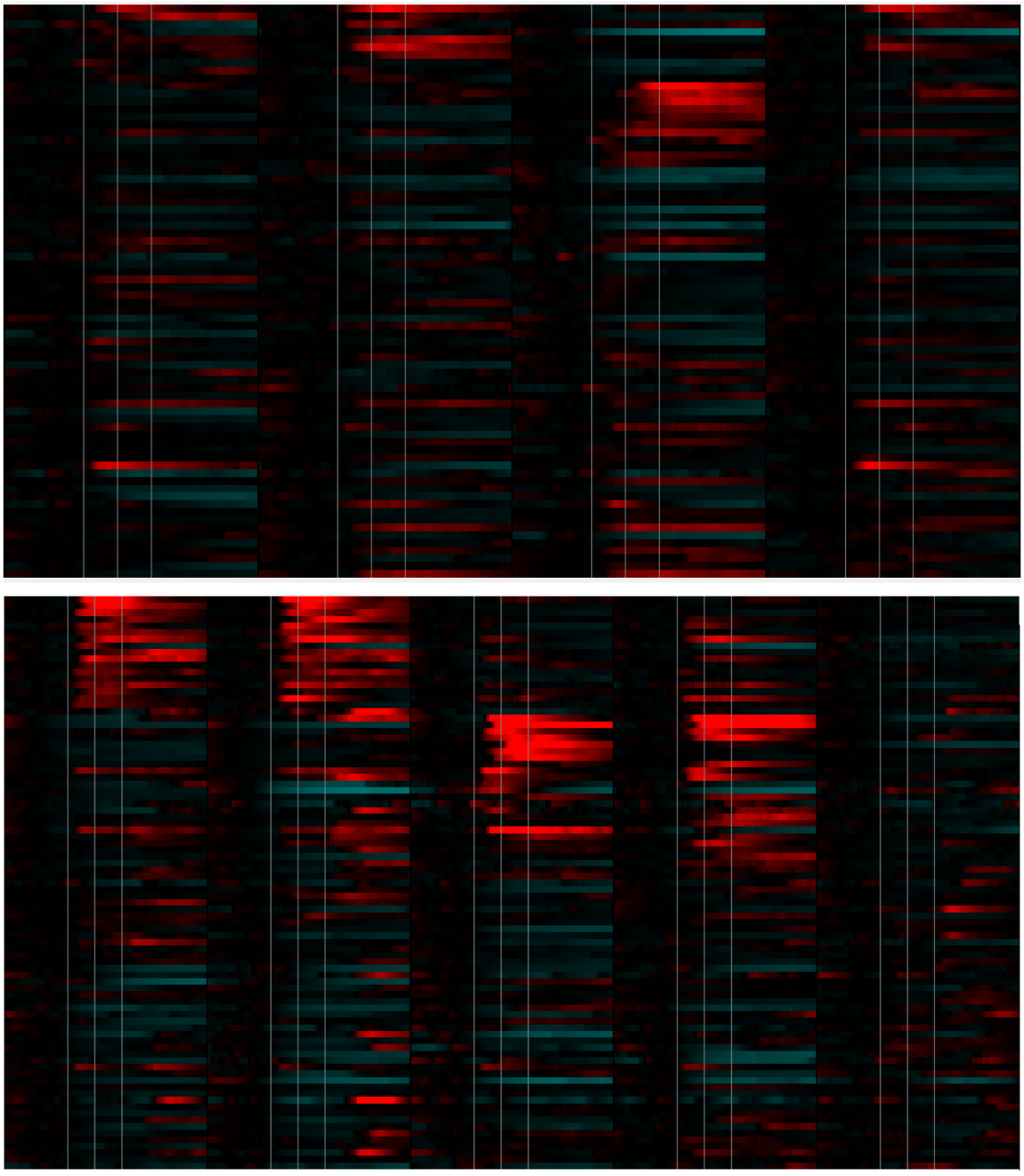

Figure 4.1. mPFC Population Activity Before and After Learning mPFC responses in an example mouse. Each row denotes a single cell's trial-averaged DF/F responses to CS+1 (PIN), CS+2 (MSY), CS-1 (EUY), CS-2 (LIM). Response to water is the 5th column (bottom). Scale bars indicate an increase in DF/F (red) or a decrease in DF/F (blue) relative to baseline. Responses prior to learning (top). 20% of neurons respond to CS+ odors after learning (bottom). Moreover, a non-overlapping set of 20% of neurons respond to CS- odors after learning.

Figure 4.2

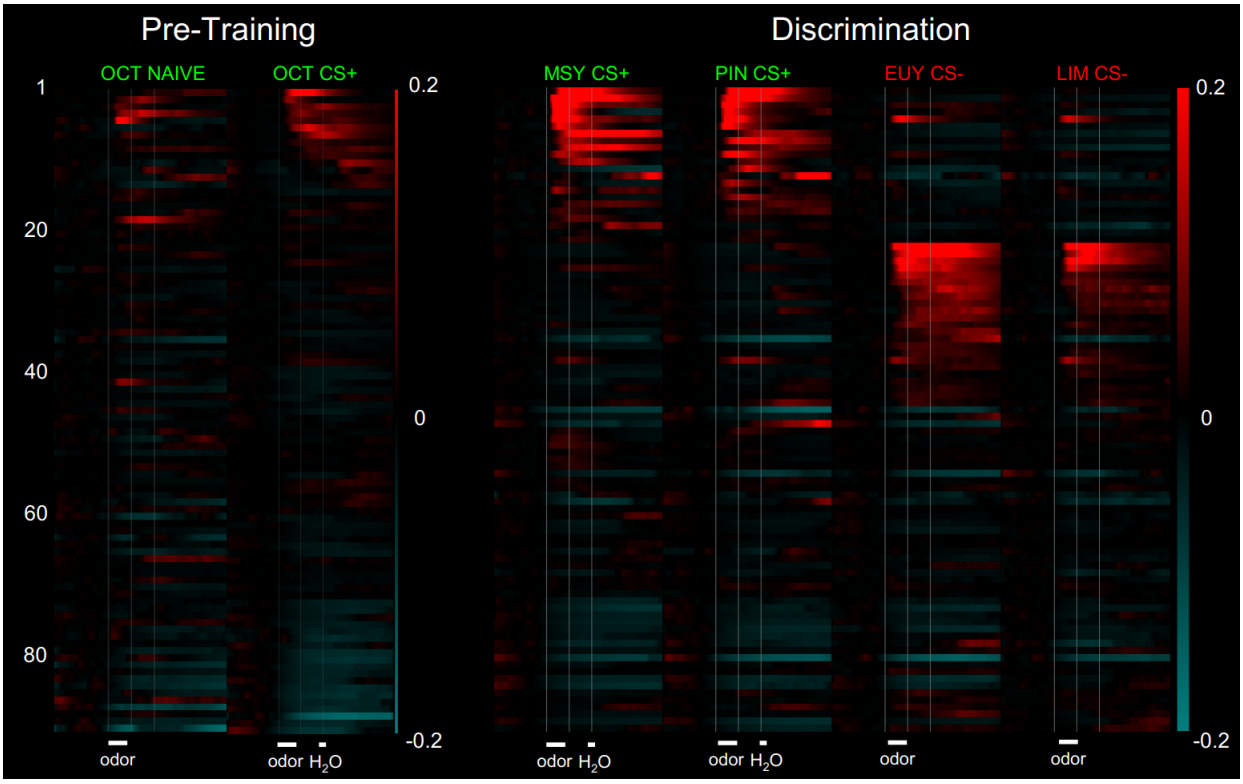
Pre-Training
Discrimination
OCT NAIVE
OCT CS+
MSY CS+
PIN CS+
EUY CS-
LIM CS-
1
20
40
60
80
0.2
0
-0.2
odor
odor H2O
odor H2O
odor H2O
odor
odor

Figure 4.2. mPFC is Engaged During Learning of Subsequent Associations Population response of mPFC neurons to CS+ and CS- odors during pre-training and discrimination. Left: the CS+ odor used was OCT, or octanal. Few potentiated responses were observed after learning the pre-training task compared to prior to pre-training. Right: responses to CS+ and CS- odors when mice have learned to lick to CS+ odors and suppress to CS- odors during subsequent discrimination training. Robust activation was observed to CS+ odors and also to CS- odors in non-overlapping sets of neurons.

Figure 4.3

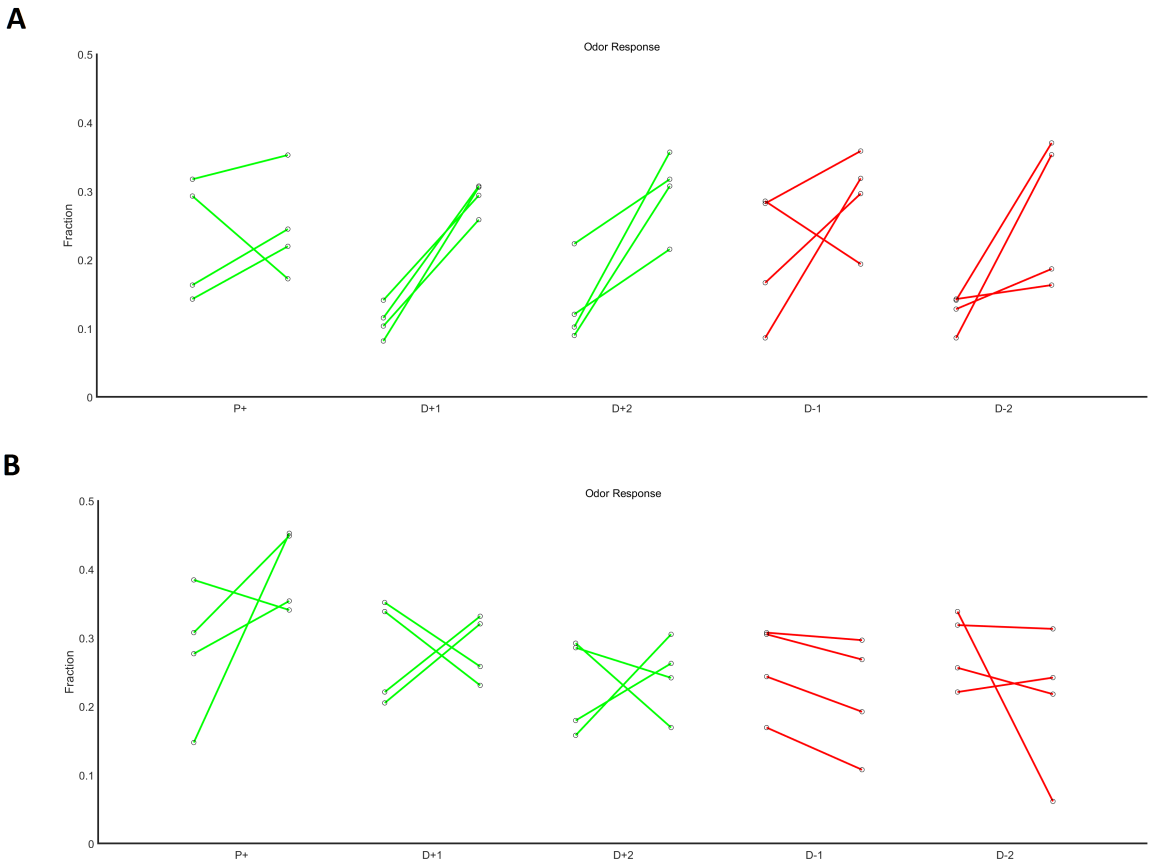
A
Odor Response
Fraction
0.5
0.4
0.3
0.2
0.1
0
P+
D+1
D+2
D-1
D-2
B
Odor Response
Fraction
0.5
0.4
0.3
0.2
0.1
0
P+
D+1
D+2
D-1
D-2

Figure 4.3. mPFC and OFC Responses Have Opposite Time-courses During Pre-Training and Discrimination Quantification of number of neurons that are responsive to the pre-trained CS+ odor, the discrimination CS+ odors, and the discrimination CS- odors before and after learning. Each line represents responses from a single mouse. **A.** mPFC responses (n = 4). **B.** OFC responses (n=4). Whereas the mPFC population did not acquire significant numbers of CS+ neurons during pre-training, a significant percentage of neurons were potentiated to either CS+ odors or CS- odors during discrimination training. In contrast, in the OFC, the most significant changes occured during pre-training, and no significant changes occured in either the CS+ or CS- ensemble during discrimination training.

Figure 4.4

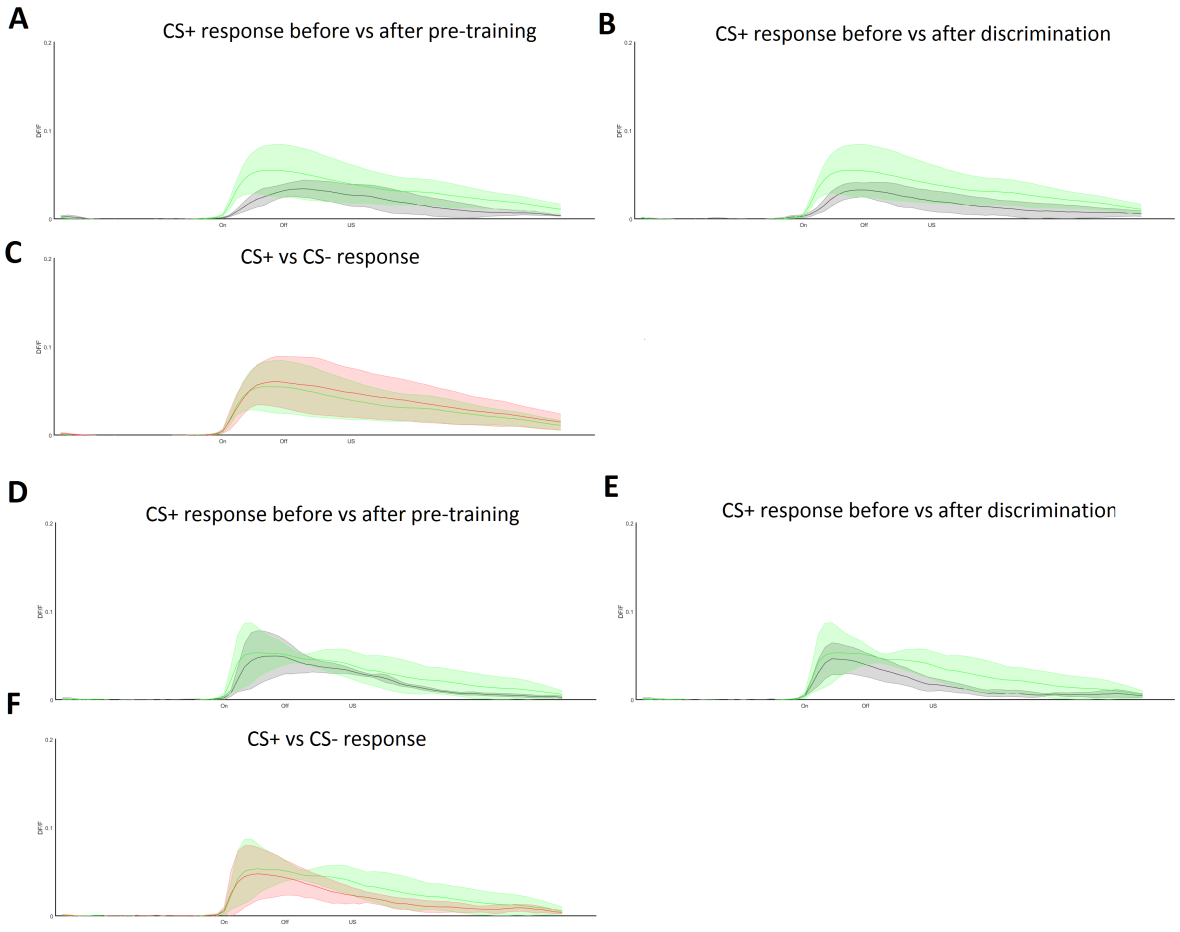
A
CS+ response before vs after pre-training
B
CS+ response before vs after discrimination
C
CS+ vs CS- response
D
CS+ response before vs after pre-training
E
CS+ response before vs after discrimination
F
CS+ vs CS- response

Figure 4.4. mPFC CS+ Responses are greater in amplitude after discrimination learning Quantification of response amplitude (power) for all responses categorized as statistically significant from baseline. The responses of all neurons that are deemed statistically significant were averaged. Shading denotes the SE of responses of different mice. Top: mPFC. Bottom: OFC. **A.** Comparing the average amplitude of significant CS+ responses after pre-training to CS+ responses after discrimination training. **B.** Comparing the amplitude of significant CS+ responses before discrimination to CS+ responses after discrimination training. **C.** Comparing CS+ and CS- responses after discrimination training. **D-F.** Same, except for OFC.

Figure 4.5

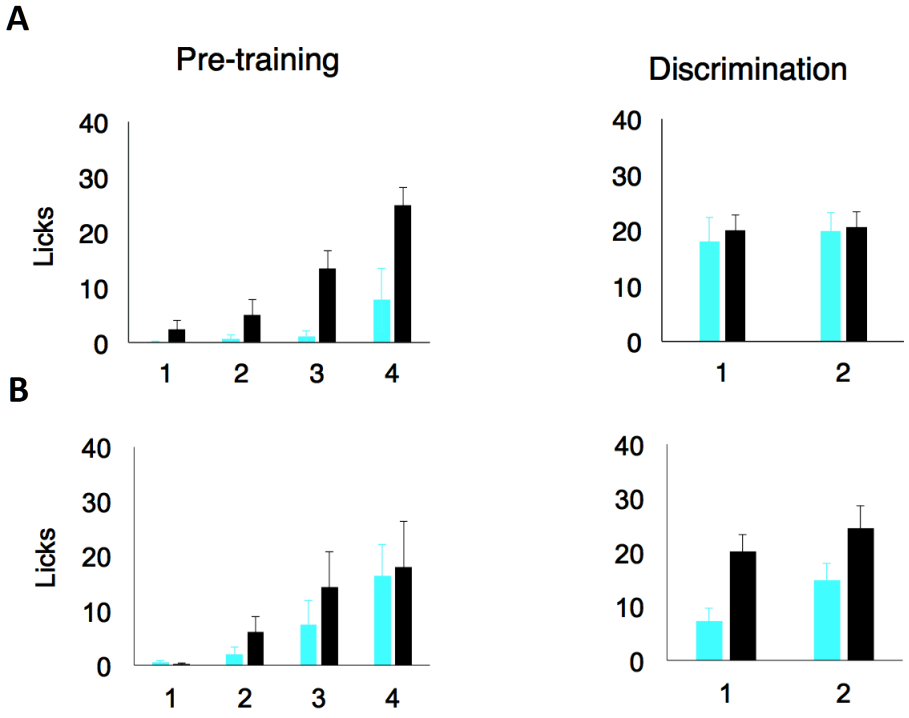
A
Pre-training
Discrimination
Licks
40
30
20
10
0
1
2
3
4
B
Licks
40
30
20
10
0
1
2
3
4

Figure 4.5. mPFC is Necessary for Learning of Subsequent Associations Quantification of learning rate during pre-training and discrimination without and without inhibition in OFC. Red: OFC inhibition with halorhodopsin. White: YFP controls. Learning performance was quantified as average anticipatory lick rate for each day of training. **A.** Silencing the OFC impairs licking to CS+ odors during pre-training but not during subsequent discrimination. **B.** The opposite phenotype is observed for mPFC silencing.

Figure 4.6

A

Anticipatory CS plus licks

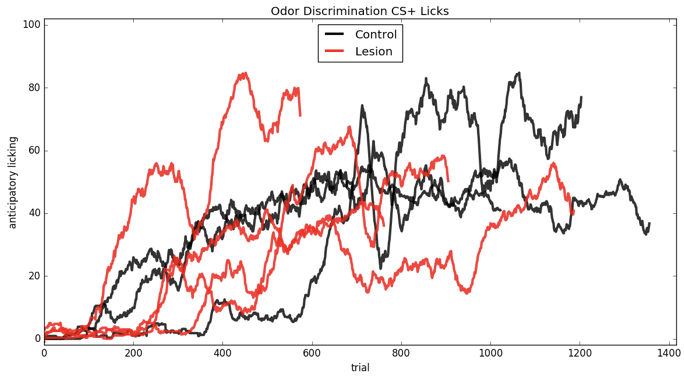

B

False negatives

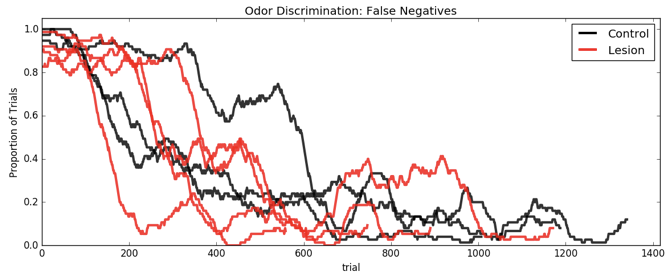

Figure 4.6. Inhibition of mPFC During Pre-training does not Impair Learning A. Amount of anticipatory licking as a function of trials during pre-training. Y axis scores the percentage of time that the mouse spent licking prior to water delivery, measured in a two second time window. Black trace are control mice, red trace are experimental mice. Control mice have YFP bilaterally injected into the mPFC, and with laser is turned on. Experimental mice have halorhodopsin bilaterally injected into the mPFC, also with laser turned on. We observe that mPFC silencing does not impair anticipatory licking **B.** mPFC inhibition also does not inhibit anticipatory licking as measured by rate of false positives (no anticipatory licking to the CS+ odor).

Figure 4.7

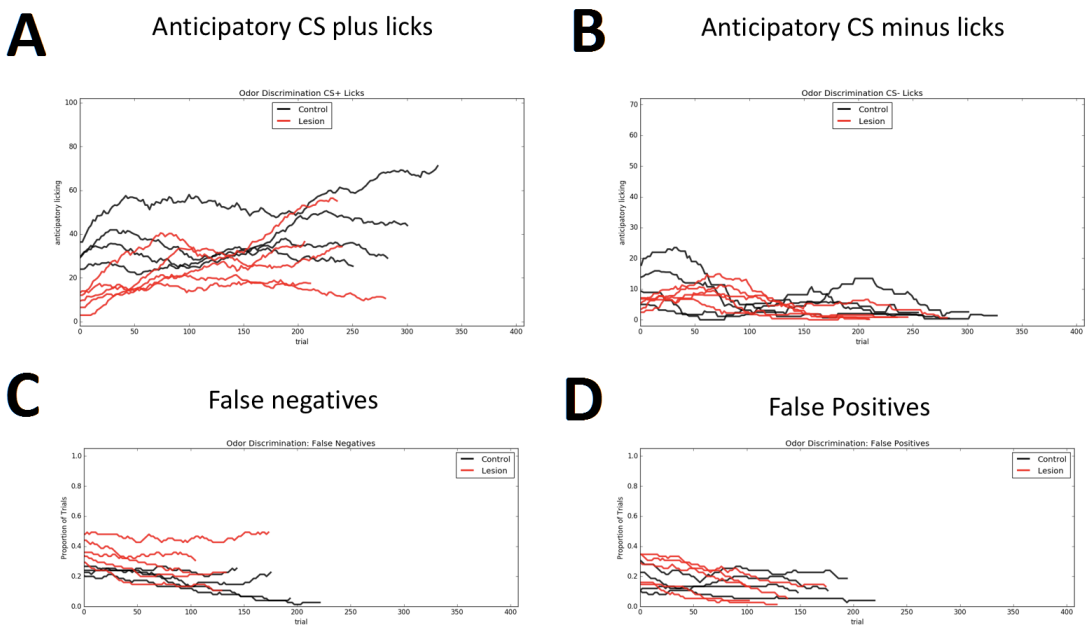
A
Anticipatory CS plus licks
B
Anticipatory CS minus licks
Odor Discrimination CS+ Licks
Odor Discrimination CS- Licks
Control
Lesion
anticipatory licking
trial
C
False negatives
D
False Positives
Odor Discrimination: False Negatives
Odor Discrimination: False Positives
Proportion of Trials

Figure 4.7. Inhibition of mPFC During Discrimination Training Impairs Learning A, B. Silencing the mPFC during discrimination training impairs the mouse's ability to generalize what it has learned during pre-training at the onset of discrimination. Licking at the onset to CS+ odors is drastically reduced, suggesting that mice have forgotten what it has previously learned. This is also reflected by the initially low lick rate to CS- odors. Mice then appear to re-learn licking to CS+ odors by initially licking to all odors (CS+ and CS- odors, during trials 0-100) and then refining anticipatory licking to only CS+ odors. **C, D.** mPFC silencing also appears to impair licking to CS+ odors in a subset of mice (false negatives to CS+ odors), but not the suppression of licking to CS- odors (false positives to CS- odors).

Figure 4.8

Figure 4.8. mPFC generates non-overlapping CS+ and CS- ensembles Quantification of overlap between CS+:CS+ ensembles,CS-:CS- ensembles, and CS+:CS- ensembles. Overlap increases between CS+:CS+ and CS-:CS- ensembles, and decreases between CS+:CS- ensembles as a result of training.

Chapter 5

The Basolateral Amygdala

5.1 Introduction

We have delineated a circuit where sensory identity from the piriform is transformed into a representation of predicted value in the OFC and mPFC. However, limbic structures have also been previously implicated in associational learning. We describe a set of imaging and inhibition experiments to assess the representation and function of the basolateral amygdala during appetitive learning.

The Basolateral Amygdala

Piriform projects to the basolateral amygdala (BLA), a structure in the medial temporal lobe that is critically required for the acquisition and expression of aversive olfactory learning (Sosulski et al. 2011; Shepherd 1998). Subjects with lesions in the BLA are unable to form associations between auditory, visual, gustatory, or olfactory cues with aversive outcomes (Campeau and Davis 1995; Cousens and Otto 1998). Therefore, BLA activity is required for both the acquisition and expression of learned fear.

The BLA receives extensive sensory input from all modalities through both cortical and subcortical routes (Sah et al. 2003; Romanski and LeDoux 1992; Shi and Davis 2001).

Moreover, input from neuromodulatory systems onto the BLA has been proposed to convey additional information about unconditioned stimuli (Schultz 2001). BLA is also innervated by structures implicated in cognitive processes. For example, the BLA receives dense innervation from the orbitofrontal cortex, which may afford the amygdala access to rapid updates to the expected value of the CS cues (Carmichael and Price 1995).

The BLA also sends projections to both cortical and subcortical structures to mediate the cognitive, behavioral, and physiologic output integral to an emotional response (Sah et al. 2003). Efferent projections to cortical areas have been implicated in numerous cognitive processes, such as memory consolidation (Quirk et al. 1997). Projections to striatum may support instrumental learning (Stuber et al. 2010), and projections to the extended amygdala may elicit changes in autonomic reactivity, such as increases in anxiety-related behaviors (Kim et al. 2013).

In summary, the amygdala receives input from sensory areas and from neurmodulatory areas that convey information regarding unconditioned stimuli, and projects to downstream structures are capable of eliciting behavior. These facts suggest that the amygdala may be capable of associating sensory stimuli with unconditioned stimuli to generate appropriate learned responses. Indeed, electrophysiological recordings have observed that both the amplitude and the number of CS-evoked BLA responses increased when the CS has been repeatedly paired with US (Tye et al. 2008; Rosenkranz and Grace 2002; Rosenkranz and Grace 2003). Moreover, this potentiation appears to occur in a dopamine-dependent manner (Rosenkranz and Grace 2002; Rosenkranz and Grace 2003). This plasticity appears to precede the development of learned behavioral responses to the cue and is therefore believed to drive learning (Quirk et al. 1997). Further support comes from studies that show

that depression of synaptic inputs into the BLA conveying sensory information can abolish previously acquired cue-evoked fear memory (Nabavi et al. 2014).

How does the BLA link associations between the CS and US during learning? Recent studies have demonstrated that the exogenous activation of US-responsive cells in the BLA elicits valence-specific responses (Gore et al. 2015). US ensembles driving behaviors of opposing valence are non-overlapping, and the activation of US-responsive BLA neurons is both sufficient and necessary for the expression of a conditioned response. During learning, it appears from immediate-early gene data that the representation of CS cues increases in overlap with the US representation, suggesting that US responsive neurons acquired CS responses (Gore et al. 2015). This convergence of a CS representation onto a US ensemble in the BLA is required for the expression of the conditioned response. Therefore, representations of sensory stimuli connect to a US representation in the BLA to elicit both innate and learned responses.

Given these facts, we believe that the BLA may encode the long-term memory of a simple olfactory association. We therefore imaged the BLA during an appetitive task to assess whether BLA neurons potentiate CS+ responses in a mechanism that is consistent with Hebbian learning. We expect that CS+ responses are only acquired by neurons that respond to US. On the other hand, recently published results using calcium imaging have found that aversive learning-related changes are not predicted by US responses, suggesting that Hebbian potentiation does not drive learning-dependent changes in the BLA (Grewe et al. 2017). We also assessed whether this representation remains stable during the entire course of learning, consistent with an brain area whose function is to store a long-term memory of a learned association.

Extensive evidence has established the importance of BLA in aversive learning, but its role in appetitive learning is more nuanced (Balleine and Killcross 2006; Everitt et al. 2003; LeDoux 2000). While experiments have demonstrated that the activation of appetitive US representation in the BLA can elicit appetitive innate responses (Tye et al. 2008; Gore et al. 2015), lesion and pharmacological inactivation studies indicate that BLA is not necessary for the formation of simple appetitive associations (Hatfield et al. 1996; Holland 1997). We thus also ask whether inhibition of BLA impairs appetitive learning.

5.2 Results

BLA Encode Predicted Value

As detailed in Chapter 1, we again implanted microendoscopes above the BLA of transgenic GCaMP6S mice (VGLUT2-ires-Cre X rosa-FLEX-GCaMP6S) and imaged BLA population responses during the same head-fixed olfactory appetitive learning task (Vong et al. 2011; Madisen et al. 2015). We were able to track an average of 35 BLA neurons per animal across multiple training days. CS+, CS-, and US responses were imaged before, during, and after learning.

Compared to the OFC, calcium activity rarely increase without cue presentation, so BLA neurons display low levels of spontaneous activity. Prior to learning, 10% of neurons were responsive to odor, and as in the OFC, these responses were non-selective (Figure 5.1.A). As a consequence, a binary decoder performed at near chance level at distinguishing between all pairs of odors, suggesting that odor identity is not encoded in the BLA prior to

learning (Figure 5.2.A). We also found that 35% of BLA neurons were responsive to the US.

As in the OFC, BLA neurons acquired potentiated responses to CS+ odors but not CS- odors during learning (Figure 5.1.B, 3.4). Again, the representations of the different CS+ odors are almost identical (Figure 3.4). The level of overlap between the two CS+ odors increased from 30% prior to learning to 90% post learning (Figure 3.5). Moreover, responses to CS+ odors also appear identical in a majority of neurons. Given the similarity between population responses to different CS+ odors, linear decoders were unable to successfully decode their identity as well. Value, on the other hand, was easily decoded when comparing the responses between any pair of CS+ and CS- odor (Figure 5.2.B). A major difference between BLA and OFC responses is that most CS+ responses are acquired by neurons that are US-responsive (Figure 3.5). Almost all neurons (90%) that are US-responsive acquired CS+ responses. Conversely, 80% of neurons that are responsive to CS+ also respond to the US. This suggests that a Hebbian mechanism may elicit potentiation of CS+ responses through the convergence of sensory and US information.

Responses to CS+ odors in the BLA appear temporally homogeneous and had similar waveforms, durations, and onset times (Figure 5.5). To confirm this observation, we performed a principal component analysis (PCA) on the population PSTH of all BLA neurons to quantify the variability of activity evoked by BLA neurons in response to cue delivery. We observed that almost all the variance (80%) was accounted for by the first principal component. Therefore, the first PC is essentially an exemplar neuron which displays robust odor-locked responses to both CS+ odors and the US, and to a good approximation, all CS+ responses in the BLA are approximately scaled copies of the first PC. In addition to

the temporal homogeneity of responses, we also observe that BLA responses are far more consistent across days compared to OFC responses (Figure 3.5). 80% of CS+ responses and 75% of US responses were retained across consecutive imaging days.

We also tested whether the BLA encodes predicted value by imaging the BLA during manipulations of internal state, context, and reversal learning. Conclusions derived from these experiments were identical to that of the OFC. The majority of CS+ neurons in the BLA completely reversed their selectivities to CS+ and CS- odors during reversal learning (Figure 5.6.A, B, C). After reversal, all neurons (40% of the BLA representation) lost their responses to the old CS+ odors and acquired responses to new CS+ odors. Moreover, BLA responses were also sensitive to state and context (Figure 5.6.E,F). Again, nearly all neurons that are responsive to CS+ odors (40% of BLA representation) lost their CS+ responses when mice were not thirsty or when the lick port was not present. The average DF/F of CS+ responsive neurons decreased from 10% DF/F to 1% DF/F after manipulating state or context. Therefore, nearly all BLA neurons updated their responses in a way that is consistent with the encoding of expected value.

BLA Is Not Necessary for Appetitive Learning

The OFC and BLA share dense direct reciprocal connections and also interact through thalamic relays (Barbas and Pandya 1984; Cavada et al. 2000). A number of papers have suggested that functional interactions between BLA and OFC contribute at least in part to a battery of goal-directed behaviors (Baxter et al. 2000; Saddoris et al. 2005; Takahashi et al. 2009; Pickens et al. 2003; Lichtenberg et al. 2017). Moreover, associative encoding

in one region has generally been shown to be altered by lesions of the other (Saddoris et al. 2005; Schoenbaum et al. 2003; Rudebeck et al. 2013). However, the unique contribution of each region towards associative learning and towards a representation of value is still up to debate. We therefore wanted to ask if either region is necessary for appetitive learning, and whether they have differential roles during the learning process.

We therefore used optogenetics to bilaterally inhibit the OFC while assessing the effects of that inhibition through behavior and through the representation in the BLA. We also did the converse experiment of inhibiting the BLA and simultaneously imaging the OFC. The red-shifted rhodopsin, JAWS, provided an activation wavelength that is separated from the excitation and emission spectra of GCaMP6, and we combined JAWS activation with smultaneous GCaMP imaging (Chuong et al. 2014) (Figure 3.13).

Inhibition of BLA did not appear to inhibit behavioral performance. Mice took, on average, the same number of trials to learn to lick to CS+ odors compared to controls (average of 38 trials for control mice as compared to 36 trials for mice with BLA inhibition) (Figure 5.7). Moreover, the learned representation in the OFC appeared to be spared. A similar proportion (35%) of CS+ responsive neurons were observed in the OFC when the BLA is silenced compared to when the BLA is intact (Figure 5.7). Moreover, these responses had similar attributes as those without BLA inhibition, including the fraction overlap between two different CS+ ensembles (60 % overlap), and responses to US before and after learning (20% of OFC were US-responsive) (Figure 5.7). Moreover, we further replicated this task in freely moving mice and found that again, BLA inhibition did not impair either pre-training or discrimination learning if discrimination was preceded by pre-training (not shown).

In contrast, as we have already described in chapter 3, OFC inhibition caused profound learning deficits in most mice. We observe fewer CS+ responsive BLA neurons compared to controls (50% vs 30% in control vs inhibited conditions, Figure 5.7). Moreover, these responses were weak in amplitude and also inconsistent across trials compared to controls. To quantify response consistency, we used AUC (area under Receiver Operating Characteristic) to measure the extent of the difference between odor-evoked trials relative to baseline, with the baseline defined as the 5 second period prior to odor delivery. An AUC of 1 implies that the odor evoked a robust excitatory response that is perfectly distinguishable from baseline fluctuations on every single trial. We averaged the AUC values of the top 20% responders for CS+ odors on each day, and compared BLA responses with and without inhibition. The AUC values of BLA responses with OFC inhibition in the 2 mice with learning deficits were smaller than that without BLA inhibition, averaging under 0.8 compared to over 0.95. Given that the top 20% of responders also attained an average of .8 AUC in the three days of training prior to learning in the control mice, this suggests that learning did not cause CS+ odors to drive activity in the BLA in a consistent way when the OFC was silenced (Figure 5.7). Equivalent results were obtained choosing the top 10-40% of responders.

The degree of impairment in BLA CS+ responses was variable across different mice. 2 of 5 OFC-inhibited mice learned normally, whereas 3/5 mice were unable to learn the task. If the BLA representation was causally driven by OFC activity, we would expect that OFC silencing to abolish the CS+ representation in the BLA regardless of whether they learned the task or not. Conversely, if the BLA representation tracked behavior and was independent of OFC silencing, we would expect that BLA activity tracked learning

performance. In support of the latter, we found that the BLA representation of a OFC-silenced mouse that learned normally was unimpaired (Figure 5.9). After analyzing the degree of viral infection, optrode placement, and light loss through the optical fiber post-mortem, there was no reason to assume that OFC silencing did not work. Therefore, the BLA representation appears to track learning independent of OFC silencing.

5.3 Discussion

BLA

Our imaging of the BLA agrees with the large corpus of slice and anesthetized recording data suggesting that Hebbian learning drives synaptic potentiation of sensory inputs onto US-responsive cells in the BLA. In our study, the vast majority of US-responsive neurons acquire CS+ responses after learning; likewise, most CS+ responsive neurons are US-responsive, and very few arise from cells that are not US-responsive. Our BLA imaging results differ from a recently published paper that also images calcium dynamics in the BLA during learning. Schnitzer and colleagues observe that learning-related changes are not predicted by the neuron's response to US before learning (Grewe et al. 2017). In their study, the majority of US responsive cells do not acquire a CS+ response, suggesting that Hebbian potentiation does not drives learning-dependent changes. Several experimental differences may explain the discrepancy in our results. First, auditory cues are used in place of olfactory cues in their task. Second, mice are subjected to fear learning instead of appetitive conditioning. Third, instead of using transgenic mice, viral vectors were used to

express GCaMP in their study. These two expression strategies drive significantly different levels of GCaMP expression. In our particular mouse line, we observe no instances of over-expression in all of our imaging data, and expression levels were relatively uniform across different neurons (Madisen et al. 2015). Viral vectors generate more non-uniform and far greater expression levels, and over-expression of calcium sensors may tax cell integrity, leading to errant responses that may not be representative of normal neuronal function.

Several previous studies have shown that the BLA is necessary for fear learning (Gore et al. 2015; Walker et al. 2005; Cousens and Otto 1998). Recent studies have shown that the photoactivation of nicotine-responsive BLA neurons can generate appetitive behavioral responses and also reinforce appetitive olfactory learning, and we have now shown that a representation of CS+ odors is maintained in the BLA throughout learning. However, the necessity of this representation for appetitive learning has not been demonstrated. We have now shown that BLA activity does not appear to be required for an appetitive discrimination task in which a mouse is trained to lick in response to an odor that predicts a water reward. This is in agreement with previous inactivation studies showing that the BLA is not necessary for the formation of simple appetitive CS-US associations in other sensory modalities (Hatfield et al. 1996; Holland 1997). Moreover, recent unpublished results from our lab have shown that while the projection from piriform to the BLA is necessary for olfactory fear learning, it is not necessary for olfactory appetitive learning (Felicity Gore, unpublished). Therefore, while a representation of CS+ odors is maintained throughout learning, and while the BLA activity is sufficient to drive innate appetitive responses, it is not necessary for learning appetitive olfactory associations either early or late during learning. We believe that there must be a subtle behavioral function that the BLA must subserve

during appetitive learning, ones in which our task is not designed to reveal.

Figure 5.1

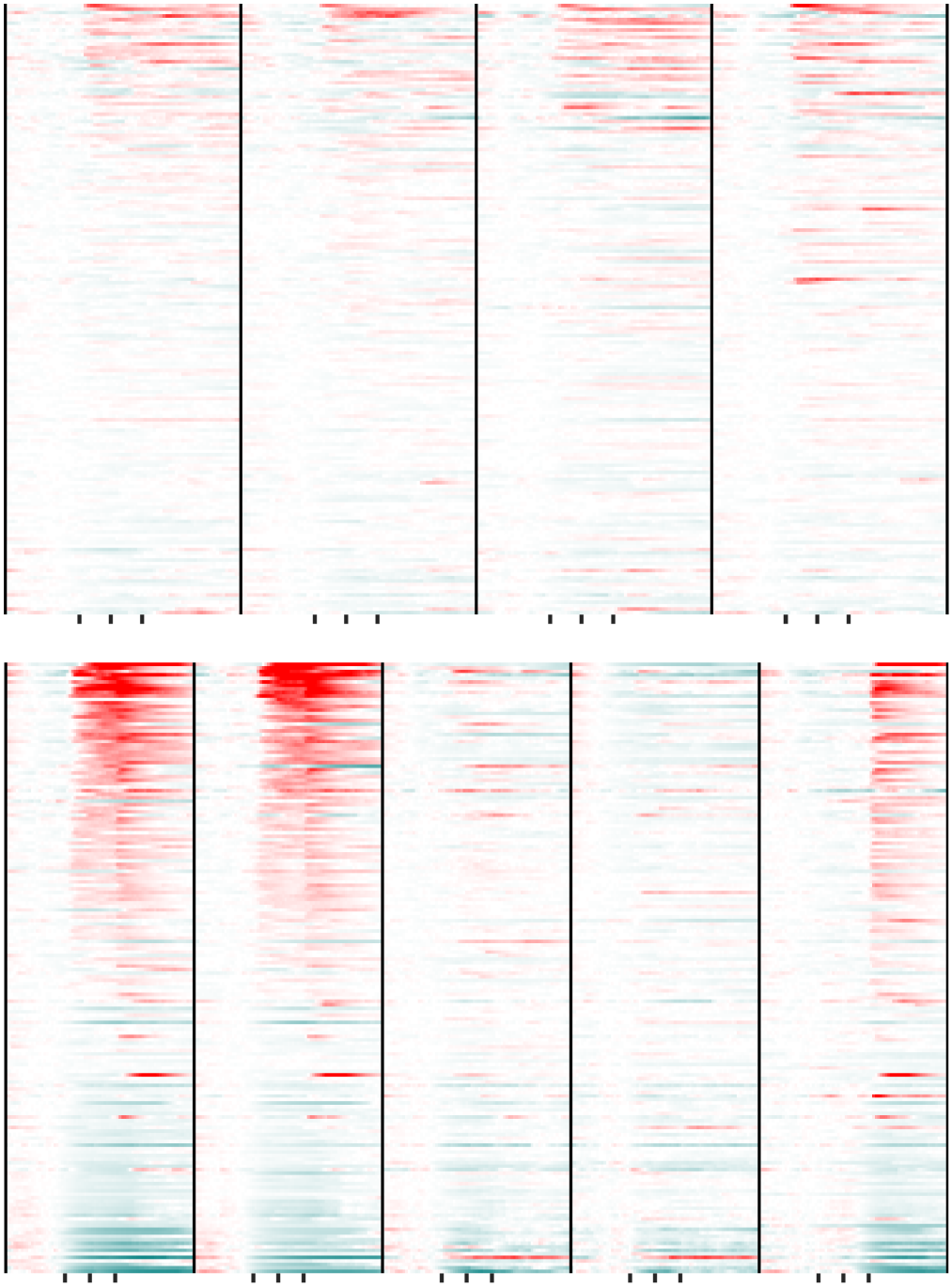

Figure 5.1. BLA Population Activity Before and After Learning BLA responses in all neurons recorded from 5 mice. Each row denotes a single cell's trial-averaged DF/F responses to CS+1 (PIN), CS+2 (MSY), CS-1 (EUY), CS-2 (LIM). Response to water is the 5th column in the part b. Scale bars indicate an increase in DF/F (red) or a decrease in DF/F (blue) relative to baseline. Responses prior to learning are non-selective (top). 35% of neurons respond to CS+ odors after learning (bottom). Responses are almost identical for two distinct CS+ odors paired with the same reward.

Figure 5.2

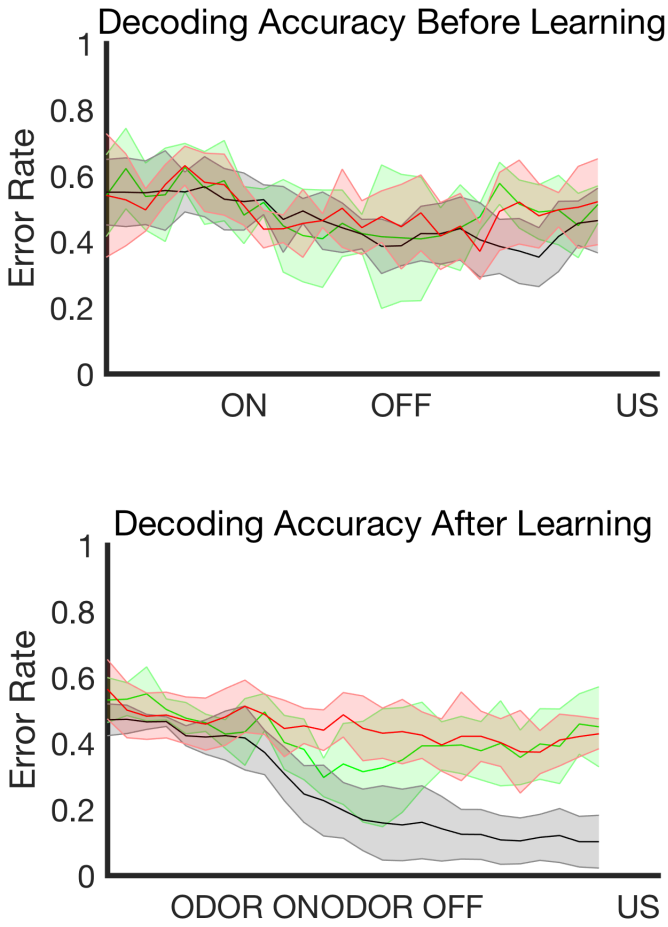
Decoding Accuracy Before Learning
Error Rate
1
0.8
0.6
0.4
0.2
0
ON
OFF
US
Decoding Accuracy After Learning
Error Rate
1
0.8
0.6
0.4
0.2
0
ODOR ON
ODOR OFF
US

Figure 5.2. Pairwise Decoding of Odors Using BLA Population Activity For each mouse, a binary linear decoder was trained on population activity from a subset of odor trials and was then asked to decode the identity of the odor using held-out trials. Green curve indicates decoding between CS+1/CS+2 odors, red curve indicates decoding between CS-1/CS-2 odors, and gray indicates all 4 pairwise combinations of CS+/CS- odors. Error bars indicate standard deviations of decoding performance across different mice. The decoder was trained and tested at each time-point (see Methods). Prior to learning, decoding accuracy was poor for all odor pairs (top). After learning, decoding performance only improved for pairs of CS+/CS- odors, suggesting that BLA acquired a representation of expected value (bottom).

Figure 5.3

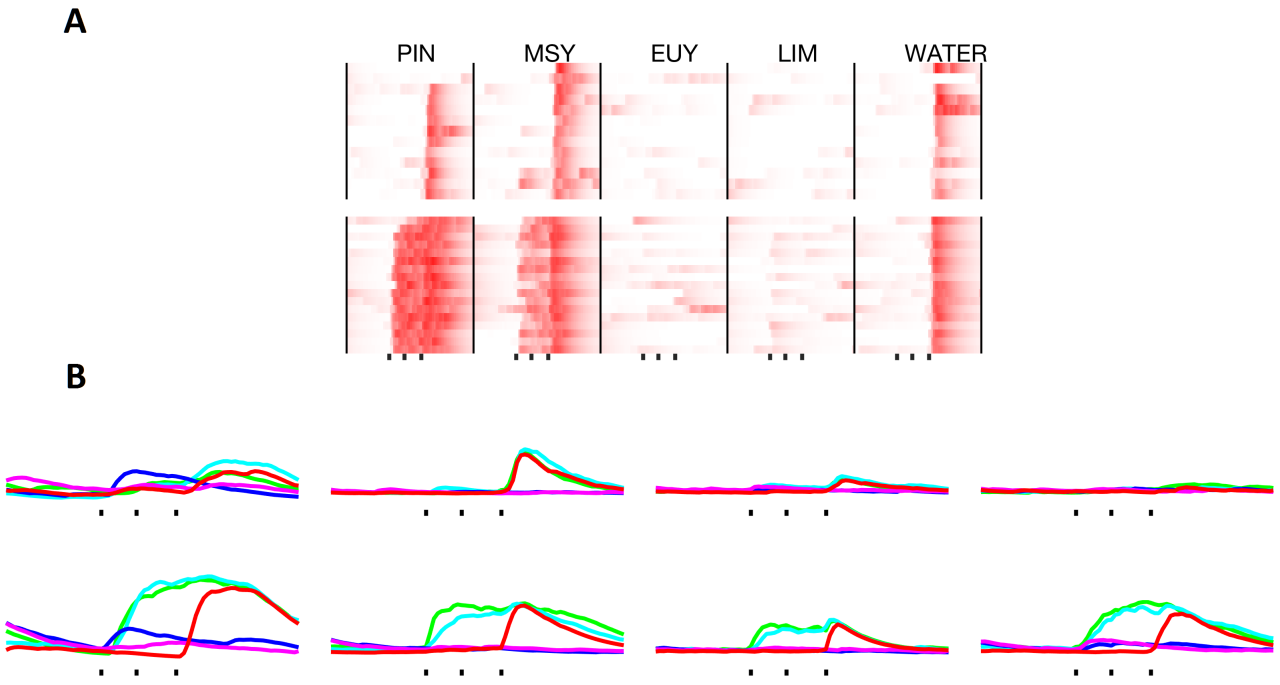

Figure 5.3. BLA neurons acquire responses to CS+ odors during learning A. Trial by trial responses of a BLA neuron during learning. This US-responsive neuron acquires responses to CS+ odors. **B**. Tracking responses of 4 example cells to odors before learning (naive odor presentation), during learning (anticipatory licking in 50%), and fully learned (anticipatory licking in >90% of CS+ trials). All 4 US-responsive cells acquire responses to CS+ odors.

Figure 5.4

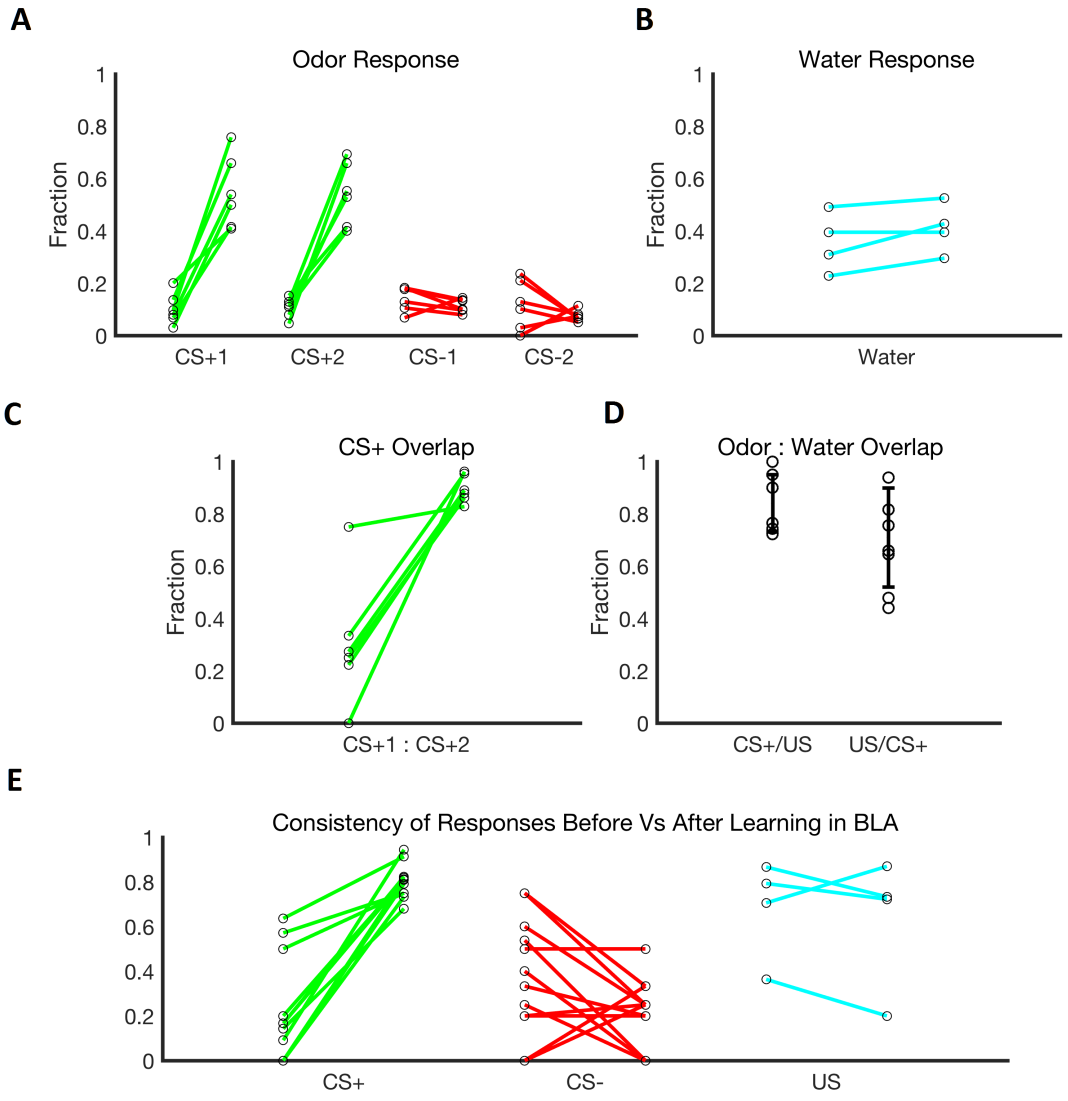
A
Odor Response
Fraction
1
0.8
0.6
0.4
0.2
0
CS+1
CS+2
CS-1
CS-2
B
Water Response
Fraction
Water
C
CS+ Overlap
Fraction
CS+1 : CS+2
D
Odor : Water Overlap
Fraction
CS+/US
US/CS+
E
Consistency of Responses Before Vs After Learning in BLA
CS+
CS-
US

Figure 5.4. Quantification of Odor-Evoked Responses Before and AFter Learning A, B. Fraction of neurons responsive to CS+ odors increased, while responses to CS- odors and to the US remained constant after learning. **C.** Fraction of cells responsive to both CS+ odors increased as a function of learning. **D.** CS+/US: 60% of neurons responsive to US acquired an CS+ response. US/CS+: 40% of CS+ responsive neurons are US responsive **E.** Consistency of BLA responses across consecutive days post-learning

Figure 5.5

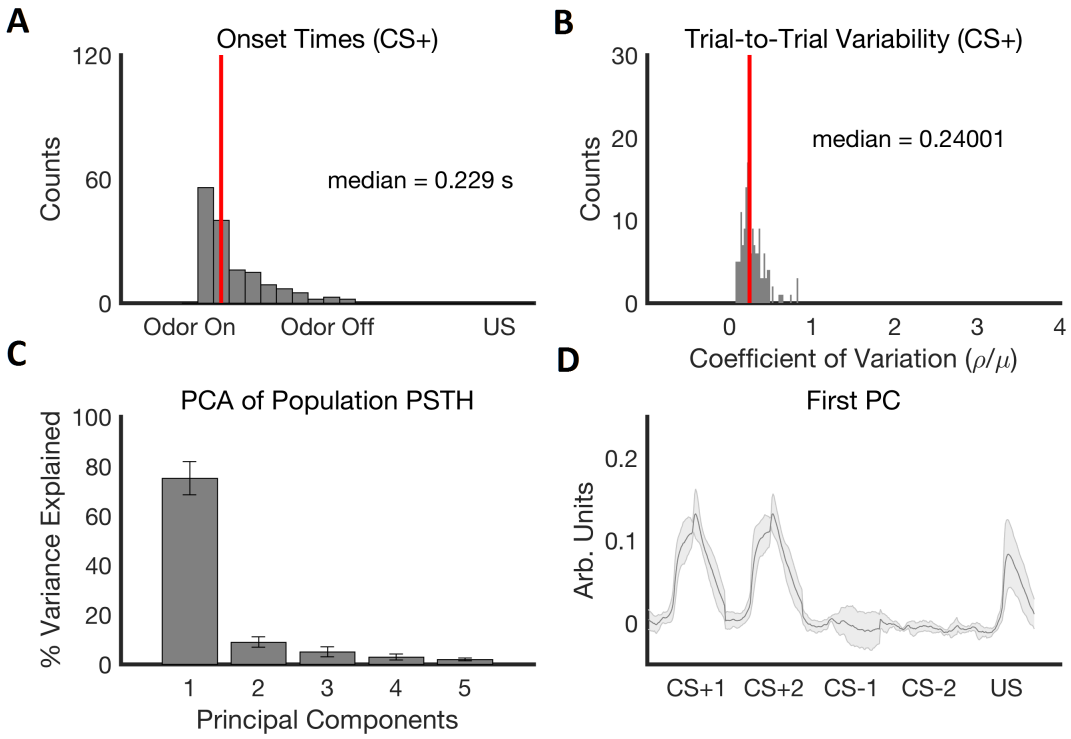
A
Onset Times (CS+)
120
60
0
Counts
median = 0.229 s
Odor On
Odor Off
US
B
Trial-to-Trial Variability (CS+)
30
20
10
0
Counts
median = 0.24001
0
1
2
3
4
Coefficient of Variation (ρ/μ)
C
PCA of Population PSTH
100
80
60
40
20
0
% Variance Explained
1
2
3
4
5
Principal Components
D
First PC
0.2
0.1
0
Arb. Units
CS+1
CS+2
CS-1
CS-2
US

Figure 5.5. BLA responses are temporally homogeneous A. The onsets of CS+ responses in the BLA mostly occur at odor onset. **B.** OFC responses exhibit similar trial-by-trial variability as compared to piriform responses. **C.** Principal component analysis (PCA) was performed on the population PSTH of the BLA to quantify the variance of the population. The first PC accounted for the majority of variance within the entire population (80%). **D.** The first PC illustrates that almost all neurons exhibit similar responses to different CS+ odors, and these responses are acquired only in US-reponsive neurons.

Figure 5.6

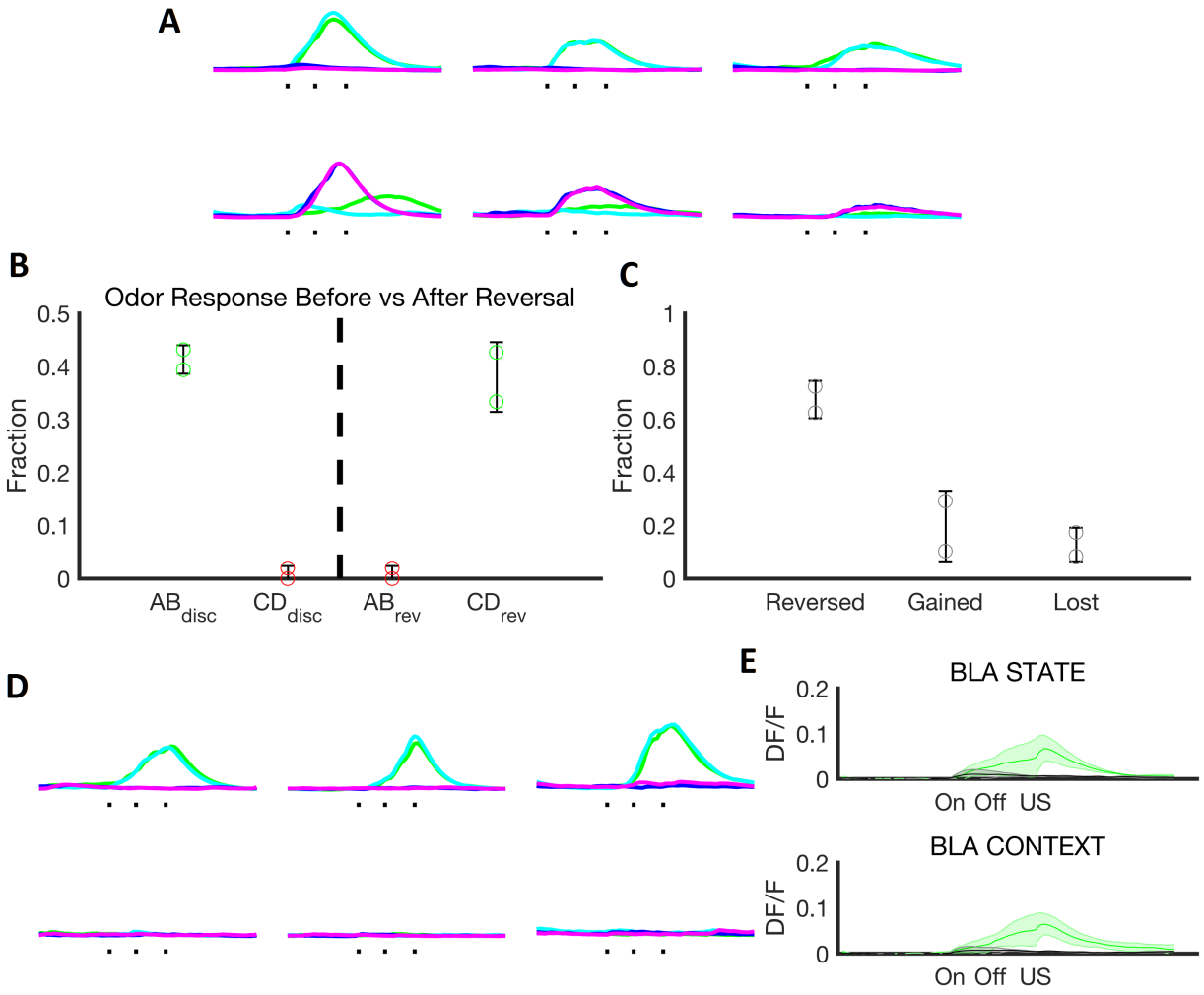
A
B
Odor Response Before vs After Reversal
Fraction
0.5
0.4
0.3
0.2
0.1
0
AB disc
CD disc
AB rev
CD rev
C
Fraction
1
0.8
0.6
0.4
0.2
0
Reversed
Gained
Lost
D
E
BLA STATE
DF/F
0.2
0.1
0
On Off US
BLA CONTEXT
DF/F
0.2
0.1
0
On Off US

Figure 5.6. BLA responses are temporally homogeneous A. Tracking the odor responses of 3 example cells before and after reversal learning. Prior to reversal learning, robust responses are observed to CS+ odors. After reversal, these responses diminish and are replaced by responses to new CS+ odors. **B.** Quantification of fraction of cells responsive to CS+ and CS- odors before and after learning. Green color denotes CS+, red color denotes CS-. **C.** For all cells that display significant responses to CS+ odors either before or after reversal, we found that 70% of cells fully reversed their responses during reversal. 15% of neurons were not responsive to CS+ odors pre-reversal but gained a response post-reversal, whereas 15% of neurons were responsive to CS+ odors pre-reversal but were not responsive to the new CS+ odors post-reversal. **D.** Tracking responses of 3 example cells before and after quenching thirst. When mice are sated, responses to CS+ responses vanish. **E.** Top: average DF/F of all CS+ responsive neurons before and after satiation. Bottom: same as above, except for water port removal.

Figure 5.7

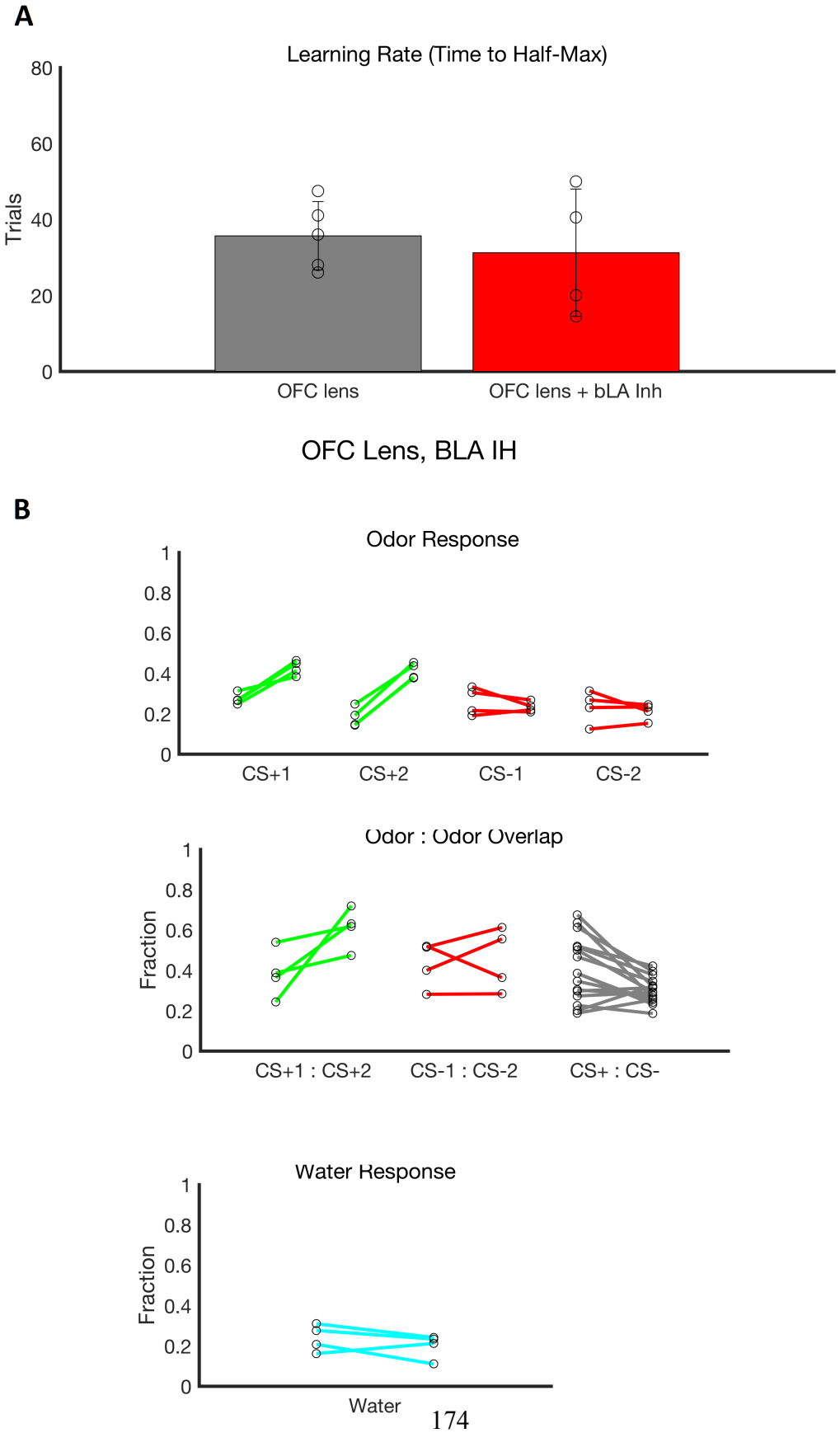
A
Learning Rate (Time to Half-Max)
Trials
80
60
40
20
0
OFC lens
OFC lens + bLA Inh
OFC Lens, BLA IH
B
Odor Response
1
0.8
0.6
0.4
0.2
0
CS+1
CS+2
CS-1
CS-2
Odor : Odor Overlap
Fraction
CS+1 : CS+2
CS-1 : CS-2
CS+ : CS-
Water Response
Water

Figure 5.7. Inhibition of BLA has no effect on behavior or on OFC representation **A**. The number of trials it takes for mice to display anticipatory licking is unaffected by BLA inhibition. **B**. OFC responses imaged during BLA inhibition are quantitatively similar to response without inhibition. Analyzed statistics include percentage of CS+ neurons, overlap between CS+ neurons, and fraction of US responsive neurons.

Figure 5.8

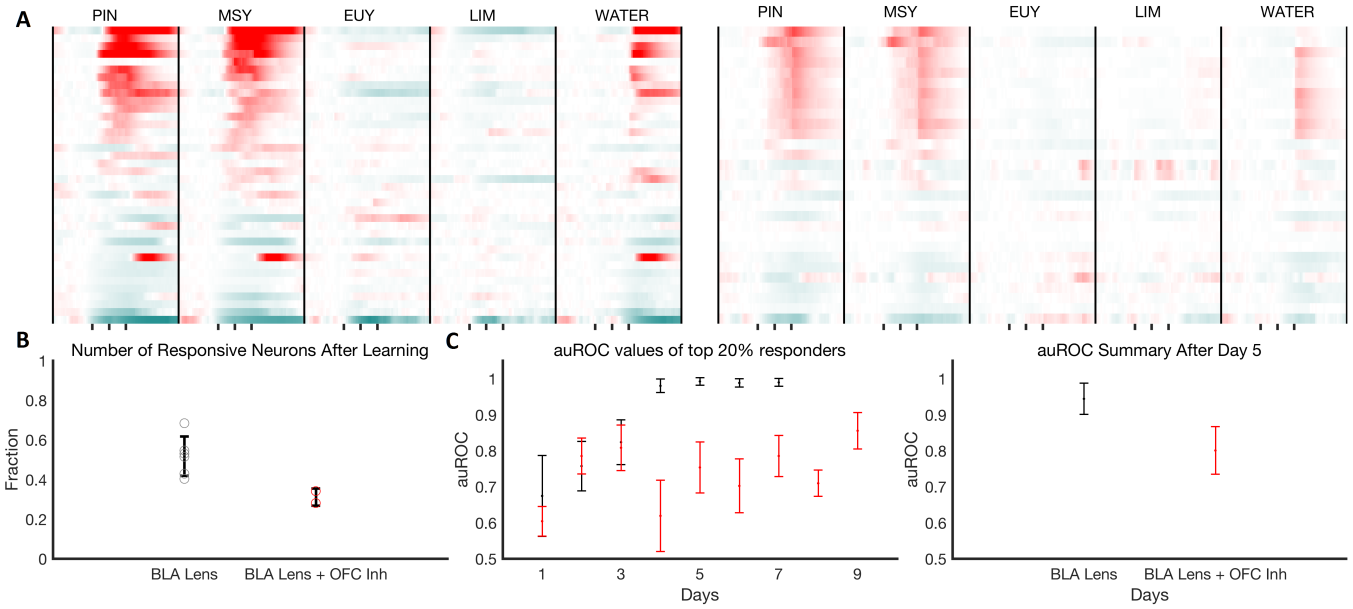
A
PIN
MSY
EUY
LIM
WATER
PIN
MSY
EUY
LIM
WATER
B
Number of Responsive Neurons After Learning
Fraction
1
0.8
0.6
0.4
0.2
0
BLA Lens
BLA Lens + OFC Inh
C
auROC values of top 20% responders
auROC
1
0.9
0.8
0.7
0.6
0.5
1
3
5
7
9
Days
auROC Summary After Day 5
auROC
1
0.9
0.8
0.7
0.6
0.5
BLA Lens
BLA Lens + OFC Inh
Days

Figure 5.8. Inhibition of OFC impairs the BLA representation A. BLA population response to odors on day 5 of training without OFC inhibition (left) and with OFC inhibition (right). **B**. Far fewer neurons were responsive to odor cues in the BLA with OFC inhibition **C**. BLA neurons that were responsive to CS+ odors during OFC inhibition were also far more inconsistent as compared to controls.

Figure 5.9

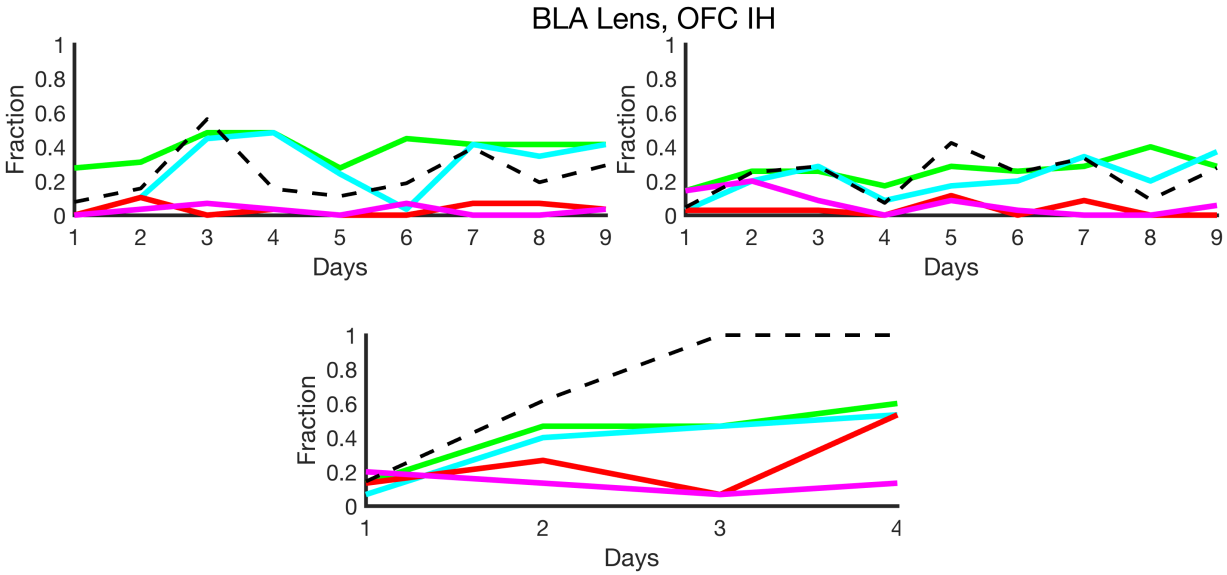

Figure 5.9. Inhibition of OFC impairs learning A. Fraction of BLA neurons responsive to CS+ and CS- odors during OFC inhibition as a function of learning. Black dotted line denotes fraction of CS+ trials that showed anticipatory licking. Representations of learners (bottom) were similar as compared to controls whereas the representations of non-learners were impaired (top).

Chapter 6

Discussion and Conclusion

6.1 Piriform Cortex Provides a High Dimensional Odor Representation

The cerebellar theory developed by Marr and Albus has provided a simple and powerful framework to understand why so many brain areas involved in associative learning are defined by sparse coding in a large homogeneous populations of neurons (Marr 1971; Marr 1969). This theory proposes that within the cerebellum, the abundance of granule cells exist to support a high dimensional representation of sensory information conveyed by a far lower number of mossy fiber inputs, and the large number of synapses that granule cells make with the the principal neurons of the cerebellum (Purkinje cells) allows them to form precise associations during learning. This theory is characterized by two key parameters: that mossy fibers make sparse and random connections to granule cells, and that there is a large expansion ratio, where granule cells outnumber their mossy fiber inputs 10-100 fold (Huang et al. 2013; Chabrol et al. 2015; Ishikawa et al. 2015; Stettler and Axel 2009). Indeed, each granule cell receives input from an average of only 4 mossy fibers, and granule cells outnumber mossy fibers by 30-fold.

This feature is shared by neurons that play roles similar to granule cells in other neural

circuits, such as the dorsal cochlear nucleus, the electrosensory lobe of the electric fish, or the insect mushroom body (Caron et al. 2013; Keene and Waddell 2007; Bell et al. 2008; Mugnaini et al. 1980; Eccles et al. 1966). Indeed, multiple modeling studies have observed that this sparse input connectivity is well-suited for producing high-dimensional representations that can then be read out by densely connected downstream output neurons for learning (Litwin-Kumar et al. 2017; Babadi and Sompolinsky 2014; Barak et al. 2013; Rigotti et al. 2013). Moreover, dimensionality quickly saturates as synaptic degree grows, implying that sparse connectivity present within these learning systems have evolved to be optimal (Litwin-Kumar et al. 2017; Babadi and Sompolinsky 2014).

Under this framework, piriform neurons should provide a high dimensional representation of odors that is fed to downstream associative areas to be modified by learning. Indeed, previous work have shown that piriform neurons are characterized by large expansion ratios, outnumbering their inputs by 30 fold (1 million piriform neurons to 30000 bulbar inputs). Moreover, current and prior work have shown that piriform neurons appear to encode stimuli with sparse and non-overlapping ensembles (Huang et al. 2013; Chabrol et al. 2015; Ishikawa et al. 2015; Stettler and Axel 2009).

Learning can either occur on piriform's synaptic inputs or downstream in other brain regions. There are several important benefits of not imposing changes upstream but rather downstream. First, random connectivity from bulb to piriform is optimized to decorrelate odor ensembles. If learning induces non-random changes in input strengths that made them more structured, this would induce odor ensembles to become more correlated, and therefore less discriminable. This problem can be solved by dedicating separate areas downstream to learn structured odor representations that reflect learning, salience, and value,

etc. Additional read-out circuits can thus perceive both the perceptual qualities of odors from the piriform as well as its value and meaning from regions downstream.

Conversely, if learning induced no loss or growth of new input synapses but simply made existing ones stronger, this learning rule will quickly suffer from the overlap problem. Each odor occupies a random 10% of all inputs onto the piriform, so if 10 individual odors are paired with reward, then 65% of all piriform inputs will be strengthened. If the animal now experiences a novel odor, this odor will activate 65% of strengthened piriform inputs which have been previously paired with reward, therefore driving learned behaviors even when the behavior is not desired. The overlap problem is mitigated by having learning take place in multiple downstream areas, each of which drives a different behavior, such as licking or escape. In this scenario, piriform outputs are strengthened onto a particular downstream area to drive a specific behavior, and over-generalization would only occur if many piriform ensembles are strengthened onto the same downstream area. However, if multiple piriform ensembles are each paired with a different downstream area to drive a different behavior, over-generalization will not exist. In conclusion, the avoid false generalization and to preserve discriminability, learning should occur downstream of the piriform. Indeed, in our chronic imaging experiments, we observe that piriform ensembles are not modified by learning.

6.2 OFC Provides a Blank Slate for Learning New Tasks

We have shown that the entrainment of piriform inputs can drive a representation of expected value in the OFC. How could piriform inputs, which encode a representation of

odor identity, transform into a cognitive representation of expected value in the OFC? The question can be rephrased as how unique odor ensembles in the piriform can converge and potentiate the same set of OFC neurons during learning. In our model, we first make the simplifying assumption that OFC neurons receive sufficiently large and random collections of piriform inputs such that every odor will activate a subset of piriform neurons. For instance, odors activate 10% of the entire piriform, and if 100 piriform inputs impinge onto an OFC neuron, then every odor will on average activate 10 of those piriform inputs. Consequently, piriform projections from distinct odor ensembles could then be independently reinforced onto the same OFC neuron. Therefore, having random piriform projections onto the OFC offers a simple mechanism that allows distinct odor ensembles to activate the same set of OFC neurons. While we have assumed that direct piriform projections are responsible for learning in the OFC, indirect pathways can also accommodate a random connectivity profile. For instance, anatomical studies have also revealed piriform projects indirectly to the OFC through the mediodorsal thalamus (Mitchell 2015).

We observe that CS+ responsive neurons constitute 35-40% of the entire OFC population. If learning was Hebbian, then we have to assume that 35-40% of the OFC receives water US input, and we also would predict that almost all US-responsive neurons acquire a CS+ response. However, the majority of US responsive neurons are not CS+ responsive, so the mechanism underlying the potentiation of CS+ responses in the OFC is unlikely to be Hebbian. An alternative hypothesis is that the potentiation of piriform inputs may also be gated by neuromodulation, such as by dopamine input. Only specific subsets of OFC neurons may be receptive to neuromodulators to account for the fact that only 35-40% of the OFC is CS+ responsive after learning. Frontal lobes indeed receive strong projections

from dopaminergic (DA) neurons in the midbrain (Goldman-Rakic et al. 1992; Swanson 1982). Specifically, dopamine release in the OFC has been linked to associative reward processing and reward-related behavior (Walker et al. 2009; Cetin et al. 2004). Therefore, the coincidence of neuromodulation and active piriform inputs may drive the formation of an CS+ ensemble in a select subset of OFC neurons. Once dopamine has reinforced piriform inputs onto the OFC, the activation of piriform inputs may be sufficient to drive OFC activity absent neuromodulation.

What mechanism underlies OFC sensitivity to state and context? The activity of these neurons must gate OFC activity in response to learned sensory CS+ inputs. One potential mechanism would be to require that OFC neurons behave like 'AND' gates, where output activity is only generated by the coincident activation of all inputs: motivational inputs (internal state), contextual inputs (reward is predicted by the CS+ in this given context), and learned sensory inputs. If any of the required inputs are inactive, CS+ neurons in the OFC will not fire. The regulation of internal state may be accommodated by inputs from the periaqueductal gray, basal forebrain and brainstem nuclei, and hypothalamic regions, all of which send projections to the OFC (Cavada et al. 2000). Likewise, contextual inputs may be sent to the OFC through its connections with other prefrontal and associative areas. Future work should be directed to understand the circuitry underlying the gating of OFC activity.

Once the task has been learned with a single odor, CS+ neurons in the OFC gradually vanish, and the OFC remains silent even when mice encounter novel odors they haven't previously experienced. Because OFC responses vanish, learning must be transfered onto other brain areas for behavioral performance to be maintained. Why would a learned rep-

resentation ever vanish? It seems counter-intuitive that a brain area should lose what it has learned only to waste resources transferring knowledge to other brain areas. However, the process of forgetting may allow the OFC to start again as a clean slate to learn novel tasks without having prior knowledge interfere with learning in a new context. If the OFC did not forget or lose what it has learned, prior learning may accumulate and erroneous recall may interfere with the learning of new task parameters. Therefore, to continually learn new tasks throughout an animal's lifetime, the OFC may function within a wider learning circuit as a playground where experimentation and hypothesis testing takes place. Once it solves a task, it may unload what it has learned to storage units located elsewhere to free up space to learn new tasks.

Many studies point to the transfer of learning from the hippocampus to the consolidation of long-term memories in the cortex (Zola-Morgan and Squire 1990; Bontempi et al. 1999; Kitamura et al. 2017). This framework suggests that every new memory is first cached in the hippocampus before stored within the cortex. However, while our results are similar to the idea that short and long term memory formation are accommodated by different brain areas, there is a key difference. Once task structure has been learned, the OFC no longer serves as a relay, and information flows directly to other brain regions to be learned and stored. OFC functions more like a teacher that configures the neural circuitry of other brain regions such that they are learn independently to acquire new associations.

6.3 mPFC Stores Task Information and Drives Behavior Downstream

When OFC activity is robust, mPFC is inactive; when OFC activity degrades, mPFC activity grows robust. As predicted by these imaging experiments, OFC is only important during initial learning, and mPFC is only important after task acquisition. While these experiments strongly suggest that the OFC transfers information to the mPFC, this connection has not been made explicit. Further experiments need to be conducted to demonstrate that OFC connects directly to the mPFC. Additional experiments should be done to ask 1) whether perturbations to the OFC representation affects the acquisition of a learned representation in the mPFC, and conversely, 2) whether perturbing the mPFC representation causes the OFC to retain its learned representation for longer, as it cannot use the mPFC to store what it has learned.

Assuming the OFC transfers learning to the mPFC, the mPFC does not create an exact replica of the learned OFC representation. Its representation is simpler in that neurons no longer tile the task duration but respond homogeneously with similar dynamics and at odor onset. However, it is also more complex in that we observe an unique CS- representation that is non-overlapping with that of the CS+. The emergence of a CS- ensemble is particular to the mPFC; we did not observe CS- responses during in piriform, OFC, or the BLA. What does this representation encode? It likely represents a negative value signal. Once CS+ odors are learned, the animal develops an expectation that at least some odor predicts reward. This expectation is met with disappointment if an odor now informs mice that no reward will be delivered. Therefore, the emergence of an expectation should dictate the

emergence of a CS- representation that signals negative value.

The big question, however, is why the CS- representation is even necessary. In other words, what function does this representation serve that a CS+ representation by itself cannot already accomplish? Conceptually, our task has only two possible actions, to lick and to not lick. If the default behavior is to not lick, which is what mice do prior to learning, then a CS+ representation that drives licking is sufficient to accomplish this task. Indeed, if we assume that mice do not lick in response to any novel odor, then a CS- ensemble that drives lick suppression is never necessary. However, mice change their default behaviors because they generalize past knowledge to lick to odors it has not previously encountered. In this regime, the CS+ representation that signals high value serves no purpose as it does not change the animal's default response. Rather, a CS- representation is necessary to suppress generalized licking to all odors. Therefore, if the default action is liable to change, the animal may require that CS+ and CS- ensembles to drive licking and suppression of licking. This may be why the mPFC must bind both CS+ and CS- odors to specific actions through non-overlapping ensembles.

There has to be a mechanism in place that allows prior learning to remain intact. Another value of having a CS- ensemble is that during extinction learning, the animal does not have to unlearn the CS+ representation. If during extinction learning, reward is no longer paired with a CS+ odor, the animal needs to suppress licking. The emergence of a CS- representation that suppresses licking allows the CS+ representation to remain intact without being unlearned. If the animal now has to learn again to lick to new CS+ odors, the CS+ representation can immediately inform the animal to start licking without having to learn afresh.

How could a representation of CS- odors be generated in the mPFC? One hypothesis is that there exists distinct sets of glutamatergic neurons in the mPFC that responds to different neurotransmitters. Receipt of reward releases neurotransmitters that signal over-expectation, and this will potentiates sensory inputs onto one set of mPFC neurons, forming the CS+ ensemble. Conversely, omission of reward releases neurotransmitters that signals under-expectation, or disappointment, and this will potentiate sensory inputs onto a non-overlapping set of mPFC neurons, forming the CS- ensemble. Neurotransmitter release that signals positive and negative reward prediction error may be transmitted through dopamine neurons in the VTA (Schultz 2001).

6.4 BLA's Role in Learning

The existence of distributed representations in the prefrontal cortex raises the question of whether there are multiple redundant pathways for learning elsewhere in the brain. Indeed, further imaging in another associative area, the BLA, has revealed a CS+ representation that is stable, low dimensional, and consistent from trial-to-trial. However, BLA silencing does not impair any observable behavioral changes during the learning of a simple appetitive association. Why must the brain expend resource to encode a learned representation if it is not necessary for learning or task performance? One potential reason is that these representations encode task variables that are not present within our simple appetitive association task. Second, each area may seem redundant but may be optimized to perform functions that are only somewhat overlapping. Indeed, all three regions, the BLA, OFC, and mPFC, encode value in different ways. Therefore, within any learning task, the brain may take a conser-

vative approach and recruit the activation of multiple redundant pathways, and whichever pathway that learns the task the fastest will be used to dictate behavior downstream.

Moreover, there must exist additional learning pathways that are independent of the OFC, mPFC, and BLA. The deficits that we observed during OFC and mPFC silencing were always relegated to a subset of animals. For instance, when we silenced the OFC during discrimination training, 3/5 mice could not learn discrimination training even after 10 days of training, whereas 2/5 mice were unimpaired. The heterogeneity of these results suggest that mice that are unimpaired may be learning the association through a pathway that is independent of OFC, mPFC, and BLA activation. Such a brain area may reside in the striatum, mid-brain, thalamus, and motor regions.

6.5 Model of Circuit

A simple model that illustrates how learning can be transferred from a complex task representation in the OFC to a simple representation in the mPFC. During initial learning, piriform inputs are strengthened onto the OFC, forming the CS+ representation. This representation allows a downstream region X (analogous to the VTA) to form an association between the cue and reward. After forming the association between odor and reward, region X projects back to the mPFC and releases two kinds of neurotransmitters, one signaling a positive value and the other a negative value. These neurotransmitters gate plasticity in distinct and non-overlapping sets of mPFC neurons, allowing non-overlapping CS+ and CS- ensembles to emerge in the mPFC. For example, when the US is delivered after a CS+ odor, neurotransmitter signaling positive value is released onto the mPFC, and coincident

piriform activation strengthens active synapses and drives the emergence of the CS+ ensemble. Conversely, when US is not delivered, opposing neurotransmitters signaling negative value drives the emergence of a CS- ensemble. We note that a negative value signal is only present once the animal has formed an expectation that some odors predict reward. Once the mPFC representation is robust, the OFC representation is not necessary anymore and therefore vanishes.

6.6 Conclusion

In summary, we have delineated a circuit whereby a sensory representation of odor identity is transformed into a representation of learning in multiple downstream brain regions. In particular, the representation in the OFC is necessary for learning the task structure, and this is transfered onto the mPFC and other brain regions after task structure has already been learned. The simplicity of the olfactory system makes it an invaluable system to understand how animals learn to associate sensory stimuli with specific outcomes. Continued investigation of associative circuitry downstream of olfactory centers will impact tremendously on our understanding of the neural origins of learned behavior.

Chapter 7

Methods

General

Vglut2-ires-cre mice (016963, Jackson Laboratories) were crossed to Ai96 (floxed-STOP-GCaMP6s, 024106, Jackson Labs). Adult female and males were used in all imaging and optogenetic experiments. Syn1-cre mice (003966, Jackson Laboratories) were crossed to Ai96. Adult female and males were used in bLA imaging experiments. All animals were group housed under a normal 12 hour light/dark cycle with littermates until surgery.

For all experiments, mice underwent surgeries when they were 8 - 12 weeks old. Mice were anesthetized with ketamine (100 mg/kg) and xylazine (10mg/kg) through intraperitoneal injection and then placed in a stereotactic frame. Ophthalmic ointment (Puralube) and a topical anesthetic (2% Lidocaine) was applied during surgeries. Body temperature was stabilized using a heating pad attached to a temperature controller. Following surgery, mice received buprenorphone (.05 - .1 mg/kg) subcutaneously every 12 hours over the next three days. Mice recovered for at least 4 weeks before the start of any imaging or optogenetic experiment.

For learning experiments, mice were water-restricted (water bottles taken out of cage) and was delivered water (water bottle put back into a cage) for 4-5 minutes everyday. Behavioral training began when mice weighed less than 90% of free drinking weight (3 days

for all experiments). Mice were also weighed everyday to ensure good health. No health problems related to dehydration arose at any point.

All experimental procedures were performed in accordance with the guide of Care and Use of Laboratory Animals (NIH) and were approved by the Institutional Animal Care and Use Committee at Columbia University.

Virus Injection

The UNC Vector Core packaged all viruses (AAV-CamKII-Jaws-KGC-GFP-ER2, AAV-Syn-ChrimsonR-tdTomato). Virus injections were administered unilaterally (for activation experiments) or bilaterally (for silencing experiments) targeting OFC or BLA. Injection coordinates used were all relative to bregma. For Piriform: AP, +2.20mm; ML , ±1.2mm; DV, -3.35mm. For OFC: AP, +2.40mm; ML , ±1.0mm; DV, -2.40mm. For BLA: AP, -1.60mm; ML , ±3.3mm; DV, -4.90mm. For mPFC: AP, +2.05mm; ML , ±0.40mm; DV, -2.05mm. All virus injections were diluted to 1/3 of original titer and 300 nL was injected per side for both unilateral and bilateral viral injections.

Optogenetics

For optogenetic experiments, 200 um core fibers (ThorLabs) were implanted bilaterally, approximately .3 mm above GRIN lens implantation coordinates. OFC coordinates: AP, +2.40mm; ML ±1.00mm; DV, −2.05mm. BLA coordinates: AP, -1.60mm; ML ±3.30mm; DV, −4.60mm. mPFC coordinates: AP, +1.65mm; ML ±0.40mm; DV, −1.70mm.

For photo-activation manipulations in Chrimson or control mice, the LED (660 nM)

was turned on for 10 Hz pulses. For photo-inhibition experiments in Jaws or control mice, laser (660 nM, CrystalLaser) did not pulse. The power was adjusted such that the power coming out of the fiber tip was approximately 3-4 mW for activation experiments, and 8-10 mW for inhibition experiments. The same trial structure was employed except that laser was turned on 2 seconds prior to odor delivery and lasted for two seconds after US delivery, for a total of 9 seconds. Laser was also turned on for 9 seconds for CS- trials, except US was never delivered.

For experiments involving simultaneous imaging and photo-activation or inhibition, the activation wavelength (660 nM) and LED power that we used neither bleached GCaMP levels nor bled through the collection filters. To confirm that the optical fibers were working properly during the experiment, fiber implants were extracted immediately after perfusion and output power levels at the fiber tip was tested to confirm the fibers were properly transmitting LED light. As exclusion criteria, we only included mice where viral expression within the target area of interest was robust.

Lens Implantation

First, a 1-1.5mm round craniotomy centered on the implantation coordinate was made using a dental drill. Dura and .5mm - 1mm of underlying cortex was then aspirated. Blood was washed off at the top constantly through aspiration. A .5mm diameter microendoscope (Grinch GmBH) was then inserted slowly. Lens coordinates are identical to the viral injection coordinates. After implantation, the microendoscopes were fixed in place using dental cement (Metabond). Usually, about 1-2 mm of lens stuck outside of the skull. To pro-

tect the lens on top from damage, we put a metal enclosure surrounding it (Dytran thread adapter) and then covered the enclosure with an acorn nut (Amazon Supplies). Lastly, a custom-made head plate (stainless steel) was attached to the skull during surgery to allow for head-fixation.

Head-fixed Behavior

Mice were head-fixed on a large Styrofoam ball, where they are free to only run forwards and backwards. All mice were habituated for at least one day prior to all experiments. During training, white noise was played to mute the sound of laser scanning. white imaging, mouse behavior was visualized through an UV camera (FlyLight). Water delivery was driven by a quiet solenoid-controlled valve (Lee Instruments) and delivered through a lick port. Licking was collected through a capacitive touch sensor (Phidgets) attached to the same lick port. All data was collected at 1000 Hz. Input/output and acquisition was all done through custom MATLAB scripts.

Odors

Odor delivery was driven by a custom-made olfactometer. All olfactometer parts, including valves and manifolds, were obtained from Lee Instruments. Air (Medical air) was streamed at 900 mL / minute, and split into two equal lines carrying 450 mL / minute. One line was directed towards the mouse's nose. Air flows perpendicular to the nose through a teflon tube, and a narrow slit was made in the opening at where the mouse's nose was located for odors to be detected. The other line routes to the PID (photo-ionization device) to mea-

sure odor ionization, a proxy for odor identity and concentration. All odors are diluted in mineral oil at concentrations of 2% (100 uL odor / 5000 uL solvent). All odors were obtained through Sigma-Aldrich. Odors used were: isoamyl acetate, methyl salicylate, pinene, 4-methylthiazole, peanut oil, 2-phenylethanol, limonene, eucalyptol, geranyl acetate, fenchone, benzaldehyde, octanol, hexanol. In most experiments, methyl salicylate and pinene served as the CS+ odors, and eucalyptol and limonene served as CS-. Odor-reward contingencies were reversed in reversal experiments.

Trial Structure

Before discrimination training, mice were trained to lick to the water port by placing the water port extremely close to the mouth, with water delivered for on average 2-3 trials. After, the lick port was moved further away such that there was spatial separation between skin and the delivered water drop. Mice usually learned to lick to collect water when water was delivered in such a manner in about 5 water deliveries. Water detection is presumably accommodated by fine hairs and whiskers located below the mouth. After this, training began. Baseline licking for most mice was extremely low, so all mice had to learn to lick to CS+ odors instead of suppressing to CS- odors.

All trials were as follows: 5 seconds baseline, 2 seconds odor, 3 seconds delay, and if a trial is a CS+, water is given. Then, there is an intertribal interval of 25 seconds. During pre-training, only one CS+ was given. On average, 40-60 pre-training trials was given in a day. During discrimination training, there were 5 different conditions: 2 CS+ odors that predicted water delivery, 2 CS- odors, and US trials where water was delivered

without being preceded by odor. Cues were delivered in a pseudorandom manner. On average, 12-15 trials of each of the 5 conditions were given per day of training. In initial pilot experiments, imaging during training on consecutive days caused slight bleaching in imaging planes. Therefore, most imaging experiments were conducted every other day to minimize bleaching.

Imaging

A two-photon microscope (Bruker Instruments, formerly Prairie Technologies) was equipped with the following to allow imaging of deep brain areas in vivo: a tunable mode-locked 2-photon laser (Coherent Laser, laser set to 920 nm, 100 fs pulse width); a GaAsp-PMT photo-detector with adjustable voltage, gain, and offset feature; a single green/red NDD filter cube (580 dcxd dichroic, hq525/70 m-2p bandpass filter); a long working distance 10X air objective with 0.3 NA (Olympus).

A 260 pixel X 260 pixel region of interest (400 um X 400 um FOV) was chosen, with 1.6 us dwell time per pixel. This allowed for image collection at 4.5 Hz. Prior to imaging, the imaging plane (z-axis) that was used from previous imaging days was located. This was done by using the top of the GRIN lens as the reference location. Sample image stacks of planes at every 10 um intervals was taken on a new imaging day. The mean intensity image of each image stack was registered to the previous day's image stack, and the best registered plane was chosen for subsequent imaging. During each odor trial, two-photon scanning was triggered immediately at the start of the baseline period (5 seconds prior to odor delivery), and a 19 second (75 frames / trial) video was collected for each trial. Data

was acquired using custom acquisition software (Bruker Instruments).

Image Analysis

Image analysis was all performed using custom MATLAB scripts. First, images were motion corrected using sub-pixel image registration. Imaging sessions are usually 4-7 thousand frames. Motion correction was first applied within each trial (75 frames per trial), and then it was applied across trials by registering the mean intensity image of different trials. In some FOVs, we often observe small fluorescence changes occurring in large areas (> 100 um X 100 um) that are presumably due to calcium transients in out-of-focus planes. We thus got rid of large diffuse calcium fluctuations through a spatial low-pass Gaussian filter (length constant, 50 um).

For ROI identification, we used a MATLAB package for calcium transient analysis based on nonnegative matrix factorization (NMF). The algorithm is specialized for separating signals from overlapping structures by relying on the fact that signals from different structures often have different time signatures. This algorithm also allows for removal of activity from sources such as axonal and dendritic processes. ROIs that corresponded to neurons were selected, and neuropil and other signals that do not appear to correspond to neural cell bodies were deleted. Sometimes, the algorithm will classify distinct neurons lying in close proximity as the same neuron, in which case the spatial filters were split manually. On average, 70-100 neurons were extracted, and 10-20 were deleted in a given mouse. Traces were extracted using selected regions of interest, and delta F / F was computed using baseline extracted using NMF.

To register neuronal identities across multiple days of imaging sessions, we first used rigid body rotation and translation (MATLAB rigid body registration and sub pixel registration) on the mean intensity averages of image stacks collected on different days. We then applied the angular rotation and translation to both the image stacks and the ROIs on different days to register across days. For instance, 5 different imaging days, day 3 was used as a reference, and all image stacks on other days were registered relative to day 3. After, we then manually took the union of all unique and spatially non-overlapping cells identified in all imaging days to produce a large set of spatial filters. Neuronal cell counts at this stage usually exceeded standard single-day cell count results by a multiple of 1.2 - 1.4.

Once done, we then back-applied these spatial filters to the original imaging data from each data. Small warping occurs in the brain across different days. As a result, different ROIs will move in different directions, but the shapes of each ROI is well-preserved across days. Back-application of spatial filters involves first morphologically dilating the spatial filter and searching for the best spatial filter within this dilated area. Thus, one can use a spatial filter that corresponds to a cell on a day's imaging to derive a new, updated filter corresponding to the outline of a cell on a different day provided that the cell has not changed its shape or location by a reasonable threshold. Finally, we then visually assessed whether the back-applied spatial filters corresponded to the same cell on different days. Sometimes, the back-application process results in spatial filters that do not correspond to the same cell on different imaging days. Commonly, while the center of mass of the back-applied spatial filters is fixed across days, they appear to correspond to the outlines of different cells. Thus, we cannot use any metric based of center of mass to exclude cells. Moreover, metrics based

on cross-correlation also did not agree with visual inspection. Thus, we simply looked at the shapes of the spatial filters while being blind to the fluorescence data and spatial location of the cell, and picked only cells whose spatial filters on multiple days appeared to correspond to the same cell outline. This usually led to the exclusion of 20% of all ROIs from the master list when aligning across 4 or more imaging days.

Optrode Experiments

NeuroNexus optrode probes with 32 sites and 200 um core fiber was used to assess efficacy of Chrimson inhibition and Jaws excitation using 660 nM light. Recordings were performed 4 weeks after virus injection. On recording days, mice were anesthetized with ketamine/xylazine and were head-fixed to the recording stage. On the day of recording, the hole used for the virus injection was enlarged using a drill and the dura was removed. The optrode was then fixed onto a micro manipulator and lowered into the brain. The hole was then sealed with liquid agar (1.5%) applied at body temperature.

For Jaws inhibition experiments, we lowered optical probes down to 2-3 mm below bregma towards the OFC and performed a series of inhibition recordings with varying power levels (.5 mW, 1 mW, 2 mW, 5 mW, 10 mW, 15 mW) at fiber tip. At each power level, laser was turned on for 10 seconds with an ITI of 30 seconds for a total of 15 consecutive blocks. This same protocol was used for Chrimson activation experiments, except that optical fibers were lowered down to 3-4 mm below bregma to target the anterior piriform cortex, and the laser was pulsed at 5 Hz.

After recording, cells were sorted using KlustaKwik using a EM algorithm for

maximum-likelihood fitting of a mixture of arbitrary-covariance Gaussians. Manual correction of automatic clustering was then subsequently done with KlustaViewa. This was described in https://www.ncbi.nlm.nih.gov/pmc/articles/PMC4817237/. Data was then analyzed by aligning and averaging light on periods and comparing spike rates to periods of no light.

Histology

Mice were killed by transcardial perfusion with 10 mL PBS followed by 10 mL 4% paraformaldehyde. Brains were extracted and coronal sections were cut on a vibratome. The slices were labeled with far-red neurotrace to label neuronal cell bodies. All images were taken using a Zeiss LSM-710 confocal microscope system. Histology was done to confirm locations of implanted lenses, implanted optical fibers, and level of GCamP6, Jaws, and Chrimson expression.

Data Collection

The number of mice that are required for each experiment is generally 4-6 per group. Investigators were not blind to either imaging or ontogenetic experiments. For imaging experiments, mice were excluded if there were less than 20 neurons within the field of view or if the lens was not placed directly above region of interest (n=2, all conditions). For optogenetic experiments, mice were excluded if histology revealed low expression within the region of interest, if optic fibers were misplaced, or if optic fibers did not transmit excitation light properly (n=0, head-fixed).

Data Analysis

Statistically Significant Response

For each cell, we pooled all the DF/F values of all trials during the baseline period to form a reference distribution. This was then compared to the distribution formed by pooling DF/F values at a given frame after odor onset with a moving average of 3 frames. A Mann-Whitney U test was performed on the reference and test distributions to obtain a P-value. Thus, a P-value was obtained for every frame after odor onset. A cell was deemed significantly active if the P-value was < 0.01 for at least 8 consecutive frames after odor onset.

Metrics for Significance and Selectivity

Quantification of a significant odor response in piriform cortex depended upon satisfying two criteria, that it must be greater than 0.1 DF/F and also must be statistically significant ($P < 0.01$). Many odor responses in the piriform are robust and have high signal, often above 0.3 DF/F. While odor responses that are much lower in amplitude (< 0.1 DF/F) are still significant statistically, they are less consistent trial-to-trial and are often not locked to odor onset. We therefore required that response be greater than 0.1 DF/F to be considered a significant odor response. Evoked responses in OFC, BLA, or mPFC were often much weaker, with statistically significant responses within the range of 0.05 – 0.1 DF/F. Therefore, we did not use an absolute threshold on DF/F for any region other than piriform.

In piriform, we often observe cells that robustly respond to odor A with >80% DF/F, and odor B with 10% DF/F. While both responses are statistically significant compared to baseline, response to A was much greater than B. We thus interpret this cell to be exclusively

selective for odor A. Therefore, for analysis of odor selectivity in piriform, we require that significant responses satisfy the additional criterion that the odor response has to be greater than 0.1 DF/F and also greater than 20% of the maximum odor response.

Using this criterion, a cell's response to the 4 tested odors can then be subdivided into two categories, selective responders and non-selective responders. Selective neurons respond to a subset of all odors, whereas non-selective neurons respond to all odors. We observe that on average, 3% of neurons were non-selectively responsive to all 4 tested odors with similar amplitude profiles. Like before, we discarded non-selective responders in the analysis of piriform odor selectivity because their odor tuning cannot be accounted by sparse inputs from the olfactory bulb (Stettler and Axel 2009).

Response Consistency Across Days

We use Union(A,B) / Max (A,B) to assess overlap between two neuron ensembles. For instance, if 50 cells are in ensemble A, and 100 cells are in ensemble B, and 40 cells are active on both days, this gives an overlap of 40 / 100 = 0.4 between the two ensembles.

We reason that this metric is fairer than other metrics, such as the Szymkiewicz-Simpson coefficient, defined as Union (A,B) / Min (A,B), to assess overlap because these metrics severely overestimates overlap if the number of cells between days differ significantly. In the above example, this alternative metric would produce a value of 80% overlap, which we believe is a severe over-estimation.

This metric was used to assess 1) the consistency of water-responsive cells across consecutive days (US-responsive cells on Day X and Day X+1), 2) the consistency of odor-responsive cells across consecutive days (Odor-responsive cells on Day X and Day X+1),

and 3) the overlap of responsive cells to different odors on the same day (odor A and odor B on Day X)

Quantifying Response Onset, Variability, Power

For all cells deemed to be significantly responsive to any CS+ odor based on previously explained criteria, we marked the onset of the significant response to be the first frame where the P-value was less than 0.01 relative to baseline. The onset times of each significant CS+ response in a given neuron were treated independently and were pooled together. A median onset time was then derived from this distribution. This was then averaged across all days after learning.

DF/F values for all trials, centered on a given frame with a time window of 3 frames, was pooled together to form a distribution, and the CV (coefficient of variation, or standard deviation/mean) was calculated for each frame. The minimum CV value between odor onset and water onset was used to assess the trial-by-trial variability of the odor response. All significant responses in all neurons were pooled together to form a distribution of CV values. The median CV was then derived from this distribution, and then averaged across all days after learning.

Power is defined as averaging the absolute value of the DF/F across the entire population for each condition.

Decoding

Binary linear decoders were constructed in MATLAB. We concatenated the DF/F values between odor onset and water onset for all neurons to form a population activity vector

of a single odor trial. We trained decoders to discriminate between the population activity vectors of all pair-wise odor conditions. We determined the error rate as the mean error rate over a fivefold cross-validation. For cross-validation we split all the trials (10-15 trials per odor condition per imaging session) into 5 equally sized blocks. We used 4 blocks for decoder training and 1 for testing.

We also applied the same method to decode between the 4 odor conditions at every imaging frame. We concatenated DF/F values with a moving average of 3 frames to form a population activity vector centered at a given frame. We then trained decoders to discriminate between the population activity vectors of two odors at every frame. This approach revealed when the population activities of different odors were most separable following odor delivery.

We also assessed whether licking was encoded by asking whether trials in which mice did not lick to the CS+ odor (false negative trials) were more similar to trials in which mice licked to CS+ odor (true positive) or to trials in which mice withheld licking to the CS- odors (true negative). We trained decoders to distinguish between CS+ lick trials and CS- non-lick trials using the above approach and then tested with CS+ non-lick trials. When making comparisons across decoders involving unequal numbers of cells…

Bibliography

Alexander, Georgia M et al. (July 2009). "Remote control of neuronal activity in transgenic mice expressing evolved G protein-coupled receptors." In: *Neuron* 63 (1), pp. 27–39.

Apicella, Alfonso et al. (2010). "Pyramidal cells in piriform cortex receive convergent input from distinct olfactory bulb glomeruli." In: *Journal of Neuroscience* 30.42, pp. 14255–14260.

Azzi, João C B, Angela Sirigu, and Jean-René Duhamel (Feb. 2012). "Modulation of value representation by social context in the primate orbitofrontal cortex." In: *Proceedings of the National Academy of Sciences of the United States of America* 109 (6), pp. 2126–2131.

Babadi, Baktash and Haim Sompolinsky (Sept. 2014). "Sparseness and expansion in sensory representations." In: *Neuron* 83 (5), pp. 1213–1226.

Balleine, Bernard W and Simon Killcross (May 2006). "Parallel incentive processing: an integrated view of amygdala function." In: *Trends in neurosciences* 29 (5), pp. 272–279.

Barak, Omri, Mattia Rigotti, and Stefano Fusi (Feb. 2013). "The sparseness of mixed selectivity neurons controls the generalization-discrimination trade-off." In: *The Journal of neuroscience : the official journal of the Society for Neuroscience* 33 (9), pp. 3844–3856.

Barbas, H and D N Pandya (1984). "Topography of commissural fibers of the prefrontal cortex in the rhesus monkey." In: *Experimental brain research* 55 (1), pp. 187–191.

Barbey, Aron K, Michael Koenigs, and Jordan Grafman (Apr. 2011). "Orbitofrontal contributions to human working memory." In: *Cerebral cortex (New York, N.Y. : 1991)* 21 (4), pp. 789–795.

Barretto, Robert P J et al. (Jan. 2015). "The neural representation of taste quality at the periphery." In: *Nature* 517 (7534), pp. 373–376.

Baxter, M G et al. (June 2000). "Control of response selection by reinforcer value requires interaction of amygdala and orbital prefrontal cortex." In: *The Journal of neuroscience : the official journal of the Society for Neuroscience* 20 (11), pp. 4311–4319.

Bechara, A, H Damasio, and A R Damasio (Mar. 2000). “Emotion, decision making and the orbitofrontal cortex.” In: *Cerebral cortex (New York, N.Y. : 1991)* 10 (3), pp. 295–307.

Bekkers, John M and Norimitsu Suzuki (July 2013). “Neurons and circuits for odor processing in the piriform cortex.” In: *Trends in neurosciences* 36 (7), pp. 429–438.

Bell, Curtis C, Victor Han, and Nathaniel B Sawtell (2008). “Cerebellum-like structures and their implications for cerebellar function.” In: *Annual review of neuroscience* 31, pp. 1–24.

Belluscio, L and L C Katz (Mar. 2001). “Symmetry, stereotypy, and topography of odorant representations in mouse olfactory bulbs.” In: *The Journal of neuroscience : the official journal of the Society for Neuroscience* 21 (6), pp. 2113–2122.

Beyer, Frederike et al. (2014). “Orbitofrontal cortex reactivity to angry facial expression in a social interaction correlates with aggressive behavior.” In: *Cerebral cortex* 25.9, pp. 3057–3063.

Biran, Roy, David C Martin, and Patrick A Tresco (Sept. 2005). “Neuronal cell loss accompanies the brain tissue response to chronically implanted silicon microelectrode arrays.” In: *Experimental neurology* 195 (1), pp. 115–126.

Bontempi, B et al. (Aug. 1999). “Time-dependent reorganization of brain circuitry underlying long-term memory storage.” In: *Nature* 400 (6745), pp. 671–675.

Boulougouris, Vasileios, Jeffrey W Dalley, and Trevor W Robbins (May 2007). “Effects of orbitofrontal, infralimbic and prelimbic cortical lesions on serial spatial reversal learning in the rat.” In: *Behavioural brain research* 179 (2), pp. 219–228.

Bozza, Thomas et al. (Apr. 2004). “In vivo imaging of neuronal activity by targeted expression of a genetically encoded probe in the mouse.” In: *Neuron* 42 (1), pp. 9–21.

Broussard, Gerard J, Ruqiang Liang, and Lin Tian (2014). “Monitoring activity in neural circuits with genetically encoded indicators.” In: *Frontiers in molecular neuroscience* 7, p. 97.

Buck, L and R Axel (Apr. 1991). “A novel multigene family may encode odorant receptors: a molecular basis for odor recognition.” In: *Cell* 65 (1), pp. 175–187.

Burgos-Robles, Anthony, Hector Bravo-Rivera, and Gregory J Quirk (2013). “Prelimbic and infralimbic neurons signal distinct aspects of appetitive instrumental behavior.” In: *PloS one* 8 (2), e57575.

Butter, C M, D R Snyder, and J A McDonald (July 1970). “Effects of orbital frontal lesions on aversive and aggressive behaviors in rhesus monkeys.” In: *Journal of comparative and physiological psychology* 72 (1), pp. 132–144.

Buzsáki, György (May 2004). “Large-scale recording of neuronal ensembles.” In: *Nature neuroscience* 7 (5), pp. 446–451.

Calu, Donna J et al. (June 2007). “Associative encoding in posterior piriform cortex during odor discrimination and reversal learning.” In: *Cerebral cortex (New York, N.Y. : 1991)* 17 (6), pp. 1342–1349.

Campeau, S and M Davis (Mar. 1995). “Involvement of the central nucleus and basolateral complex of the amygdala in fear conditioning measured with fear-potentiated startle in rats trained concurrently with auditory and visual conditioned stimuli.” In: *The Journal of neuroscience : the official journal of the Society for Neuroscience* 15 (3 Pt 2), pp. 2301–2311.

Carmichael, S T and J L Price (Dec. 1995). “Limbic connections of the orbital and medial prefrontal cortex in macaque monkeys.” In: *The Journal of comparative neurology* 363 (4), pp. 615–641.

Caron, Sophie J C et al. (May 2013). “Random convergence of olfactory inputs in the Drosophila mushroom body.” In: *Nature* 497 (7447), pp. 113–117.

Cavada, C et al. (Mar. 2000). “The anatomical connections of the macaque monkey orbitofrontal cortex. A review.” In: *Cerebral cortex (New York, N.Y. : 1991)* 10 (3), pp. 220–242.

Cetin, Timur et al. (Nov. 2004). “Dopamine in the orbitofrontal cortex regulates operant responding under a progressive ratio of reinforcement in rats.” In: *Neuroscience letters* 370 (2-3), pp. 114–117.

Chabrol, François P et al. (May 2015). “Synaptic diversity enables temporal coding of coincident multisensory inputs in single neurons.” In: *Nature neuroscience* 18 (5), pp. 718–727.

Chen, Chien-Fu F, Dylan C Barnes, and Donald A Wilson (Dec. 2011). “Generalized vs. stimulus-specific learned fear differentially modifies stimulus encoding in primary sensory cortex of awake rats.” In: *Journal of neurophysiology* 106 (6), pp. 3136–3144.

Chen, Qian et al. (Oct. 2012). “Imaging neural activity using Thy1-GCaMP transgenic mice.” In: *Neuron* 76 (2), pp. 297–308.

Chen, Tsai-Wen et al. (July 2013). “Ultrasensitive fluorescent proteins for imaging neuronal activity.” In: *Nature* 499 (7458), pp. 295–300.

Choi, Gloria B et al. (Sept. 2011). “Driving opposing behaviors with ensembles of piriform neurons.” In: *Cell* 146 (6), pp. 1004–1015.

Chu, Monica W, Wankun L Li, and Takaki Komiyama (Oct. 2016). “Balancing the Robustness and Efficiency of Odor Representations during Learning.” In: *Neuron* 92 (1), pp. 174–186.

Chudasama, Y and Trevor W Robbins (Sept. 2003). “Dissociable contributions of the orbitofrontal and infralimbic cortex to pavlovian autoshaping and discrimination reversal learning: further evidence for the functional heterogeneity of the rodent frontal cortex.” In: *The Journal of neuroscience : the official journal of the Society for Neuroscience* 23 (25), pp. 8771–8780.

Chudasama, Y, J D Kralik, and E A Murray (May 2007). “Rhesus monkeys with orbital prefrontal cortex lesions can learn to inhibit prepotent responses in the reversed reward contingency task.” In: *Cerebral cortex (New York, N.Y. : 1991)* 17 (5), pp. 1154–1159.

Chuong, Amy S et al. (Aug. 2014). “Noninvasive optical inhibition with a red-shifted microbial rhodopsin.” In: *Nature neuroscience* 17 (8), pp. 1123–1129.

Cicerone, K D and L N Tanenbaum (1997). “Disturbance of social cognition after traumatic orbitofrontal brain injury.” In: *Archives of clinical neuropsychology : the official journal of the National Academy of Neuropsychologists* 12 (2), pp. 173–188.

Cohen, Yaniv et al. (June 2008). “Olfactory learning-induced long-lasting enhancement of descending and ascending synaptic transmission to the piriform cortex.” In: *The Journal of neuroscience : the official journal of the Society for Neuroscience* 28 (26), pp. 6664–6669.

Cousens, G and T Otto (Oct. 1998). “Both pre- and posttraining excitotoxic lesions of the basolateral amygdala abolish the expression of olfactory and contextual fear conditioning.” In: *Behavioral neuroscience* 112 (5), pp. 1092–1103.

Critchley, H D and E T Rolls (Apr. 1996). “Hunger and satiety modify the responses of olfactory and visual neurons in the primate orbitofrontal cortex.” In: *Journal of neurophysiology* 75 (4), pp. 1673–1686.

Csicsvari, Jozsef et al. (Aug. 2003). “Massively parallel recording of unit and local field potentials with silicon-based electrodes.” In: *Journal of neurophysiology* 90 (2), pp. 1314–1323.

Davison, Ian G and Michael D Ehlers (2011). “Neural circuit mechanisms for pattern detection and feature combination in olfactory cortex.” In: *Neuron* 70.1, pp. 82–94.

Eccles, J C, R Llinás, and K Sasaki (1966). "The mossy fibre-granule cell relay of the cerebellum and its inhibitory control by Golgi cells." In: *Experimental brain research* 1 (1), pp. 82–101.

Everitt, Barry J et al. (Apr. 2003). "Appetitive behavior: impact of amygdala-dependent mechanisms of emotional learning." In: *Annals of the New York Academy of Sciences* 985, pp. 233–250.

Feierstein, Claudia E et al. (Aug. 2006). "Representation of spatial goals in rat orbitofrontal cortex." In: *Neuron* 51 (4), pp. 495–507.

Franks, Kevin M et al. (Oct. 2011). "Recurrent circuitry dynamically shapes the activation of piriform cortex." In: *Neuron* 72 (1), pp. 49–56.

Frey, Stephen and Michael Petrides (Sept. 2002). "Orbitofrontal cortex and memory formation." In: *Neuron* 36 (1), pp. 171–176.

Gallagher, M, R W McMahan, and G Schoenbaum (Aug. 1999). "Orbitofrontal cortex and representation of incentive value in associative learning." In: *The Journal of neuroscience : the official journal of the Society for Neuroscience* 19 (15), pp. 6610–6614.

Galleguillos, Lorna, Teresa Parrao, and Carolina Delgado (2011). "Personality disorder related to an acute orbitofrontal lesion in multiple sclerosis." In: *The Journal of neuropsychiatry and clinical neurosciences* 23 (4), E7.

Ghosh, Sulagna et al. (2011). "Sensory maps in the olfactory cortex defined by long-range viral tracing of single neurons." In: *Nature* 472.7342, p. 217.

Giustino, Thomas F and Stephen Maren (2015). "The Role of the Medial Prefrontal Cortex in the Conditioning and Extinction of Fear." In: *Frontiers in behavioral neuroscience* 9, p. 298.

Godfrey, Paul A, Bettina Malnic, and Linda B Buck (Feb. 2004). "The mouse olfactory receptor gene family." In: *Proceedings of the National Academy of Sciences of the United States of America* 101 (7), pp. 2156–2161.

Goldman-Rakic, P S et al. (1992). "The anatomy of dopamine in monkey and human prefrontal cortex." In: *Journal of neural transmission. Supplementum* 36, pp. 163–177.

Gore, Felicity et al. (July 2015). "Neural Representations of Unconditioned Stimuli in Basolateral Amygdala Mediate Innate and Learned Responses." In: *Cell* 162 (1), pp. 134–145.

Gottfried, Jay A, John O'Doherty, and Raymond J Dolan (Aug. 2003). "Encoding predictive reward value in human amygdala and orbitofrontal cortex." In: *Science (New York, N.Y.)* 301 (5636), pp. 1104–1107.

Grewe, Benjamin F et al. (Mar. 2017). "Neural ensemble dynamics underlying a long-term associative memory." In: *Nature* 543 (7647), pp. 670–675.

Groenewegen, H J (Feb. 1988). "Organization of the afferent connections of the mediodorsal thalamic nucleus in the rat, related to the mediodorsal-prefrontal topography." In: *Neuroscience* 24 (2), pp. 379–431.

Haberly, L B and J L Price (June 1977). "The axonal projection patterns of the mitral and tufted cells of the olfactory bulb in the rat." In: *Brain research* 129 (1), pp. 152–157.

— (Apr. 1978). "Association and commissural fiber systems of the olfactory cortex of the rat." In: *The Journal of comparative neurology* 178 (4), pp. 711–740.

Hatfield, T et al. (Aug. 1996). "Neurotoxic lesions of basolateral, but not central, amygdala interfere with Pavlovian second-order conditioning and reinforcer devaluation effects." In: *The Journal of neuroscience : the official journal of the Society for Neuroscience* 16 (16), pp. 5256–5265.

Holland, Peter C (1997). "Brain mechanisms for changes in processing of conditioned stimuli in Pavlovian conditioning: Implications for behavior theory." In: *Animal Learning & Behavior* 25.4, pp. 373–399.

Huang, Cheng-Chiu et al. (Feb. 2013). "Convergence of pontine and proprioceptive streams onto multimodal cerebellar granule cells." In: *eLife* 2. Original DateCompleted: 20130308, Original DateCompleted: 20140206, e00400.

HUBEL, D H and T N WIESEL (Oct. 1959). "Receptive fields of single neurones in the cat's striate cortex." In: *The Journal of physiology* 148, pp. 574–591.

Ishai, Alumit (Feb. 2007). "Sex, beauty and the orbitofrontal cortex." In: *International journal of psychophysiology : official journal of the International Organization of Psychophysiology* 63 (2), pp. 181–185.

Ishikawa, Taro, Misa Shimuta, and Michael Häusser (Dec. 2015). "Multimodal sensory integration in single cerebellar granule cells in vivo." In: *eLife* 4.

Izquierdo, Alicia, Robin K Suda, and Elisabeth A Murray (Aug. 2004). "Bilateral orbital prefrontal cortex lesions in rhesus monkeys disrupt choices guided by both reward value and reward contingency." In: *The Journal of neuroscience : the official journal of the Society for Neuroscience* 24 (34), pp. 7540–7548.

— (Sept. 2005). “Comparison of the effects of bilateral orbital prefrontal cortex lesions and amygdala lesions on emotional responses in rhesus monkeys.” In: *The Journal of neuroscience : the official journal of the Society for Neuroscience* 25 (37), pp. 8534–8542.

Jin, Xin, Navin Pokala, and Cornelia I Bargmann (Feb. 2016). “Distinct Circuits for the Formation and Retrieval of an Imprinted Olfactory Memory.” In: *Cell* 164 (4), pp. 632–643.

Johnson, D M et al. (Sept. 2000). “New features of connectivity in piriform cortex visualized by intracellular injection of pyramidal cells suggest that ”primary” olfactory cortex functions like ”association” cortex in other sensory systems.” In: *The Journal of neuroscience : the official journal of the Society for Neuroscience* 20 (18), pp. 6974–6982.

Jones, B and M Mishkin (Aug. 1972). “Limbic lesions and the problem of stimulus–reinforcement associations.” In: *Experimental neurology* 36 (2), pp. 362–377.

Kahnt, Thorsten et al. (May 2012). “Connectivity-based parcellation of the human orbitofrontal cortex.” In: *The Journal of neuroscience : the official journal of the Society for Neuroscience* 32 (18), pp. 6240–6250.

Keene, Alex C and Scott Waddell (May 2007). “Drosophila olfactory memory: single genes to complex neural circuits.” In: *Nature reviews. Neuroscience* 8 (5), pp. 341–354.

Kennerley, Steven W, Timothy E J Behrens, and Jonathan D Wallis (Oct. 2011). “Double dissociation of value computations in orbitofrontal and anterior cingulate neurons.” In: *Nature neuroscience* 14 (12), pp. 1581–1589.

Kepecs, Adam et al. (Sept. 2008). “Neural correlates, computation and behavioural impact of decision confidence.” In: *Nature* 455 (7210), pp. 227–231.

Kikuta, Shu et al. (Mar. 2013). “Odorant response properties of individual neurons in an olfactory glomerular module.” In: *Neuron* 77 (6), pp. 1122–1135.

Kim, Sung-Yon et al. (Apr. 2013). “Diverging neural pathways assemble a behavioural state from separable features in anxiety.” In: *Nature* 496 (7444), pp. 219–223.

Kitamura, Takashi et al. (Apr. 2017). “Engrams and circuits crucial for systems consolidation of a memory.” In: *Science (New York, N.Y.)* 356 (6333), pp. 73–78.

Klapoetke, Nathan C et al. (Mar. 2014). “Independent optical excitation of distinct neural populations.” In: *Nature methods* 11 (3), pp. 338–346.

Kobayakawa, Ko et al. (Nov. 2007). “Innate versus learned odour processing in the mouse olfactory bulb.” In: *Nature* 450 (7169), pp. 503–508.

Lak, Armin et al. (Oct. 2014). “Orbitofrontal cortex is required for optimal waiting based on decision confidence.” In: *Neuron* 84 (1), pp. 190–201.

LeDoux, J E (2000). “Emotion circuits in the brain.” In: *Annual review of neuroscience* 23, pp. 155–184.

Li, Wen et al. (Mar. 2008). “Aversive learning enhances perceptual and cortical discrimination of indiscriminable odor cues.” In: *Science (New York, N.Y.)* 319 (5871), pp. 1842–1845.

Lichtenberg, Nina T et al. (Aug. 2017). “Basolateral Amygdala to Orbitofrontal Cortex Projections Enable Cue-Triggered Reward Expectations.” In: *The Journal of neuroscience : the official journal of the Society for Neuroscience* 37 (35), pp. 8374–8384.

Lin, Da Yu, Stephen D Shea, and Lawrence C Katz (June 2006). “Representation of natural stimuli in the rodent main olfactory bulb.” In: *Neuron* 50 (6), pp. 937–949.

Lin, John Y et al. (Oct. 2013). “ReaChR: a red-shifted variant of channelrhodopsin enables deep transcranial optogenetic excitation.” In: *Nature neuroscience* 16 (10), pp. 1499–1508.

Lipton, P A, P Alvarez, and H Eichenbaum (Feb. 1999). “Crossmodal associative memory representations in rodent orbitofrontal cortex.” In: *Neuron* 22 (2), pp. 349–359.

Litwin-Kumar, Ashok et al. (Mar. 2017). “Optimal Degrees of Synaptic Connectivity.” In: *Neuron* 93 (5), 1153–1164.e7.

Madisen, Linda et al. (Mar. 2015). “Transgenic mice for intersectional targeting of neural sensors and effectors with high specificity and performance.” In: *Neuron* 85 (5), pp. 942–958.

Malnic, B et al. (Mar. 1999). “Combinatorial receptor codes for odors.” In: *Cell* 96 (5), pp. 713–723.

Marek, Roger et al. (May 2018). “Excitatory connections between the prelimbic and infralimbic medial prefrontal cortex show a role for the prelimbic cortex in fear extinction.” In: *Nature neuroscience* 21 (5), pp. 654–658.

Marr, D (June 1969). “A theory of cerebellar cortex.” In: *The Journal of physiology* 202 (2), pp. 437–470.

— (July 1971). “Simple memory: a theory for archicortex.” In: *Philosophical transactions of the Royal Society of London. Series B, Biological sciences* 262 (841), pp. 23–81.

Meunier, M, J Bachevalier, and M Mishkin (July 1997). “Effects of orbital frontal and anterior cingulate lesions on object and spatial memory in rhesus monkeys.” In: *Neuropsychologia* 35 (7), pp. 999–1015.

Miller, M H and J Orbach (Sept. 1972). “Retention of spatial alternation following frontal lobe resections in stump-tailed macaques.” In: *Neuropsychologia* 10 (3), pp. 291–298.

Mishkin, M and F J Manning (Mar. 1978). “Non-spatial memory after selective prefrontal lesions in monkeys.” In: *Brain research* 143 (2), pp. 313–323.

Mitchell, Anna S (July 2015). “The mediodorsal thalamus as a higher order thalamic relay nucleus important for learning and decision-making.” In: *Neuroscience and biobehavioral reviews* 54, pp. 76–88.

Miyamichi, Kazunari et al. (2011). “Cortical representations of olfactory input by trans-synaptic tracing.” In: *Nature* 472.7342, p. 191.

Miyazaki, Katsuhiko, Kayoko W Miyazaki, and Gen Matsumoto (Mar. 2004). “Different representation of forthcoming reward in nucleus accumbens and medial prefrontal cortex.” In: *Neuroreport* 15 (4), pp. 721–726.

Mombaerts, P (Oct. 1999). “Seven-transmembrane proteins as odorant and chemosensory receptors.” In: *Science (New York, N.Y.)* 286 (5440), pp. 707–711.

Mombaerts, P et al. (Nov. 1996). “Visualizing an olfactory sensory map.” In: *Cell* 87 (4), pp. 675–686.

Morecraft, R J, C Geula, and M M Mesulam (Sept. 1992). “Cytoarchitecture and neural afferents of orbitofrontal cortex in the brain of the monkey.” In: *The Journal of comparative neurology* 323 (3), pp. 341–358.

MOUNTCASTLE, V B (July 1957). “Modality and topographic properties of single neurons of cat’s somatic sensory cortex.” In: *Journal of neurophysiology* 20 (4), pp. 408–434.

Mugnaini, E et al. (Aug. 1980). “Fine structure of granule cells and related interneurons (termed Golgi cells) in the cochlear nuclear complex of cat, rat and mouse.” In: *Journal of neurocytology* 9 (4), pp. 537–570.

Mulder, Antonius B et al. (Nov. 2003). “Learning-related changes in response patterns of prefrontal neurons during instrumental conditioning.” In: *Behavioural brain research* 146 (1-2), pp. 77–88.

Nabavi, Sadegh et al. (July 2014). “Engineering a memory with LTD and LTP.” In: *Nature* 511 (7509), pp. 348–352.

Otis, James M et al. (Mar. 2017). “Prefrontal cortex output circuits guide reward seeking through divergent cue encoding.” In: *Nature* 543 (7643), pp. 103–107.

Padoa-Schioppa, Camillo and John A Assad (May 2006). “Neurons in the orbitofrontal cortex encode economic value.” In: *Nature* 441 (7090), pp. 223–226.

Perry, Anat et al. (Dec. 2016). “The role of the orbitofrontal cortex in regulation of interpersonal space: evidence from frontal lesion and frontotemporal dementia patients.” In: *Social cognitive and affective neuroscience* 11 (12), pp. 1894–1901.

Pickens, Charles L et al. (Dec. 2003). “Different roles for orbitofrontal cortex and basolateral amygdala in a reinforcer devaluation task.” In: *The Journal of neuroscience : the official journal of the Society for Neuroscience* 23 (35), pp. 11078–11084.

Pnevmatikakis, Eftychios A et al. (Jan. 2016). “Simultaneous Denoising, Deconvolution, and Demixing of Calcium Imaging Data.” In: *Neuron* 89 (2), pp. 285–299.

Poo, Cindy and Jeffry S Isaacson (June 2009). “Odor representations in olfactory cortex: ”sparse” coding, global inhibition, and oscillations.” In: *Neuron* 62 (6), pp. 850–861.

Pratt, W E and S J Mizumori (Sept. 2001). “Neurons in rat medial prefrontal cortex show anticipatory rate changes to predictable differential rewards in a spatial memory task.” In: *Behavioural brain research* 123 (2), pp. 165–183.

Price, J L and T P Powell (Nov. 1970). “The mitral and short axon cells of the olfactory bulb.” In: *Journal of cell science* 7 (3), pp. 631–651.

Protopapas, A D and J M Bower (May 2000). “Physiological characterization of layer III non-pyramidal neurons in piriform (olfactory) cortex of rat.” In: *Brain research* 865 (1), pp. 1–11.

Quirk, G J, J L Armony, and J E LeDoux (Sept. 1997). “Fear conditioning enhances different temporal components of tone-evoked spike trains in auditory cortex and lateral amygdala.” In: *Neuron* 19 (3), pp. 613–624.

Raleigh, M J et al. (Oct. 1979). “The effects of orbitofrontal lesions on the aggressive behavior of vervet monkeys (Cercopithecus aethiops sabaeus).” In: *Experimental neurology* 66 (1), pp. 158–168.

Ramus, S J and H Eichenbaum (Nov. 2000). “Neural correlates of olfactory recognition memory in the rat orbitofrontal cortex.” In: *The Journal of neuroscience : the official journal of the Society for Neuroscience* 20 (21), pp. 8199–8208.

Rennaker, Robert L et al. (Feb. 2007). “Spatial and temporal distribution of odorant-evoked activity in the piriform cortex.” In: *The Journal of neuroscience : the official journal of the Society for Neuroscience* 27 (7), pp. 1534–1542.

Ressler, K J, S L Sullivan, and L B Buck (May 1993). “A zonal organization of odorant receptor gene expression in the olfactory epithelium.” In: *Cell* 73 (3), pp. 597–609.

— (Dec. 1994). “Information coding in the olfactory system: evidence for a stereotyped and highly organized epitope map in the olfactory bulb.” In: *Cell* 79 (7), pp. 1245–1255.

Rigotti, Mattia et al. (May 2013). “The importance of mixed selectivity in complex cognitive tasks.” In: *Nature* 497 (7451), pp. 585–590.

Rinberg, Dmitry, Alex Koulakov, and Alan Gelperin (Aug. 2006). “Sparse odor coding in awake behaving mice.” In: *The Journal of neuroscience : the official journal of the Society for Neuroscience* 26 (34), pp. 8857–8865.

Roesch, Matthew R, Adam R Taylor, and Geoffrey Schoenbaum (Aug. 2006). “Encoding of time-discounted rewards in orbitofrontal cortex is independent of value representation.” In: *Neuron* 51 (4), pp. 509–520.

Roesch, Matthew R, Thomas A Stalnaker, and Geoffrey Schoenbaum (Mar. 2007). “Associative encoding in anterior piriform cortex versus orbitofrontal cortex during odor discrimination and reversal learning.” In: *Cerebral cortex (New York, N.Y. : 1991)* 17 (3), pp. 643–652.

Romanski, L M and J E LeDoux (Nov. 1992). “Equipotentiality of thalamo-amygdala and thalamo-cortico-amygdala circuits in auditory fear conditioning.” In: *The Journal of neuroscience : the official journal of the Society for Neuroscience* 12 (11), pp. 4501–4509.

Root, Cory M et al. (Nov. 2014). “The participation of cortical amygdala in innate, odour-driven behaviour.” In: *Nature* 515 (7526), pp. 269–273.

Rosenkranz, J Amiel and Anthony A Grace (May 2002). “Dopamine-mediated modulation of odour-evoked amygdala potentials during pavlovian conditioning.” In: *Nature* 417 (6886), pp. 282–287.

— (Apr. 2003). “Affective conditioning in the basolateral amygdala of anesthetized rats is modulated by dopamine and prefrontal cortical inputs.” In: *Annals of the New York Academy of Sciences* 985, pp. 488–491.

Roy, Dheeraj S et al. (Aug. 2017). “Distinct Neural Circuits for the Formation and Retrieval of Episodic Memories.” In: *Cell* 170 (5), 1000–1012.e19.

Rudebeck, Peter H et al. (Dec. 2013). "Effects of amygdala lesions on reward-value coding in orbital and medial prefrontal cortex." In: *Neuron* 80 (6), pp. 1519–1531.

Sacco, Tiziana and Benedetto Sacchetti (Aug. 2010). "Role of secondary sensory cortices in emotional memory storage and retrieval in rats." In: *Science (New York, N.Y.)* 329 (5992), pp. 649–656.

Saddoris, Michael P, Michela Gallagher, and Geoffrey Schoenbaum (Apr. 2005). "Rapid associative encoding in basolateral amygdala depends on connections with orbitofrontal cortex." In: *Neuron* 46 (2), pp. 321–331.

Saez, A et al. (Aug. 2015). "Abstract Context Representations in Primate Amygdala and Prefrontal Cortex." In: *Neuron* 87 (4), pp. 869–881.

Sah, P et al. (July 2003). "The amygdaloid complex: anatomy and physiology." In: *Physiological reviews* 83 (3), pp. 803–834.

Sato, T, T Suzuki, and K Mabuchi (Feb. 2007). "A new multi-electrode array design for chronic neural recording, with independent and automatic hydraulic positioning." In: *Journal of neuroscience methods* 160 (1), pp. 45–51.

Schaffer, Evan S et al. (May 2018). "Odor Perception on the Two Sides of the Brain: Consistency Despite Randomness." In: *Neuron* 98 (4), 736–742.e3.

Schoenbaum, G and H Eichenbaum (Aug. 1995). "Information coding in the rodent prefrontal cortex. I. Single-neuron activity in orbitofrontal cortex compared with that in pyriform cortex." In: *Journal of neurophysiology* 74 (2), pp. 733–750.

Schoenbaum, G, A A Chiba, and M Gallagher (June 1998). "Orbitofrontal cortex and basolateral amygdala encode expected outcomes during learning." In: *Nature neuroscience* 1 (2), pp. 155–159.

Schoenbaum, Geoffrey et al. (May 2002). "Orbitofrontal lesions in rats impair reversal but not acquisition of go, no-go odor discriminations." In: *Neuroreport* 13 (6), pp. 885–890.

Schoenbaum, Geoffrey et al. (Aug. 2003). "Encoding predicted outcome and acquired value in orbitofrontal cortex during cue sampling depends upon input from basolateral amygdala." In: *Neuron* 39 (5), pp. 855–867.

Schultz, W (Aug. 2001). "Reward signaling by dopamine neurons." In: *The Neuroscientist : a review journal bringing neurobiology, neurology and psychiatry* 7 (4), pp. 293–302.

Sevelinges, Yannick et al. (2004). "Olfactory fear conditioning induces field potential potentiation in rat olfactory cortex and amygdala." In: *Learning & memory (Cold Spring Harbor, N.Y.)* 11 (6), pp. 761–769.

Shepherd, Gordon M (1998). “Synaptic Organization of the Brain pdf.” In:

Shi, C and M Davis (Dec. 2001). “Visual pathways involved in fear conditioning measured with fear-potentiated startle: behavioral and anatomic studies.” In: *The Journal of neuroscience : the official journal of the Society for Neuroscience* 21 (24), pp. 9844–9855.

Sierra-Mercado, Demetrio, Nancy Padilla-Coreano, and Gregory J Quirk (Jan. 2011). “Dissociable roles of prelimbic and infralimbic cortices, ventral hippocampus, and basolateral amygdala in the expression and extinction of conditioned fear.” In: *Neuropsychopharmacology : official publication of the American College of Neuropsychopharmacology* 36 (2), pp. 529–538.

Simmons, Janine M and Barry J Richmond (Jan. 2008). “Dynamic changes in representations of preceding and upcoming reward in monkey orbitofrontal cortex.” In: *Cerebral cortex (New York, N.Y. : 1991)* 18 (1), pp. 93–103.

Sosulski, Dara L et al. (Apr. 2011). “Distinct representations of olfactory information in different cortical centres.” In: *Nature* 472 (7342), pp. 213–216.

Soucy, Edward R et al. (Feb. 2009). “Precision and diversity in an odor map on the olfactory bulb.” In: *Nature neuroscience* 12 (2), pp. 210–220.

Stalnaker, Thomas A, Nisha K Cooch, and Geoffrey Schoenbaum (2015). “What the orbitofrontal cortex does not do.” In: *Nature neuroscience* 18.5, p. 620.

Stettler, Dan D and Richard Axel (Sept. 2009). “Representations of odor in the piriform cortex.” In: *Neuron* 63 (6), pp. 854–864.

Stuber, Garret D et al. (June 2010). “Dopaminergic terminals in the nucleus accumbens but not the dorsal striatum corelease glutamate.” In: *The Journal of neuroscience : the official journal of the Society for Neuroscience* 30 (24), pp. 8229–8233.

Suzuki, Norimitsu and John M Bekkers (Nov. 2006). “Neural coding by two classes of principal cells in the mouse piriform cortex.” In: *The Journal of neuroscience : the official journal of the Society for Neuroscience* 26 (46), pp. 11938–11947.

— (Oct. 2007). “Inhibitory interneurons in the piriform cortex.” In: *Clinical and experimental pharmacology & physiology* 34 (10), pp. 1064–1069.

Swanson, L W (1982). “The projections of the ventral tegmental area and adjacent regions: a combined fluorescent retrograde tracer and immunofluorescence study in the rat.” In: *Brain research bulletin* 9 (1-6), pp. 321–353.

Takahashi, Yuji K et al. (Apr. 2009). “The orbitofrontal cortex and ventral tegmental area are necessary for learning from unexpected outcomes.” In: *Neuron* 62 (2), pp. 269–280.

Tan, Jie et al. (Mar. 2010). "Odor information processing by the olfactory bulb analyzed in gene-targeted mice." In: *Neuron* 65 (6), pp. 912–926.

Thorpe, S J, E T Rolls, and S Maddison (1983). "The orbitofrontal cortex: neuronal activity in the behaving monkey." In: *Experimental brain research* 49 (1), pp. 93–115.

Tremblay, L and W Schultz (Apr. 1999). "Relative reward preference in primate orbitofrontal cortex." In: *Nature* 398 (6729), pp. 704–708.

Tye, Kay M et al. (June 2008). "Rapid strengthening of thalamo-amygdala synapses mediates cue-reward learning." In: *Nature* 453 (7199), pp. 1253–1257.

Vassalli, Anne et al. (Aug. 2002). "Minigenes impart odorant receptor-specific axon guidance in the olfactory bulb." In: *Neuron* 35 (4), pp. 681–696.

Vassar, R, J Ngai, and R Axel (July 1993). "Spatial segregation of odorant receptor expression in the mammalian olfactory epithelium." In: *Cell* 74 (2), pp. 309–318.

Vassar, R et al. (Dec. 1994). "Topographic organization of sensory projections to the olfactory bulb." In: *Cell* 79 (6), pp. 981–991.

Vertes, Robert P (Jan. 2004). "Differential projections of the infralimbic and prelimbic cortex in the rat." In: *Synapse (New York, N.Y.)* 51 (1), pp. 32–58.

Vidal-Gonzalez, Ivan et al. (2006). "Microstimulation reveals opposing influences of prelimbic and infralimbic cortex on the expression of conditioned fear." In: *Learning & memory (Cold Spring Harbor, N.Y.)* 13 (6), pp. 728–733.

Vong, Linh et al. (July 2011). "Leptin action on GABAergic neurons prevents obesity and reduces inhibitory tone to POMC neurons." In: *Neuron* 71 (1), pp. 142–154.

Walker, David L, Gayla Y Paschall, and Michael Davis (2005). "Glutamate receptor antagonist infusions into the basolateral and medial amygdala reveal differential contributions to olfactory vs. context fear conditioning and expression." In: *Learning & memory (Cold Spring Harbor, N.Y.)* 12 (2), pp. 120–129.

Walker, S C, T W Robbins, and A C Roberts (Apr. 2009). "Differential contributions of dopamine and serotonin to orbitofrontal cortex function in the marmoset." In: *Cerebral cortex (New York, N.Y. : 1991)* 19 (4), pp. 889–898.

West, Elizabeth A et al. (Oct. 2011). "Transient inactivation of orbitofrontal cortex blocks reinforcer devaluation in macaques." In: *The Journal of neuroscience : the official journal of the Society for Neuroscience* 31 (42), pp. 15128–15135.

Wilson, Robert C et al. (Jan. 2014). “Orbitofrontal cortex as a cognitive map of task space.” In: *Neuron* 81 (2), pp. 267–279.

Zhan, Cheng and Minmin Luo (Dec. 2010). “Diverse patterns of odor representation by neurons in the anterior piriform cortex of awake mice.” In: *The Journal of neuroscience : the official journal of the Society for Neuroscience* 30 (49), pp. 16662–16672.

Zhang, Xinmin and Stuart Firestein (Feb. 2002). “The olfactory receptor gene superfamily of the mouse.” In: *Nature neuroscience* 5 (2), pp. 124–133.

Ziv, Yaniv et al. (Mar. 2013). “Long-term dynamics of CA1 hippocampal place codes.” In: *Nature neuroscience* 16 (3), pp. 264–266.

Zola-Morgan, S M and L R Squire (Oct. 1990). “The primate hippocampal formation: evidence for a time-limited role in memory storage.” In: *Science (New York, N.Y.)* 250 (4978), pp. 288–290.